NUMERICAL ANALYSIS OF GAS FLOW WITHIN A MUNICIPAL SOLID WASTE LANDFILL

A Thesis

Submitted to the College of Graduate Studies and Research

in Partial Fulfillment of the Requirements

for the Degree of Master of Science

in the Department of Civil Engineering

University of Saskatchewan

Saskatoon

by

Natalya Viktorovna Usova

PERMISSION TO USE

The author has agreed that the library, University of Saskatchewan, may make this thesis freely available for inspection. Moreover, the author has agreed that permission for copying of this thesis in any manner, in whole or in part, for scholarly purposes may be granted by the professors who supervised the thesis work recorded herein or, in their absence, by the Head of the Department or the Dean of the College in which the thesis work was done. It is understood that due recognition will be given to the author of this thesis and to the University of Saskatchewan in any use of the material in this thesis. Copying or publication or any other use of the thesis for financial gain without approval by the University of Saskatchewan and the author's written permission is prohibited.

Requests for permission to copy or to make any other use of material in this thesis in whole or part should be addressed to:

Head of the Department of Civil and Geological Engineering
University of Saskatchewan
Engineering Building
57 Campus Drive
Saskatoon, Saskatchewan
Canada, S7N 5A9

ABSTRACT

Numerical analysis and modelling of gas flow within a municipal solid waste (MSW) landfill has the potential to significantly enhance the efficiency of design and performance of operation for landfill gas (LFG) extraction and utilization projects. Over recent decades, several numerical models and software packages have been developed and used to describe the movement and distribution of fluids in landfills. However, for the most part, these models have failed to gain widespread use in the industry because of a number of limitations. Available simple models implement a simple theoretical basis in the numerical solution, for example various approaches that treat the landfilled waste fill purely as a porous medium with the conservation of mass inherently assumed and the ongoing gas generation within the landfill thus ignored. Alternatively, researchers have developed some highly complex models whose use is rendered difficult as a result of the uncertainty associated with the large number of required inputs.

Ultimately, more efficient design and operation of well-fields for LFG extraction will provide a benefit in the cost of construction and efficiency of operation as well as with a reduced potential of underground fire resulting from over-pumping or localized excessive wellhead vacuum. Thus, the development of tools for improved understanding and prediction of the gas flows and pressure distribution within MSW will potentially enhance operation of LFG extraction systems at existing landfills as well as the design for new LFG projects. In the simplest terms, a more accurate estimate of the relationship between flow rates and wellhead vacuum will allow for improved analysis of the network of LFG extraction wells, header pipes and valves and blowers.

The research described in this thesis was intended to evaluate the error introduced into estimates of the intrinsic permeability of waste from LFG pumping tests if the ongoing gas generation within the landfilled MSW is ignored when the pumping tests are evaluated to yield estimates of the permeability. The City of Saskatoon's Spadina Landfill Site was chosen as the research site. The landfill contains over six million tonnes of waste of age ranging from days and weeks old to almost 60 years and which

continue to generate significant landfill gas. It was determined that during the pumping tests, the estimated volume of gas generated within the radius of influence of each well during the time of pumping ranged from 20% to 97% of the total volume of the gas actually pumped during the time of the pumping, depending on the well and the flow rate in question. Fleming (2009) reported that the landfill is estimated to generate about 250[m^3/hour] of landfill gas containing up to 60% of methane.

Two different approaches were used to simulate gas flow in the unsaturated waste fill. The first modelling tool was the GeoStudio 2007 software suite. The second approach used a very simple 1-dimensional axisymmetric finite difference (1-D FD) solution to estimate the radial distribution of pressures within the waste associated with gas flow toward an applied wellhead vacuum under conditions where the waste fill is estimated to generate landfill gas at a constant rate per unit volume. This 1-D FD solution was used to compare the flow rate and pressure distribution in the waste with that predicted using widely-available geotechnical software for 2-dimensional axisymmetric flow in an unsaturated porous medium. It is proposed that the correction charts so developed may represent a first step toward a reliable method that would enable such widely used software to be used with a correction factor to enable improved simulations of flow and pressure within the system.

The results from both approaches support the previously reported intrinsic permeability values determined for the Spadina Landfill. The 1-D FD solution results show that there is some effect of the gas generation on the best-fit estimates of the value of intrinsic permeability. In addition, the 1-D FD solution shows better fit to the field data (when the gas generation is taken into account) compared with simulations carried out using AIR/W (GeoStudio 2007).

Nevertheless, the AIR/W computer package was found to be simple, powerful and intuitive for simulating two-phase flow toward LFG extraction wells. The addition of an option to include a gas generation term in the commercial software package would enable more accurate results for evaluation of flow of landfill gas, however as a first step in this direction, charts of correction factors are proposed.

ACKNOWLEDGEMENTS

I would like to express my appreciation and respect to my supervisor, Prof. Ian Fleming, for his invaluable support, guidance, and advice. His critical appraisal and recommendations have been priceless at every stage of this research and the evolution of the writing of this thesis.

I would like to extend my acknowledgement to my committee chair, Dr. Moh Boulfiza, and my advisory committee members, Dr. Jit Sharma, Dr. Grant Ferguson, and Dr. Chris Hawkes, for their valuable suggestions and feedback.

I take this opportunity to thank graduate students, colleagues and staff at the Department of Civil and Geological Engineering for making my stay at the University of Saskatchewan one of the most memorable moments of my life.

Furthermore, I would like to thank NSERC, the City of Saskatoon, and SALT Canada Inc. for providing the financial support for this research work.

DEDICATIONS

The thesis is dedicated to my husband for his priceless motivation, encouragement, and guidance and to my daughter, two sisters, father, and grandmother for their valuable support.

TABLE OF CONTENTS

LIST OF TABLES

LIST OF FIGURES

LIST OF VARIABLES

a,n,m = curve fitting parameters (eq.[3.3]);

A = surface area of the screened portion of a well [m^2];

d = representative length dimension of the porous matrix [m];

$\frac{dh}{dx}$ = gradient of hydraulic (total) head [m/m];

$\frac{dP}{dx}$ = gas pressure gradient [Pa/m];

D_T = total depth of the mode [m];

D_{waste} = entire depth of waste [m];

e = natural number *2.71828;*

f_{CH_4} = methane fraction;

g = gravitational acceleration [m/s^2];

h_{pw} = hydraulic pressure head [m];

i = interval between the range of j to N;

j = least negative pore-water pressure to be described by the final function;

I_i = rate at which mass of the i-species is produced per unit volume of the system by the chemical reaction [$kg/(m^3*s)$];

$I_{k.}$ = intrinsic permeability ratio [dimensionless];

K_w = hydraulic conductivity [m/s];

K_w^* = calculated hydraulic conductivity for a specified water content or negative pore-water pressure [m/s];

K_s = saturated hydraulic conductivity [m/s];

K_{sm} = measured saturated conductivity [m/s];

K_x and K_z = horizontal and vertical hydraulic conductivity respectively [m/s];

k_i = intrinsic permeability [m^2];

k_{ir} = intrinsic permeability in radial direction [m^2];

k_{iz} = intrinsic permeability in vertical direction [m^2];

$k_i^{F/P}$ = best-fit value of intrinsic permeability determined using the AIR/W model assuming a geometry that is closest to a fully-penetrated well screen, within the constants of convergence described above [m^2];

$k_i^{initial}$ = best-fit value of intrinsic permeability using the AIR/W model with the actual partially-penetrating geometry of each well as actually constructed [m^2];

k_i^* = intrinsic permeability determined using the 1-D FD solution with the total gas generation rate included ($R_g>0$) [m^2];

k_i^o = intrinsic permeability determined using the 1-D FD solution but where the total gas generation rate was ignored ($R_g=0$) [m^2];

k_{ra} = relative permeability of air [dimensionless];

k_{rnw} = relative permeability of non-wetting fluid[dimensionless];

k_{rw} = relative permeability of water (or wetting fluid)[dimensionless];

k_a = air effective permeability [m^2] (= $k_{ra} \cdot k_i$);

k_w = water effective permeability [m^2] (= $k_{rw} \cdot k_i$);

k_x/k_z = anisotropy ratio [dimensionless];

L_{DS} = depth to the screen [m];

L_S = screen length [m];

L_{SB} = distance from the screen bottom to the model bottom [m];

L_S/D_T = partial penetration ratio [dimensionless];

MW = molecular weight of gas [kg/mole];

N = vector norm, *i* is a counter and *n* is the total number of nodes (eq. [3.1]);

N = maximum negative pore-water pressure to be described by the final function (eq. [3.2])

μ_g = gas viscosity [kg/(m·s)];

μ_w = absolute (dynamic) viscosity of water [N s/m^2];

P = gas pressure [Pa];

P_{atm} = ambient gas pressure [Pa];

ρ_g = gas density [kg/m^3];

ρ_i = density of the *i*-species [kg/m^3];

ρ_w = density of water [kg/m^3];

ρ_{waste}^{app} = apparent density of waste [Mg/m^3];

Q_g = gas flow rate (Darcy's Law) [m^3/s];

θ_g = volumetric gas content, equal the product of the gas –phase saturation and the porosity [m^3/m^3];

θ_w = volumetric moisture content [m^3/m^3];

q_i = specific discharge of the *i*-species [m/s];

q_g = specific discharge of gas (Darcy's Law) [m/s];

q_w = specific discharge of water [m/s];

r = distance from the pumping well [m];

r_p = Pearson's correlation coefficient;

r_w = well radius [m];

R = ideal gas law constant (taken as 8.314 [Pa*m^3/(K*mole)]);

R_{CH_4} = methane generation rate [m^3/Mg/year],

R^2 = coefficient of determination;

Re = Reynolds number [dimensionless];

R_{eg} = Reynolds number for gas flow [dimensionless];

R_g = total gas generation rate [kg/(m^3*s)];

R_g^{**} = total gas generation rate [m^3/m^3/hour];

R_M = radius of the model [m];

S = saturation which is defined as the ratio of the volume of wetting fluid to the volume of interconnected pore space in bulk element of the medium [dimensionless];

S_e (or θ_e) = effective saturation [dimensionless];

S_{nw} = non-wetting fluid saturation (i.e. S_{nw0} is residential).

S_r = residual saturation [dimensionless];

S_{xx} and S_{yy} = statistics: that used to measure variability in variable "x" and "y" correspondently [dimensionless];

S_{xy} = statistic that used to measure correlation [dimensionless];

S_w = wetting fluid saturation (i.e. S_{w0} is irreducible);

t = time [s];

T = absolute temperature [K];

U_a and U_w = correspondently the air and the water pressures;

$(U_a\text{-}U_w)_i$ = individual nodal matric pressure;

V_{screen} = screen volume [m^3];

V_{waste} = waste volume [m^3];

x = distance from the pumping well [m];

y = a dummy variable of integration representing the logarithm of negative pore-water pressure; z is the thickness [m];

υ_g = kinematic viscosity of the gas [m^2/s];

φ_{kR} = intrinsic permeability correction factor due to gas generation [dimensionless];

Θ_s = volumetric water content [m^3/m^3];

Θ' = first derivative of the equation;

Ψ = required suction range;

Ψ^* = suction corresponding to the j^{th} interval;

λ = Brooks-Corey pore-size distribution index [dimensionless];

Λ_{waste} = gas ratio [$1/m^3$];

$£_{Rg}$ = volume of gas generated per unit time [m^3/hour].

CHAPTER 1
INTRODUCTION

1.1 Background

During recent decades in most countries, landfills have been constructed to separate waste deposits from the nearby environment and have represented the primary means of solid waste disposal. In fact, the problem of contamination from landfills has become an important international challenge (Amro 2004). During operation and subsequently, landfilled waste is exposed to various physical and biochemical effects. As a result, various processes occur, including generation of heat and landfill gas, flow of leachate and gas, and mechanical deformation and settlement (Kindlein et al. 2006, Powrie et al. 2008). The stabilization of municipal solid waste (MSW) landfills can be viewed as a two-phase process: an early aerobic decomposition phase followed by an anaerobic phase. The aerobic phase is relatively short inasmuch as biodegradable organic materials react rapidly with oxygen to form carbon dioxide, water, and microbial biomass. Thereafter, landfill gas is generated consisting of a mixture of gases which are the end products of biodegradation of organic materials in an anaerobic environment (El-Fadel et al. 1997a).

Increasing awareness of and concern regarding the potential environmental impact of municipal waste landfills have combined with evolving technology for landfill gas capture and utilization. MSW landfills have thus increasingly become a focus of research for both economic and environmental reasons. Existing and proposed landfills must meet environmental regulations, which typically specify minimum standards for protecting the environment and thus impose potential economic costs, for example by requiring collection and flaring of landfill gas (LFG).

The minimization of environmental impact has been significantly reinforced by research. In many cases, continuing improvements to the efficiency, performance, and economics of current or prospective LFG projects usually require expensive and time consuming testing and evaluation and the resulting well-field designs may not in any event attain the best possible efficiency and optimization.

Numerical analysis and modelling can thus play an important role in this rapidly developing field. In general, for many projects, including design of landfill barrier systems, numerical analysis and modelling have become an inalienable part of engineering because of the ability to be used in at least three generic categories such as interpretation, design, and prediction of different scenarios (Barbour and Krahn 2004). Modelling of landfill gas generation and extraction, particularly relating to well-field design and optimization is relatively less advanced.

The fundamental theory of fluid flow in porous media was developed for groundwater, oil and gas, and related flow phenomena. Jain et al. (2005), White et al. (2004); Kindlein et al. (2006), and others commonly refer to the governing equations for multiphase flow and transport in porous media, the models that were earlier presented by various authors including Bear (1972).

Published papers related to multiphase flow in waste fill, in most cases, attempt to apply established models developed for groundwater flow or related phenomena to the particularly conditions found in a landfill. As a result, applications of such modified models may be quite limited in terms of the range of applicability as a result of the restrictive assumptions and limited cases of applications. For example, available software packages and numerical models treat the landfilled waste as a porous medium with the inherent assumption of conservation of mass, thereby by necessity ignoring in-situ LFG generation. Also, depending on the approach, a landfill investigation can represent different space and time scales. For example, White et al. (2004) described the biochemical landfill degradation processes of solid waste using a numerical model of various coupled processes where they make several assumptions, for instance, that any gas with pressure in excess of the local pore-pressure is vented immediately. It is

evident that this assumption can never be completely realized as for the real spatial dimensions of the landfill, some finite duration of time would be required.

To improve the understanding of gas flow processes in unsaturated landfilled MSW, this research was intended to assess the effect of ignoring gas generation in estimating the intrinsic permeability of waste from LFG pumping test data. Efficient well-field design requires accurate knowledge of the flow/vacuum relationship for the wells, and it will be demonstrated that the relationship between flow and wellhead vacuum is affected to a significant degree by the in-situ generation of gas within the waste fill. In addition, a potential safety consideration reflects the fact that waste degradation goes along with high subsurface temperature. Overpumping of wells as a result of underestimating the relationship between gas flow rate and pumping pressure (vacuum) may thus increase the risk of underground fire. Therefore, the ability to accurately define the material properties of a landfill can be considered important from the perspective of health and safety, and more accurate estimates of permeability and relationship between flow rate and wellhead vacuum will provide a benefit in the cost of construction and efficiency of landfill's operation.

1.2 Research objective and scope

This research is carried out using pumping test data that have been previously collected by Stevens (2012) from the City of Saskatoon's Spadina Landfill Site, and the author's work is therefore strictly confined to the analysis of combined LFG generation and flow using these test data. This landfill site has operated since 1955 and by 2007 stored over six million tonnes of waste. The ongoing degradation of MSW generates landfill gas at a relatively moderate rate. Fleming (2009) reported that the demonstration well-field (10-test wells) was capable of producing on average about 250[m^3/hour] of landfill gas where the methane fraction ranged from 50% to 60%. The rate of gas generation at Spadina Landfill Site was estimated to be approximately equal to 4 m^3 of methane per Mg of waste in-situ per year. Moreover, if a modest increase in the in-situ moisture content may be achieved, the stable methane generation rate could reach 10 to 20[m^3/Mg/year] (Fleming 2009). During the pumping tests, the estimated volume of gas

generated within radius of influence of each well during the pumping time ranged from 20% to 97% of the total volume of gas that was actually pumped during the time of pumping depending on the well and the flow rate. Thus, the purpose of this work is to investigate the effect of ignoring or including the gas generation rate when carrying out analyses of the data collected from LFG pumping tests and to determine the magnitude of this effect in estimating the (intrinsic) permeability of the waste mass using numerical analysis and modeling.

The general objective of this research project is to define an appropriate conceptual basis and a numerical model for combined gas generation and flow in MSW, based on the principle of intrinsic permeability; and to determine the effect of the gas generation rate on the permeability estimates determined from pressure/flow data collected from LFG pumping tests in MSW.

The specific objectives are as listed below:

- To conduct a literature review of existing numerical techniques for unsaturated flow in MSW landfills;
- To evaluate the intrinsic permeability of MSW using test data collected from the City of Saskatoon's Spadina Landfill Site;
- To develop two approaches for a gas flow model for MSW:
    - The first model tool was the commercial software package called AIR/W (GeoStudio 2010), which was used to evaluate the conceptual model for gas flow to extraction wells within unsaturated MSW;
    - The second approach used a simple 1-dimensional axisymmetric finite difference solution to estimate the radial distribution of pressures when the effect of gas generation within the waste mass is included.
- To determine if gas generation occurring in the landfill may be ignored in the evaluation of the (intrinsic) permeability of the landfilled waste;
- To propose correction charts that incorporate gas generation term, so the results from the widely used software could be improved within a correction factor; and

- To offer recommendation for future research.

The research was restricted to analysis based on the data previously collected by Stevens (2012), and thus the data collection, instruments, and test methods used to gather the data are not considered in this research.

1.3 Research Methodology

No previous research has been found that addresses this issue of the effect of the gas generation rate on the estimated permeability of MSW. The research program for this thesis followed a standard modelling methodology. A simple version of the scientific methodology covers four steps which are: to observe, to measure, to explain, and to verify (Barbour and Krahn 2004). The methodology for each approach was followed during the four main steps in this thesis:

- Step 1. Observe – develop the conceptual model. The three key processes were included such as defining the purpose of the model, gathering existing information, and developing a conceptual model.
- Step 2. Measure – define the theoretical model. Discussion of the important processes occurring in association with the most relevant equations and theories. Statement of the essential assumptions and approximations used in definitions including available data sets of all known information.
- Step 3. Explain – develop and verify the numerical model. Define the model geometry and set boundary conditions and material properties. The obtained solution was compared with an alternative solution and published field studies to establish its accuracy. Possible sources of error were determined and the limitation of the solution obtained.
- Step 4. Verify – interpret, calibrate, validate. After the solution was obtained, the results were interpreted within the context provided by the observed physical reality and calibrated and validated to capture defects in the solution if they existed. The range of reasonable and acceptable responses to the solutions was defined. A sensitivity analysis was carried out through a selected range of

relevant parameters. The sensitivity analysis involved a series of simulations in which only one parameter was varied at a time and then reviewed for defining what was the effect of these variations against the key performance. Confirm the model by applying the calibrated model to the new set of responses. The results of both approaches were recorded, compared, and the work was submitted for review.

1.4 Thesis Outline

This research study delivers the background which is needed for the development of a numerical analysis of gas generation and flow within a MSW landfill. The thesis includes five chapters and four appendices.

The first chapter introduces the problem, lists the objectives and the scope, and briefly describes the research methodology.

Chapter 2 provides the literature review, which includes the summary of the related research conducted previously and describes the physical problems.

Chapter 3 presents a description of the investigated site together with the methodology for both modelling approaches. The first approach is the transient axisymmetric two-phase saturated/unsaturated flow model built using the widely-available commercial software, GeoStudio 2007 (AIR/W). The second approach is a simple one-dimension finite difference numerical solution for combined gas generation and flow. The detailed parametric study for both approaches is shown in Chapter 3.

Chapter 4 shows what have been learned through the presentation, analysis, and discussion of the results obtained from both modelling approaches.

Chapter 5 summarizes the work described in this thesis together with one worked example of the proposed methodology. The need for the further research is outlined there as well.

The appendices present the outputs from both approaches in graphical or/and in tabular forms, as well as additional information that helps to improve understanding of the research described in this thesis. The field data and properties together with its test-well geometry, conducted previously (Stevens 2012 and Fleming 2009), are provided in Appendix A. The models' geometry and their boundary conditions for both approaches can be found in Appendix B. The outputs of the AIR/W models' simulations conducted through the parametric study are shown in Appendix C. The outputs of the 1-D FD solution conducted through the parametric study are shown in Appendix D. Appendix D provides extra information for the correction factors and charts for intrinsic permeability, which have been newly defined through this research.

CHAPTER 2
LITERATURE REVIEW AND BACKGROUND

2.1 Introduction

Gas flow within a MSW landfill is governed by the well-established principles of flow in porous media, and in this chapter, the background is presented for the development of a rigorous analysis of the problem. This chapter is divided into three sections. The first section provides the background of the physical problem under consideration, and a review of related previous research. The next section describes the material-specific properties of MSW along with factors that affect the gas flow in MSW based on earlier research. The last section presents a discussion regarding available software packages that may be used to investigate a one or two-phase flow of fluids in a MSW landfill.

2.2 Multiphase Flow in Porous Media

The following section describes the theoretical background of unsaturated porous medium theory required to develop the equations for the numerical analysis.

The complexity of two-phase flow in porous media is discussed by Knudsen and Hansen (2002) and by Bravo et al. (2007) who highlight problems such as the difference between unsteady and transient response, the relations of properties at different length scales and the existence of a variety of flow patterns. It is well established that when two or more fluids occur in porous media, two types of flow are possible to observe, miscible displacement and immiscible displacement (Bear 1972). In the case of simultaneous flow of two-phases (liquid and gas) immiscible displacement flow occurs under conditions such that the free interfacial energy is non-zero and a distinct fluid-fluid interface separates the fluid within each pore (Bear 1972). The research carried out for this work covered unsaturated flow, which is a special case of

the flow of two immiscible fluids. Unsaturated (air-water) flow represents the flow of water and water vapour through a soil where the void space is partly occupied by air (i.e. the flow of water that has the degree of saturation less than 100% with stagnant air that is partially occupied the void space not filled with water) (Bear 1972).

Experimental results have demonstrated that when two-phase flow of immiscible fluids occurs simultaneously through a porous medium, each of them creates its own tortuous flow paths, forming stable channels (Bear 1972). Therefore, in many cases it is assumed that a unique set of channels acts in conformity with a given degree of saturation (Bear 1972 and Bravo et al. 2007). Relative permeability, soil structure and stratification, depth to the ground water, and moisture content are the major parameters that are used to evaluate permeability of porous media.

A fundamental property of an unsaturated porous media is reflected by the moisture retention curve, which describes the relationship between suction (or the negative pore-water pressure) and moisture content (Bear 1972, Fredlund and Rahardjo 1993, McDougall et al. 2004). When the gravimetric moisture retention curve is determined through the pore-size distribution, it is assumed that the moisture lost as a result of an increase in suction corresponds to the volume of pores drained (Simms and Yanful 2004). In an unsaturated soil, the permeability is significantly affected by combined changes in the soil moisture content (or saturation degree) and the soil void ratio (Fredlund and Rahardjo 1993). Both parameters may be readily incorporated if the saturation condition is expressed in terms of an effective degree of saturation. The effective degree of saturation can be expressed in the following form as (Corey 1954, 1956):

$$S_e = \frac{S - S_r}{1 - S_r} \qquad [2.\ 1]$$

where S_e is the effective saturation [dimensionless], S is the saturation which is defined as the ratio of the volume of wetting fluid to the volume of interconnected pore space in bulk element of the medium [dimensionless], 1 is the volumetric moisture content at saturation 100%, and S_r is the residual saturation [dimensionless].

The moisture retention curve is commonly determined experimentally; however, the shape of moisture retention curve can be also estimated predominantly by the grain-size distribution data and secondarily by the density of the soil through a mathematical approach (Fredlund et al. 2002). Fredlund et al. (2000) proposed a unimodal equation for uniform or well graded soils and a bimodal equation for gap-graded soils, essentially enabling fitting to any grain-size distribution data set (Fig. 2.1).

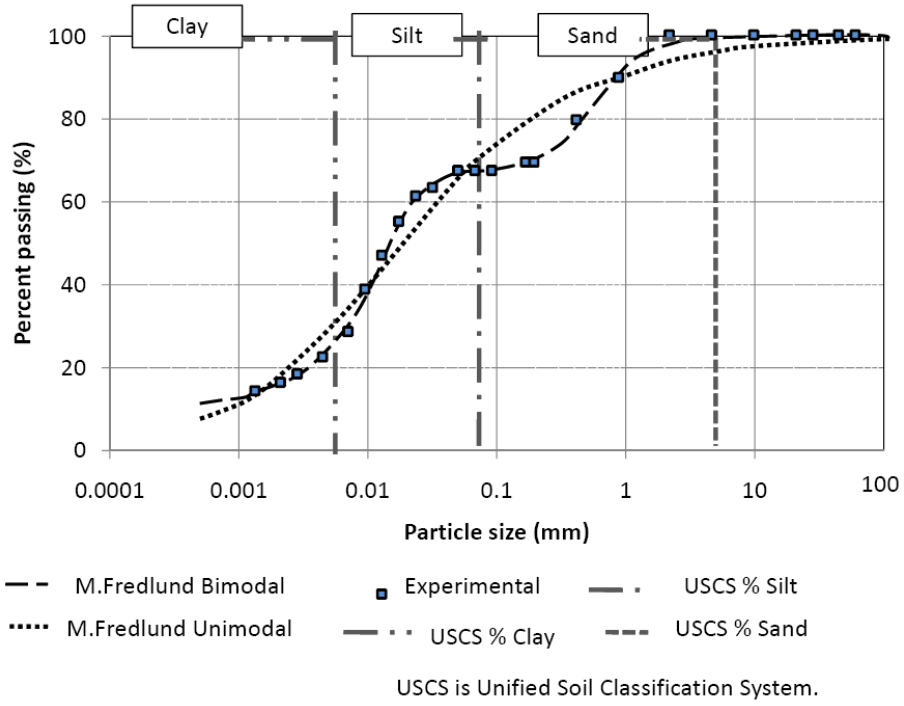

Fig. 2. 1. Fitting a gap-graded soil with the unimodel and bimodel equations (after Fredlund et al. 2000).

Later Fredlund et al. (2002) proposed a method to estimate a moisture retention curve from the grain-size distribution calculated using this method. They reported good fits for the estimated moisture retention curves for sand and silt and reasonable results for clay, silt, and loam. Huang et al. (2010) compared the estimated and measured grain-size distribution curves presented by Fredlund et al. (2000) with their samples and found that results differed with a lower root mean square error of 0.869%. The authors' research was based on a data set of 258 measured grain-size distribution and moisture retention curves (Huang et al. 2010). Additional investigation is still required in testing

the algorithms on finer soils and on soil with more complex fabrics, or indeed, non-conventional "soil-like materials" such as MSW.

When the moisture retention curve for two-phase immiscible flow is analyzed, it is necessary to consider the more complicated porosity model. In porous media there can be several conceptual models used to idealize the pore size distribution such as single-, dual-, and multiple-porosity. Since this research focused on two-phase flow in a MSW landfill, the dual-porosity becomes a point of interests.

Fluid flow in MSW has been shown to exhibit behaviour characteristic of a dual porosity model, with large easily-drained pores and a matrix of smaller pores (Kazimoglu et al. 2006, White et al. 2011, and Fleming 2011). Thus, it is possible that a gap-graded particle size approach might be suitable for estimating or predicting the moisture retention properties of landfilled MSW.

Dual-porosity models differ from single-porosity models by the presence of an additional transfer function (Tseng et al. 1995). Dual-porosity models have been extended and used since 1960 when Barenblatt and Zheltov (1960) and Barenblatt et al. (1960) introduced a conceptual double-continua approach for water flow in fissured groundwater systems. In general, the dual-porosity model appears to approximate the physical unit of a structured porous medium with two distinct, but at the same time with interacting, subunits that represent macro-pores and porous-blocks inherent in the field soil or rock formations. Because of its complexity, existing formulations of the dual porosity model have been developed with many simplifications and idealized assumptions. Moreover, in case of the dual-porosity for the two-phase MSW landfill flow there are further complications that needed to be better researched (i.e. it was not found how the ignorance of a dual-porosity might affect the results).

The fundamental parameter which affects flow (i.e. single-phase and two-phase) in porous media is the intrinsic permeability. First of all, it is obvious that the ability of a soil to transmit gas is reduced by the presence of soil liquid, which blocks the soil pores and reduces gas flow. Therefore, intrinsic permeability, a measure of the ability of soil

to transmit fluid, is the key factor in determining the amount of gas transportation (US EPA 1994).

Typically the intrinsic permeability can be calculated based on the saturated hydraulic conductivity value (Bear 1972, Strack 1989, Fredlund and Rahardjo 1993). The relationship between intrinsic permeability and the saturated hydraulic conductivity can be stated in the following form (Fredlund and Rahardjo 1993):

$$K_w = k_i \cdot \frac{\rho_w \cdot g}{\mu_w} \qquad [2.\ 2]$$

where K_w is the hydraulic conductivity [m/s]; ρ_w is the density of water [kg/m^3]; μ_w – absolute (dynamic) viscosity of water [N*s/m^2]; g is the gravitational acceleration [m/s^2]; and k_i is the intrinsic permeability [m^2].

The range of intrinsic permeability values for unconsolidated natural sediments is wide. According to Bear (1972) intrinsic permeability can vary from 10^{-7}[m^2] to 10^{-20}[m^2]. Fetter (2001) suggests that the range for intrinsic permeability is somewhat narrower, 10^{-9}[m^2] to 10^{-18}[m^2]. Nevertheless, it is well to keep in mind the intrinsic permeability of natural materials can vary by one to three orders of magnitude across a site and might be estimated from boring log data within an order of magnitude (Collazos et. al. 2002, McDougall 2007). For MSW, on the other hand, due to anisotropic material characteristics and varaibility of material across a site, the intrinsic permeability value strongly depends on several factors (more information is provided below in this Chapter) such as depth, porosity, age and type of the waste (Bleiker et al. 1995, El-Fadel et al. 1997a, Powrie and Beaven 1999, Jain et al. 2005, and Beaven et al. 2008).

Numerous sources including Fredlund and Rahardjo (1993), Kindlein et al. (2006), Beaven et al. (2008), and GeoStudio (2010) use the Brooks and Corey model to describe the water and air permeability of porous media. The relative permeability of a phase (i.e. water or air) is a dimensionless measure of the effective permeability of that particular phase in multiphase flow (Bear 1972). In other words for this research, the relative permeability is the ratios of the effective permeability of water or landfill gas phase to its absolute permeability.

The relative air and water permeability respectively could be expressed in the following forms, shown in equations [2.3] and [2.4], (Brooks and Corey 1964):

$$k_{ra} = (1 - S_e)^2 \left[1 - S_e^{\left(\frac{2+\lambda}{\lambda}\right)}\right] \qquad [2.\ 3]$$

and

$$k_{rw} = S_e^{\left(\frac{2+3\lambda}{\lambda}\right)} \qquad [2.\ 4]$$

where k_{ra} is the relative permeability of air [dimensionless], k_{rw} is the relative permeability of water [dimensionless], and λ is the Brooks-Corey pore-size distribution index [dimensionless].

A typical relationship between relative permeability curves for wetting and non-wetting phases versus degree of saturation is shown in Fig. 2.2 (Bear 1972). In this context the water represents the wetting fluid, and the landfill gas the non-wetting fluid; thereby the subscript *nw* in the non-wetting relative permeability variable k_{rnw} shown in Fig. 2.2 can be changed to k_{ra} since non-wetting phase is air.

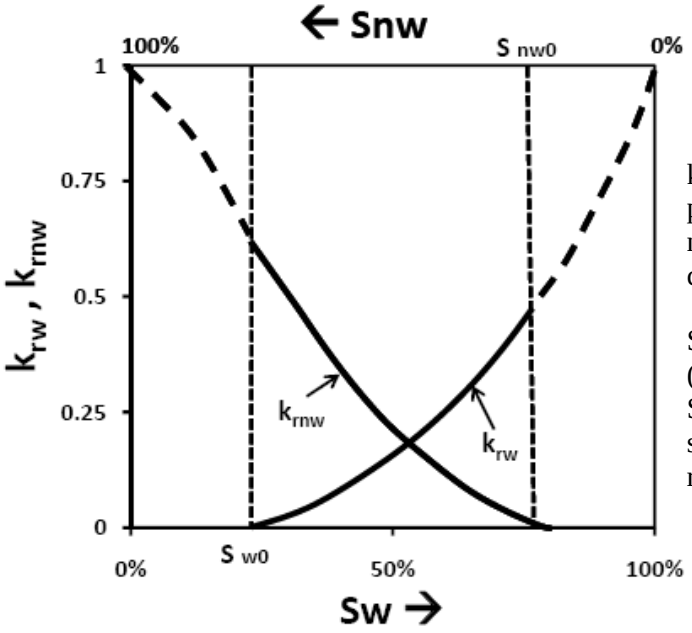

k_{rw} and k_{rnw} are the relative permeability of wetting and non-wetting fluid correspondently.

S_w is wetting fluid saturation (i.e. S_{w0} is irreducible); and S_{nw} is the non-wetting fluid saturation (i.e. S_{nw0} is residential).

Fig. 2. 2. Typical relative permeability curves (after Bear 1972).

The product of the intrinsic permeability and the relative permeability of fluid is equal to the effective permeability of that fluid, which is used to describe flow of one fluid in a porous media when another fluid is also presented in the pore spaces (Bear 1972). Air effective permeability may be expressed in the following form (Brooks and Corey 1964):

$$k_a = k_i \cdot k_{ra} \qquad [2.\ 5]$$

where k_a is the air effective permeability [m^2].

Water effective permeability is defined as (Brooks and Corey 1964):

$$k_w = k_i \cdot k_{rw} \qquad [2.\ 6]$$

where k_w is the water effective permeability [m^2].

To derive the partial differential equation (PDE) for gas and/or liquid flow in porous media four fundamental steps can be used (Fig. 2.3) (after Barbour 2010). The four steps include:

- Define a representative elementary volume;
- Make the statement of mass conservation;
- Apply Darcy's Law; and
- Simplify PDE.

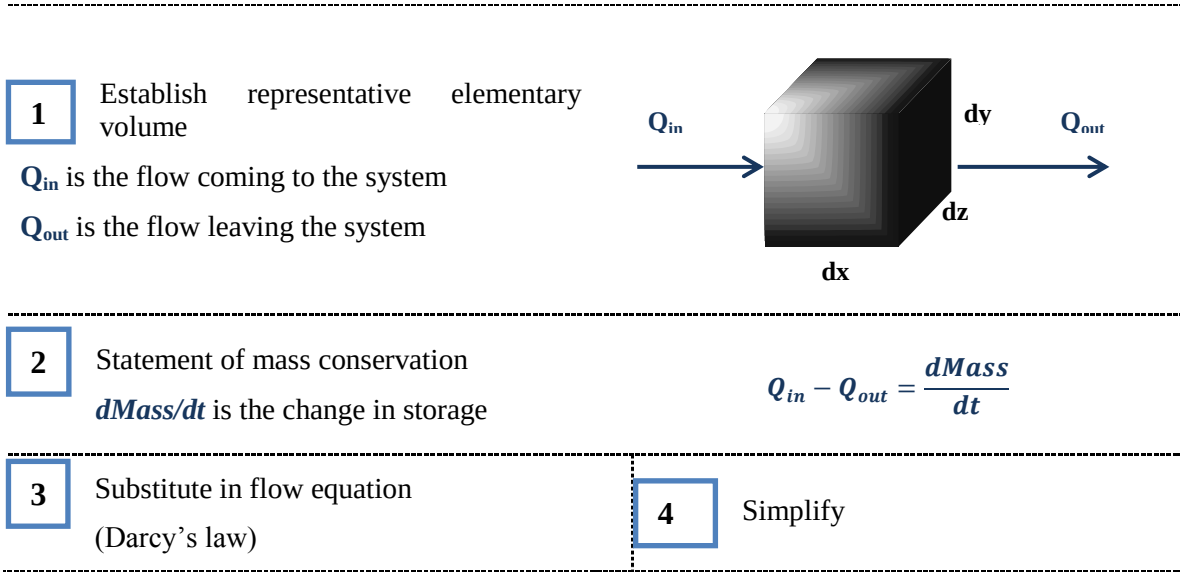

Fig. 2. 3. Schematic for the partial differential equation (after Barbour 2010).

However, all of these four steps are for porous media. In MSW, at the same time as a flow is coming into the system and leaving it, a landfilled waste generate some amount of gas which is depended on many factors more information about it is provided below in this chapter and the next ones.

In the various equations presented below for flow of water, gas or two-phases together it is assumed that the water and the gas are the viscous fluids and Darcy's Law is valid. In order to verify that liquid and gas flows in porous media are laminar (Darcy's Law is valid), the Reynolds number is used (Bear 1972, Fredlund and Rahardjo 1993, Fetter 2001).

In soil hydraulics, the Reynolds number used to distinguish the laminar and turbulent flow is defined as (Fetter 2001):

$$R_e = \frac{\rho_w \cdot q_w \cdot d}{\mu_w} \qquad [2.\ 7]$$

where *Re* is the Reynolds number [dimensionless] and *d* is the representative length dimension of the porous matrix [m].

For gas flow in porous media, the Reynolds number is calculated as (Bear 1972):

$$R_{eg} = \frac{Q_g \cdot d}{A \cdot v_g} \qquad [2.\ 8]$$

where R_{eg} is the Reynolds number for gas flow [dimensionless], Q_g is the gas flow rate (Darcy's Law) [m^3/s], A is the surface area of the screened portion of a well [m^2], and υ_g is the kinematic viscosity of the gas [m^2/s].

The fundamental porous media equation, Darcy's Law, may be expressed in terms of hydraulic head (Fetter 2001):

$$q_w = -K_w * \frac{dh}{dx} \qquad [2.\ 9]$$

where: q_w is the specific discharge of water [m/s], and $\frac{dh}{dx}$ is the gradient of hydraulic (total) head [m/m].

Gas, like liquid, can migrate under a pressure gradient, a concentration gradient (by

molecular diffusion), or both. The mass conservation of soil gas can be expressed by the following equation (Suthersan 1999):

$$\theta_g \cdot \frac{\partial \rho_g}{\partial t} = -\nabla \rho_g \cdot q_g \qquad [2.\ 10]$$

where θ_g is the volumetric gas content, equal the product of the gas–phase saturation and the porosity [m^3/m^3], ρ_g is the gas density [kg/m^3], t is the time [s], and q_g is the specific discharge of gas (Darcy's Law) [m/s].

The density of gas is a function of the pressure and temperature, where the relationship among these parameters is expressed by an equation of state. One such equation is the ideal gas law, which is simple and applicable (to a very good approximation) for both "soil gas" (in porous media) at vacuum (Bear 1972) and landfilled gas (Jain et el. 1995, Falta 1996, and Suthersan 1999). Thus the gas density can be computed by the ideal gas law as:

$$\rho_g = P \cdot \left(\frac{MW}{R \cdot T}\right) \qquad [2.\ 11]$$

where P is the gas pressure [Pa]; MW is the molecular weight of gas [kg/mole]; R is the ideal gas law constant (taken as 8.314 [Pa*m^3/(K*mole)]); and T is the absolute temperature [K].

Thereby, the partial differential equation used to analyze a porous medium for one-dimensional gas specific discharge, where the gas is assumed to be a viscous fluid and Darcy's Law is valid, can be expressed in the following form (Oweis and Khera 1998):

$$q_g = -\left(\frac{k_i}{\mu_g}\right)\frac{dP}{dx} \qquad [2.\ 12]$$

where μ_g is the gas viscosity [kg/(m·s)], and $\frac{dP}{dx}$ is the gas pressure gradient [Pa/m].

A two-dimensional partial differential formulation of Richard's equation for hydraulic unsaturated flow in which the main system variables are hydraulic pressure head and moisture content can be presented as (Richards 1931, McDougall 2007):

$$\frac{\partial}{\partial x} K_x(\theta_w)\frac{\partial h_{pw}}{\partial x} + \frac{\partial}{\partial z} K_z(\theta_w)\frac{\partial h_{pw}}{\partial z} + \frac{\partial}{\partial z} K_z(\theta_w) = \frac{\partial \theta_w}{\partial t} \qquad [2.\ 13]$$

where θ_w is the volumetric moisture content [m^3/m^3], K_x and K_z are the horizontal and vertical hydraulic conductivity respectively [m/s], h_{pw} is the hydraulic pressure head [m], x is the distance from the pumping well [m], and z is the thickness [m].

Now applying the conservation of mass to a differential volume using cylindrical coordinates gives the partial differential equation for radial flow toward a well of compressible gas in a porous medium, assumed to be transversely anisotropic and homogeneous (Falta 1996):

$$\left(\frac{\theta_g \mu_g}{P_{atm}}\right)\frac{\partial P^2}{\partial t} = k_{ir}\left[\frac{\partial^2 P^2}{\partial r^2} + \frac{1}{r}\frac{\partial P^2}{\partial r}\right] + k_{iz}\frac{\partial^2 P^2}{\partial z^2} \qquad [2.\ 14]$$

where P_{atm} is the ambient gas pressure [Pa], k_{ir} is the intrinsic permeability in radial direction [m^2], k_{iz} is the intrinsic permeability in vertical direction [m^2], and r is the distance from the pumping well [m].

Equation [2.14] is applicable for gas flow that can't be assumed incompressible, where a constant compressibility factor is $1/P_{atm}$. However, the assumption that the gas is compressible is significant when the imposed vacuum is large (on the order of 0.5[atm]); because in this case assumed incompressibility would lead to significant errors in parameter estimation from gas pump test data (Falta 1996). When intrinsic permeability expressed in terms of relative and effective permeability (equations [2.5] and [2.6]) and both these parameters are substituted in equation [2.14], it can also be presented in the form shown below in equations [2.15] and [2.16]:

$$\left(\theta_g \mu_g\right)\frac{\partial P}{\partial t} = \frac{k_{ar}}{(1-\theta_e)^2\left(1-\theta_e^{\frac{2+\lambda}{\lambda}}\right)}\left[\frac{\partial^2 P^2}{\partial r^2} + \frac{1}{r}\frac{\partial P^2}{\partial r}\right] + \frac{k_{az}}{(1-\theta_e)^2\left(1-\theta_e^{\frac{2+\lambda}{\lambda}}\right)}\frac{\partial^2 P^2}{\partial z^2} \qquad [2.\ 15]$$

and

$$\left(\theta_g \mu_g\right)\frac{\partial P}{\partial t} = \frac{k_{wr}}{\theta_e^{\frac{2+3\lambda}{\lambda}}}\left[\frac{\partial^2 P^2}{\partial r^2} + \frac{1}{r}\frac{\partial P^2}{\partial r}\right] + \frac{k_{wz}}{\theta_e^{\frac{2+3\lambda}{\lambda}}}\frac{\partial^2 P^2}{\partial z^2} \qquad [2.\ 16]$$

2.2.1 Consideration Regarding Conservation of Mass

Bear (1972) describes the equation of mass conservation for *i*-species of a

multicomponent fluid system, which can be expressed in the following form:

$$\frac{\partial \rho_i}{\partial t} + div(\rho_i \cdot q_i) = I_i \qquad [2.\ 17]$$

where ρ_i is the density of the *i*-species [kg/m^3], q_i is the specific discharge of the *i*-species [m/s], and I_i is the rate at which mass of the *i*-species is produced per unit volume of the system by chemical reaction [kg/(m^3*s)].

Later Bear and Bachmat (1990) described mass transport of multiple phases in porous medium but they were looking at a different problem (solutes etc.), rather than a situation in which the porous matrix (i.e. rock or soil) generates pore fluid (i.e. all the formulation to date fundamentally presume conservation of pore fluid mass). The research described in this thesis is focused on the gas flow within MSW, where MSW generates gas due to the biodegradation processes.

2.2.2 The Specifics of Two-Phase Flow in MSW

During the last three decades, numerous models have been developed to describe the generation and transport of gas in MSW and leachate within landfills, the migration of gas and leachate away from landfills, the emission of gases from landfill surfaces, and other flow behaviours in MSW landfills.

It is shown in many works like El-Fadel et al. (1997a), Nastev et al. (2001), White et al. (2004), Kindlein et al. (2006), and McDougall (2007) that waste degradation and landfill emission are strongly related. On the one hand, degradation process depends on environmental conditions such as temperature, pH, moisture content, microbial population, and substrate concentration. On the other hand, gas transport is driven to a certain extent by the production of gas and leachate (Kindlein et al. 2006). Changes over time of hydraulic parameters such as porosity and permeability result from the degradation of waste and the consequent effect on both pore-geometry and pore-size distribution (McDougall et al. 2004, Kindlein et al. 2006, and McDougall 2007), associated with, for example, changes in total volume of waste with decrease in solid voids from degradation (McDougall 2007). There are several factors, presented in

Fig.2.4, that influence landfill dynamics and thereby waste degradation because of their strong interconnection (Kindlein et al. 2006).

The rate of liquid and gas advection and diffusion depends on several parameters, the most important of which are refuse permeability and moisture content since these parameters have a tendency to display substantial variability within the landfill (El-Fadel et al. 1997a). In fact, the numerical modelling of two-phase flow is significantly influenced by the moisture retention properties of the porous medium (landfilled waste). In addition, as emphasized by McDougall (2007) moisture content is one of the main controls on the rate of biodegradation process in landfilled waste; and one that can be controlled most easily during the life of a landfill. The moisture content of the waste fill

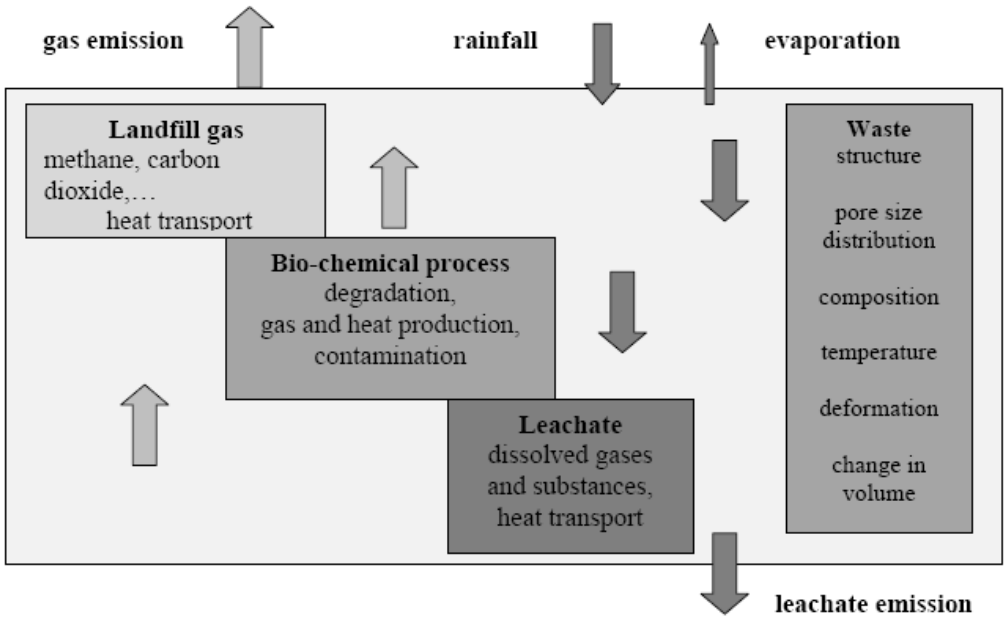

Fig. 2. 4. Factors affecting landfill dynamics (after Kindlein et al. 2006).

depends upon: rainfall, the material, topography and vegetation of the surface cover (controls runoff and evapotranspiration), groundwater intrusion, leachate collection, liner material and efforts at landfill stabilization such as irrigation or leachate recirculation (El-Fadel et al. 1997a and Powrie 2008). Sufficient moisture content is needed to encourage microbial degradation; for example, more than 35% (wet weight basis) is required for rapid methanogenesis (Powrie 2008). However, the high moisture content might increase the leachate production and reduce air permeability as well as

the effectiveness of vapor extraction by restriction the air flow through pores (Collazos et. al. 2002). On the other hand, low moisture content, in combination with high temperature might provoke the risk of underground fire in landfill. Accordingly, the control of moisture content is needed to provide sustainable landfill operations (McDougall 2007 and Powrie 2008).

The volumetric moisture content of MSW can be reduced if necessary through applying a higher stress under conditions of either low or high pore-water pressure. Powrie and Beaven (1999) reported that if applied vertical stress increases about 430[kPa], the volumetric moisture content of household waste at field capacity will increase by about 4% (from 40% to 44%). On the other hand, a sample of recent household waste (DN1), shown in Fig. 2.5, was analyzed to illustrate that the volumetric moisture content can be reduced by approximately 20% if the applied stress is raised by 150[kPa] with low pore-water pressure condition and it can be decreased by about 25% with a high pore-water pressure condition (Hudson et al. 2004). Jain et al. 2005 determined the moisture content for 50 of their samples, taken from a depth of 3 – 18[m], as 23% in average.

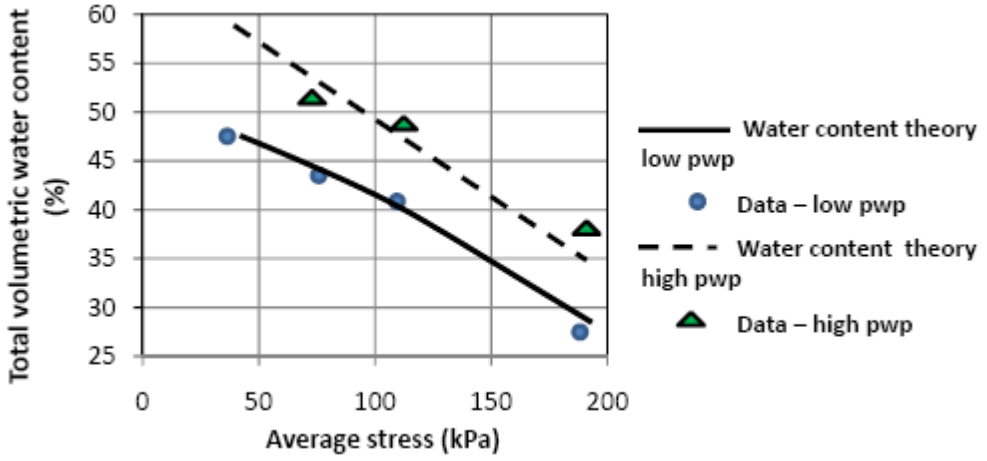

Fig. 2. 5. Theoretical curves of volumetric water content against applied stress in low accumulation conditions (after Hudson et al. 2004).

Zekkos et al. 2006 reported reliable moisture content measurements ranged from about 10 to 50%. Moreover, it was observed that the moisture content of fresh refuse may increase after landfilling through the absorption of water by some components of the waste like paper, cardboard and so on (Powrie and Beaven 1999). Synthesizing results

reported by these various authors, the range of moisture content for MSW landfills can be said to vary from approximately 10% to 52%. However, more research in this area would be beneficial for better understanding the behavior of moisture content of MSW and the effect of compression and degradation on the moisture retention properties.

In addition, the moisture retention properties of the waste affect the total unit weight of MSW landfill, which is an important material property in landfill engineering inasmuch as it is required for variety of engineering analyses such as landfill capacity evaluation, static and dynamic slope stability, pipe crushing, and so on. In fact, there are wide variations in the MSW unit weight's profiles that have been reported in the literature. Moreover, there are main uncertainties regarding the effect of waste degradation on unit weight. Zekkos (2005) reported values of in-situ MSW unit weight at 37 different landfills which varied from 3 to 20[kN/m^3]. It might be reasonably expected for a particular landfill that the unit weight should increase with depth in response to the raise in overburden stress and Zekkos et al. 2006 presented 3 hyperbolic equations fit to field data from the USA; however, these still reflect a significant range of variations. In Fig.2.6, there are data of three different landfills where the near-surface in-situ unit weight depends on waste composition, including moisture content, in addition to compaction effort and the amount of soil cover.

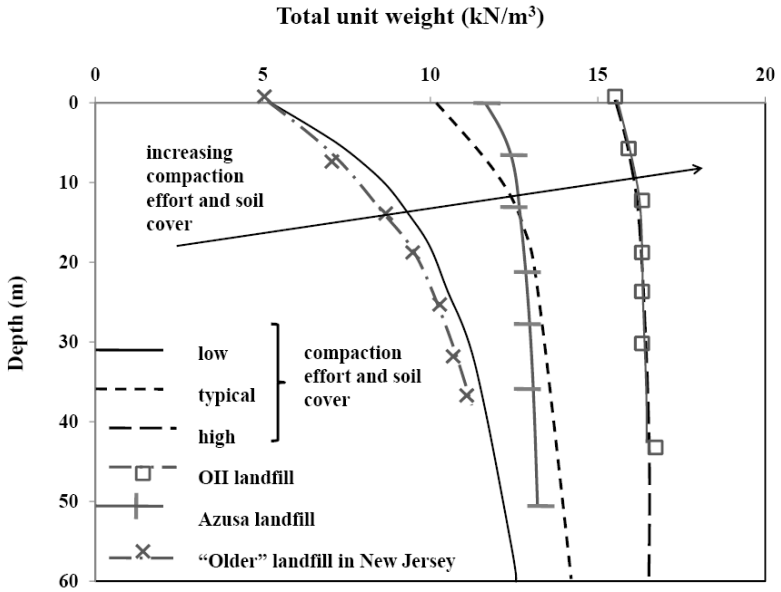

Fig. 2. 6. Unit weight profiles for conventional municipal solid-waste landfills, and the effect of confining stress is represented by depth (after Zekkos et al. 2006)

There have been made some studies that included identification of the saturated hydraulic conductivities for MSW. The range of waste hydraulic conductivity might differ over several orders of magnitude from approximately 10^{-10} to 10^{-3}[m/s] (Table 2.1). The reported hydraulic conductivity values by Jain et. al. (2005) might be suspicious as they were estimated based on an assumed anisotropy ratio of 100. Numerous reported laboratory and field tests have indicated that for landfilled MSW, the anisotropy ratio for hydraulic conductivity is most likely to be around six (Landva et al. 1998, Buchanan and Clark 2001, Kazimoglu et al. 2006, Beaven et al. 2008, and Hudson et al. 2009). Lanvda et al. (1998), Buchanan et al. (2001), Hudson et al. (2009), show that the anisotropy ratio is generally between 1 and 14 (defined as the ratio of horizontal to vertical hydraulic conductivity, K_x/K_z) as presented in Table 2.2. Schmidt (2010) reported the range of unsaturated hydraulic conductivity for the City of Saskatoon Spadina Landfill Site $8.9*10^{-9}$ to $3.5*10^{-4}$[m/s]. Making an assumption about

Table 2. 1. Range of waste hydraulic conductivity in depth profile.

Source	Depth [m]	Sample	Hydraulic conductivity [m/s]
Korfiatis et al. (1984)	~1.5	Saturated conductivity of waste sample, tested in laboratory	$7.94*10^{-5}$ to $1.29*10^{-4}$
Oweis et al. (1990)	~9.2	Saturated horizontal conductivity of MSW, based on constant pumping field test	$1.00*10^{-3}$ to $2.45*10^{-3}$
Bleiker et al. (1995)	0-50	Vertical conductivity of waste sample	$1.00*10^{-10}$ to $5.50*10^{-7}$
Powrie&Beaven (1999)	0-30	Saturated conductivity of household waste at different applied stress, tested in laboratory	$3.72*10^{-8}$ to $1.51*10^{-4}$
Jain et. al. (2005)	3-18	Unsaturated conductivity, calculated based on field data	$2.50*10^{-6}$ to $5.20*10^{-4}$
Schmidt (2010)	0-24	Spadina landfill unsaturated conductivity based on field data.	$8.91*10^{-9}$ to $3.50*10^{-4}$
Fleming (2011)	2-4.9	Spadina landfill conductivity based on field data.	$1.50*10^{-5}$ to $1.70*10^{-3}$
summary range	0-50		$1.00*10^{-10}$ to $1.00*10^{-3}$

volumetric water content and relative permeability of water fluid the intrinsic permeability can be estimated (provided in Chapter 3).

The variety in hydraulic conductivity values results in substantial variation in the distribution of water within an actual landfill which is dependent upon: the character of the leachate, waste disposal operations including shredding and compaction, temperature, and the age of the landfill (Oweis et al. 1990, McCreanor and Reinhart 2000). It has been well established (Powrie et al. 2005, McDougall 2007, and Powrie et al. 2008) that the effective stress is a significant factor controlling the hydraulic conductivity and thereby the intrinsic permeability of municipal solid waste through its impact on waste compression and density. Powrie and Beaven (1999) show if applied stress increased from 40[kPa] to 600[kPa] the hydraulic conductivity fell by approximately four orders of magnitude (Table 2.1). Later, Powrie et al. (2008) show that there is the significant decrease in hydraulic conductivity that could reach up to two orders of magnitude in low pore-water pressure condition (25[kPa]) at both stresses of 40[kPa] and 87[kPa] and a reduction of one order of magnitude for the same stresses at high pore pressure (60[kPa]).

Table 2. 2. Anisotropy of hydraulic conductivity obtained by laboratory testing waste.

Source	Waste type	K_x:K_z ratio
Landva et al. (1998)	Artificial	0.5 to 1.0
	Spruce lake landfill	8
Buchanan and Clark (2001)	Processed waste fines (<38mm)	1.2 to 2.3
Hudson et al. (2009)	20years old waste recovered from a landfill	~ 1 to 14
	Fresh Dano-processed waste	~ 2 to 13

By using the range of hydraulic conductivity in MSW landfills described above, the range of intrinsic permeability can be estimated and thereby the gas permeability assuming a moisture content, either Van Genuchten (1980) or Fredlund and Xing (1994) and Brooks-Corey parameters. Jain et. al. (2005) show that the intrinsic permeability of MSW decreased with increasing waste depth, as well as extracted gas flow rates. Table 2.3 shows the influence of intrinsic permeability of MSW on vapour

flow extraction at different depths of the compacted MSW, where the contaminated soil was assumed to be varied with an anisotropy ratio 1 to 10. They explain this behavior mainly as a result of lower waste porosity resulting from higher overburden pressure and potentially greater moisture content of waste in deeper layers of the landfill.

Table 2. 3. Intrinsic permeability of MSW in radial direction and flow rate due to depth change (after Jain et al. 2005).

Layer	Anisotropy ratio	Gas permeability*		Gas flow rate per unit screen length**
	k_x/k_z	x 10^{-12} m^2		
		Minimum	Maximum	$m^3/(min*m)$
Upper (3 – 6[m] deep)	1	3.30	32.00	0.43
	10	4.10	39.00	
Middle (6-12[m] deep)	1	2.20	14.00	0.22
	10	2.70	17.00	
Deep (12-18[m] deep)	1	0.16	7.00	0.14
	10	0.20	8.60	

*Intrinsic permeability in horizontal direction
**For example, gauge pressure at the well is 10[kN/m^2].

2.3 Available Software Packages for Analysis of Landfill Gas Flow in MSW

Municipal waste typically exhibits two fluid phases (i.e. gas and liquid) and may be idealized as a homogeneous porous medium. A key objective of this study is to investigate the potential to use readily-available software to simulate gas flow in a landfill composed of such a material. The characteristics and behavior of unsaturated flow in MSW landfill were previously monitored through in-situ experiments, at the City of Saskatoon's Spadina Landfill Site. Thus, this research used this existing data to evaluate the relative contribution of gas generation in-situ and gas flow under a pressure gradient within MSW waste fill. The focus of the research was placed on analyzing gas flow within unsaturated MSW landfills. Flow of LFG in landfilled waste is complicated because of heterogeneity and changes of its material with depth as it was summarized above. During operation and aftercare, the landfill waste is exposed to various physical and biochemical effects. As a result, the flow processes of leachate and landfill gas, heat, and mechanical deformation occur (Kindlein et al. 2006, Powrie et al. 2008).

The problem in simulation of flow of gas, liquid or both within MSW is that in reality no model exists that can simulate multiphase flow in MSW landfills with a reasonable degree of scientific certainty. Most analytical and numerical models were independently developed for gas and leachate flow. However, in reality a landfill is a complex interacting multiphase medium, which include gas, liquid, and solid phases. In fact, many previously-developed landfill models primarily focused on the liquid phase and neglect the effect of gas generation and transport. Some models have been reported in the literature to stimulate gas generation, migration, and emissions from landfills. In the case of the solid phase, as previously discussed, additional complexity results from the changes that occur over time as a result of the biodegradation of the organic materials (El-Fadel et al. 1997b, Kindlein et al. 2006, Powrie et al. 2008).

Several software packages have been reported in numerous of papers as suitable for simulation of MSW landfill gas/liquid flow behavior.

HELP (Hydraulic Evaluation of Landfill Performance)

HELP program (version 1) was developed in 1984 to evaluate the performance of proposed landfill designs (Schroeder et al. 1984). The model was subsequently modified and adapted using several programs such as the HSSWDS (Hydrologic Simulation Model for Estimating Percolation at Solid Waste Disposal Sites) model of the U.S. Environmental Protection Agency, the CREAMS (Chemical Runoff and Erosion from Agricultural Management Systems) model, the SWRRB (Simulator for Water Resources in Rural Basins) model, the SNOW-17 routine of the National Weather Service River Forecast System (NWSRFS) Snow Accumulation and Ablation Model, and the WGEN synthetic weather generator, and others. In 1994, HELP version 3 was released (Schroeder et al. 1994) incorporating these features. Gee et al. (1983), Korfiatis et al. (1984), Bleiker et al (1995), and others show the capability of using the HELP program for leachate flow in MSW landfills. On the other hand, it was found that HELP predictions of quantity of leachate are over-estimated (Oweis et al. 1990; Fleenor and King 1995). Oweis et al. (1990) data show that HELP predicts a peak daily leachate head of 34.3 feet while the actual leachate generation should be less than 30 inches per

year. Fleenor and King (1995) show that the model's prediction of HELP program demonstrated over-estimation of flux for arid and semi-arid conditions; moreover, it over-estimated moisture flux at the bottom of the landfill in all cases simulated. It is quite evident that there is some disagreement regarding the pros and cons of using the HELP program. In fact, in most of them there is no information about which version of HELP program the authors used in order to analyze its accuracy. Finally, because the gas flow algorithms incorporated in the HELP program do not reflect a rigorous analysis of two-phase flow under unsaturated conditions, this computer package was not given any further consideration.

MODFLOW

MODFLOW is a three-dimensional finite-difference ground-water flow model, originally created in the beginning of 1980s by U.S. Geological Survey, which has been broadly used and accepted in the world today. MODFLOW is easily used, even with complex hydrological conditions (Osiensky and Williams 1997). MODFLOW has a series of packages that perform specific tasks, some of which are always required for simulation and some are optional. MODFLOW was designed for and is most suitable for describing groundwater flow (Fatta et al. 2002). Several papers have reported errors that affect results of simulation. Osiensky and Williams (1997) show there are several factors that influence model accuracy, for example, selection of the proper combination of matrix solution parameters. Recently, the new version of MODFLOW–2005 (December, 2009) was released, allowing for simulation of water flow across the land surface, within subsurface saturated and unsaturated materials using single- or dual-porosity models (among other new features). Thus MODFLOW-2005 could potentially be applied for simulation of the flow within MSW landfills, but it inherently enforces conservation of mass and thus has no great advantage compared to other available software packages.

AIRFLOW/SVE

AIRFLOW/SVE is a software package that allows simulating vapor flow and multi-component vapor transport in unsaturated heterogeneous soil. Guiguer et al. (1995) have presented the first version of AIRFLOW/SVE. The software helps to visualize the

definition of a problem, specify the necessary problem coefficients, and visualize the performance of the system using user-interactive graphics (Jennings 1997). A feature of this software package is that (unlike MODFLOW or HELP) phase changes from liquid to gas can be modeled; however, the package was not set up to allow for the generation of gas from the solid phase, as occurs in MSW landfills.

TOUGH (Transport of Unsaturated Groundwater and Heat)

The original TOUGH was released in the 1980's (Pruess 1987) and revised as TOUGH2 (Pruess 1991, Pruess et al. 1999). TOUGH2-LGM (Transport of Unsaturated Groundwater and Heat - Landfill Gas Migration) was subsequently developed from TOUGH2 to stimulate landfill gas production and migration processes within and beyond landfill boundaries (Nastev 1998, Nastev et al. 2001, 2003). TOUGH2-LGM is a complex multiphase and multi-component flow system in non-isothermal conditions which for 2-phase flow requires a number of input parameters such as definition of physical properties of the fluids and the flow media, and field monitoring data for model calibration. This software was developed to aid in prediction and understanding of landfill properties and the effect of varying design components. Vigneault et al. (2004) show that TOUGH2-LGM can be used to estimate the radius of influence of a landfill gas recovery well and illustrate that TOUGH2-LGM is able to quite accurately reproduce various types of profiles obtained in the field. However, model results are sensitive to many of the large required number of input parameters and material properties. In addition, in both papers by Nastev et al. (2001, 2003), these authors point out that great attention should be paid to laboratory and in-situ measurements since the simulations require detailed inputs. Ultimately, while such a software package undoubtedly has advantages in research application, the intent of the research work described in this thesis was to provide a basis upon which readily-available and easily-used software might be used to evaluate LFG pumping tests.

GeoStudio

In the most recently available versions of the GeoStudio software suite (2007 and 2010), computer programs SEEP/W and/or AIR/W can be used for simulating one or

two-phase flow in porous media. The properties of the liquid and gas phases can be modified, analyzed, observed, and easily changed. This software package allows for two dimensional or axisymmetric simulations of homogeneous and heterogeneous isotropic or anisotropic media with various boundary conditions and simulations are easily developed and modified (GeoStudio 2010). This software has the further advantage of being widely available throughout the world. There are however, two disadvantages of using this package for MSW landfills. Firstly, and most importantly for the research described in this thesis, fluid flow in AIR/W (or SEEP/W) results solely from a potential gradient and the conservation of mass is inherently assumed; thus the gas generation, which occurs, in a landfill, is implicitly ignored. Secondly (and less critically) a flow-defined boundary condition is not available for the gas phase in AIR/W, requiring the boundary condition to be wellbore pressure rather than extraction flow rate. Thus simulations must be adjusted to match the known flow rates, rather than the simpler and more direct inverse problem. Thus, while the AIR/W program in GeoStudio has the obvious advantages of being widely available and feature-rich, there has not, to date been significant critical and analytical research made using AIR/W for landfill gas flow in MSW.

Despite the disadvantages of using GeoStudio, outlined above, it was chosen for use for this research. Its advantages include the ability to simulate unsaturated porous media with one and/or two-phase flow. Moreover, it was available for this research study, is well documented, easy to use and is broadly available around the world.

HELP was not chosen since the Spadina Landfill consists mostly of unsaturated MSW and the HELP program has shown over-estimation of flux for arid and semi-arid conditions (Oweis et al. 1990; Fleenor and King 1995). MODFLOW was reported by a few papers as discussed above, but was fundamentally designed for describing groundwater flow. Given that the principal objective of the research was to understand what is the effect of gas generation on the determination of MSW properties where the MSW is in unsaturated condition, GeoStudio provided some evident advantages. AIRFLOW/SVE may also be used to simulate vapour flow in unsaturated porous medium but it provides much less visualizing capabilities compared to GeoStudio

where the results can be displayed in listed, tabled, graphical, and video presentations and the models can be easily used in further simulation, transferred, and added the complexity. While the TOUGH program might have had some advantages, it requires detailed inputs (from either laboratory or in-situ measurements) in order to simulate field conditions and model conditions, and such detailed information was simply not available.

Ultimately, the decision was made that if the widely-available and simply-used GeoStudio software could be used to adequately simulate landfill gas pumping tests with a simple correction proposed for the effect of in-situ gas generation, that the benefit in simplicity and ease of use would outweigh any disadvantages inherent in this choice of software.

CHAPTER 3
METHODOLOGY

3.1 Introduction

Two different approaches were selected to analyze the field data mathematically. The theoretical basis was outlined in Chapter 2. This chapter will describe the selected input parameters, the material properties, and the boundary conditions that were used with each of the two approaches: GeoStudio 2007 software and the 1-D finite difference solution (1-D FD solution). The two numerical models were used to evaluate the relationship between wellhead pressure (vacuum), gas pumping flow rate and intrinsic permeability of waste fill using three data-sets from pumping tests carried out at GW01-04, GW02-04, and GW10-07 at the Spadina Landfill in Saskatoon (see Fig. 3.1).

The first modelling tool used was the commercially available GeoStudio 2007 software, which includes AIR/W, a 2-D finite element program for analyzing two-phase saturated/unsaturated flow in porous media. This approach allows for heterogeneity to be incorporated into the model as well as anisotropy and partially-penetrating wells. Because this software was developed for porous flow only, like all other readily available software it does not allow for the non-conservative of fluid mass; i.e. the in-situ generation of landfill gas during the time interval being modelled.

The second approach involved a simple numerical analysis developed specifically for gas flow within a municipal solid waste (MSW) landfill and which included a term for gas generation. This 1-D FD solution was developed for comparison with the results from AIR/W to determine if the total gas generation rate, as measured in the landfill, can be ignored when the intrinsic permeability is estimated. The 1-D FD solution is described below, including details regarding model verification using the data from the GW01-04 well pumping test. The principal input parameters included; the landfill well

geometry, the material properties, and the boundary conditions as described below. Using the 1-D FD solution, as in the case of the AIR/W simulations, the field data from the three test wells (GW01-04, GW02-04, and GW10-07) were analyzed. To better understand the effect of the gas generation and because of the simplicity of using the 1-D FD solution, the field data from one additional well pumping test (GW04-07) were also evaluated. Also, an additional verification of the 1-D FD results was made using SEEP/W for all these test-wells. Thus, the 1-D FD results of the four test wells are accordingly presented in this research, but only when the effect of the gas generation is evaluated. The description and the results for each of the two approaches are presented in Chapter 4, Chapter 5, and the Appendices.

3.2 The City of Saskatoon Spadina Landfill Site

The site of investigation, the City of Saskatoon Spadina Landfill, is located in southwest Saskatoon near the bank of South Saskatchewan River. The landfill has been operated since 1955. The total area of the landfill is about 37.4 [ha], and there is over six million tonnes of waste stored (Saskatoon waste and recycling plan 2007, Fleming 2009). In 2004 and 2007, 10 vertical test wells and 4 gas monitoring probes were installed (Fleming 2009) at locations as shown in Fig. 3.1.

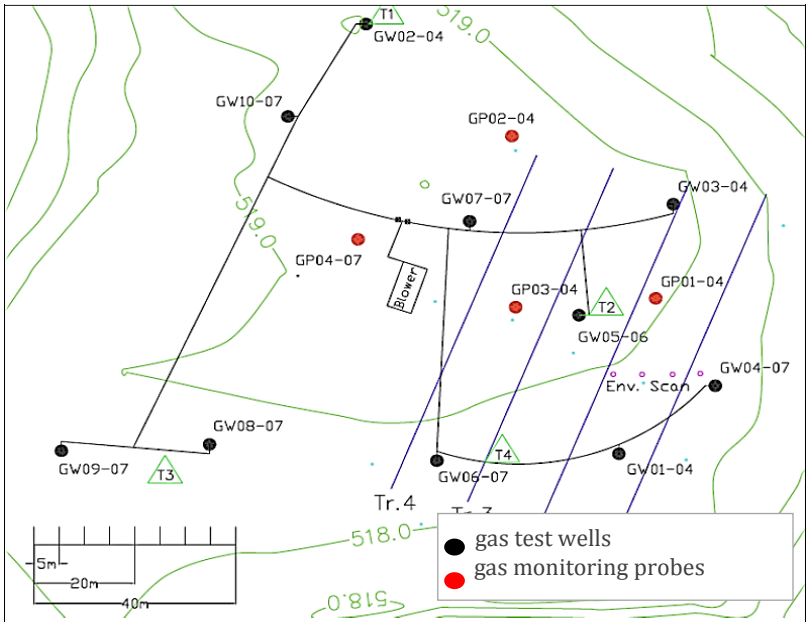

Fig. 3. 1. Test well and monitoring probe locations at the Spadina Landfill Site (after Fleming 2009).

3.3 AIR/W Models

3.3.1. Geometry and Boundary Conditions

As discussed in Chapter 2, the GeoStudio 2007 software suite can be used to model two-phase flow in porous media, including landfilled waste, except that the software inherently ensures conservation of the mass of pore fluid. Thus it cannot account for the in-situ generation of gas during the course of the pumping test. Three transient numerical models were built in AIR/W for use with the three data-sets collected during pumping test of GW01-04, GW02-04, and GW10-07 at the Spadina Landfill (Fleming 2009).

The simulations developed using AIR/W for two-phase flow in a MSW landfill were then used to estimate material properties based on matching the gas flow rates to those that were actually measured in the field for each of the three test-wells.

All three transient two-phase saturated/unsaturated flow models were set up in an axisymmetric view. In order to run a model in AIR/W, its geometry, boundary conditions, and material properties must be set up.

The following geometry parameters, schematically shown in Fig. 3. 2, must be defined:

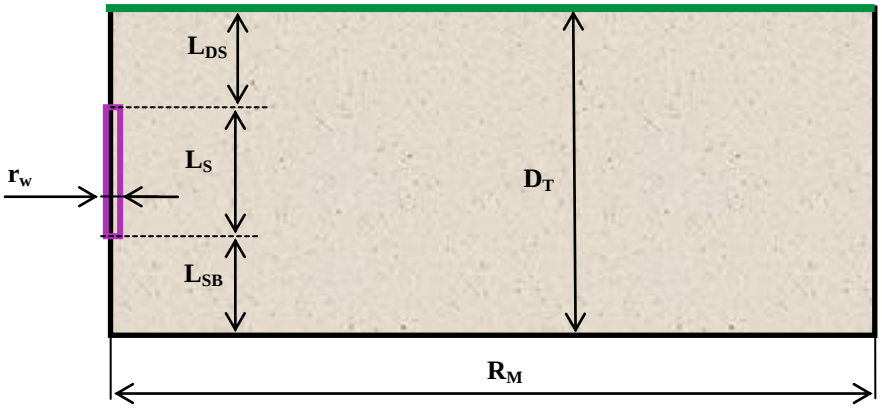

Fig. 3. 2. Schema of an AIR/W model geometry.

- Radius of the model (R_M);
- Total depth of the model (D_T);
- Depth to the screen (L_{DS});

- Screen length (L_S);
- Distance from the screen bottom to the model bottom (L_{SB})
- Well radius (r_w).

A major limitation of coding for the use of AIR/W, for this particular problem, is that the program does not allow for a non-zero gas flow rate to be applied as a boundary condition (GeoStudio, 2010). Therefore, the wellbore gas pressure measured in the field was applied as a boundary condition at the wellbore area and the program used to calculate the resulting gas flow. The following approach was therefore used for all three models. The wellbore gas pressure data that were collected during the field pumping test at each of the wells were used to determine a corresponding continuous pressure function which could be applied in GeoStudio as a wellbore boundary condition. The upper surface boundary condition was set as atmospheric pressure (P_{atm}). No-flow boundaries were applied on all other sides of the models. The typical boundary conditions for all three models are schematically shown in Fig. 3.3. The models' detailed characteristics and their material properties are provided in the Appendices.

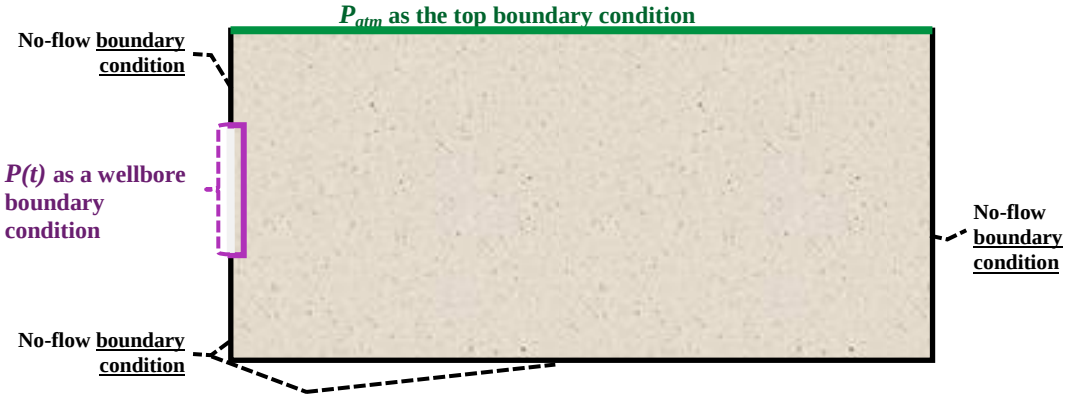

Fig. 3. 3. Boundary conditions for an AIR/W model.

The measurements of wellbore pressure actually made at each of the three test wells during testing were not continuous; rather they were discrete measurements at particular times. In order to apply a transient pressure boundary condition at the wellbore, it was necessary to fit the measured data with a logarithmic expression (Fig. 3.4). Fig. 3.4 (a) shows the wellbore pressure functions that were used as wellbore pressure boundary conditions for the AIR/W simulations.

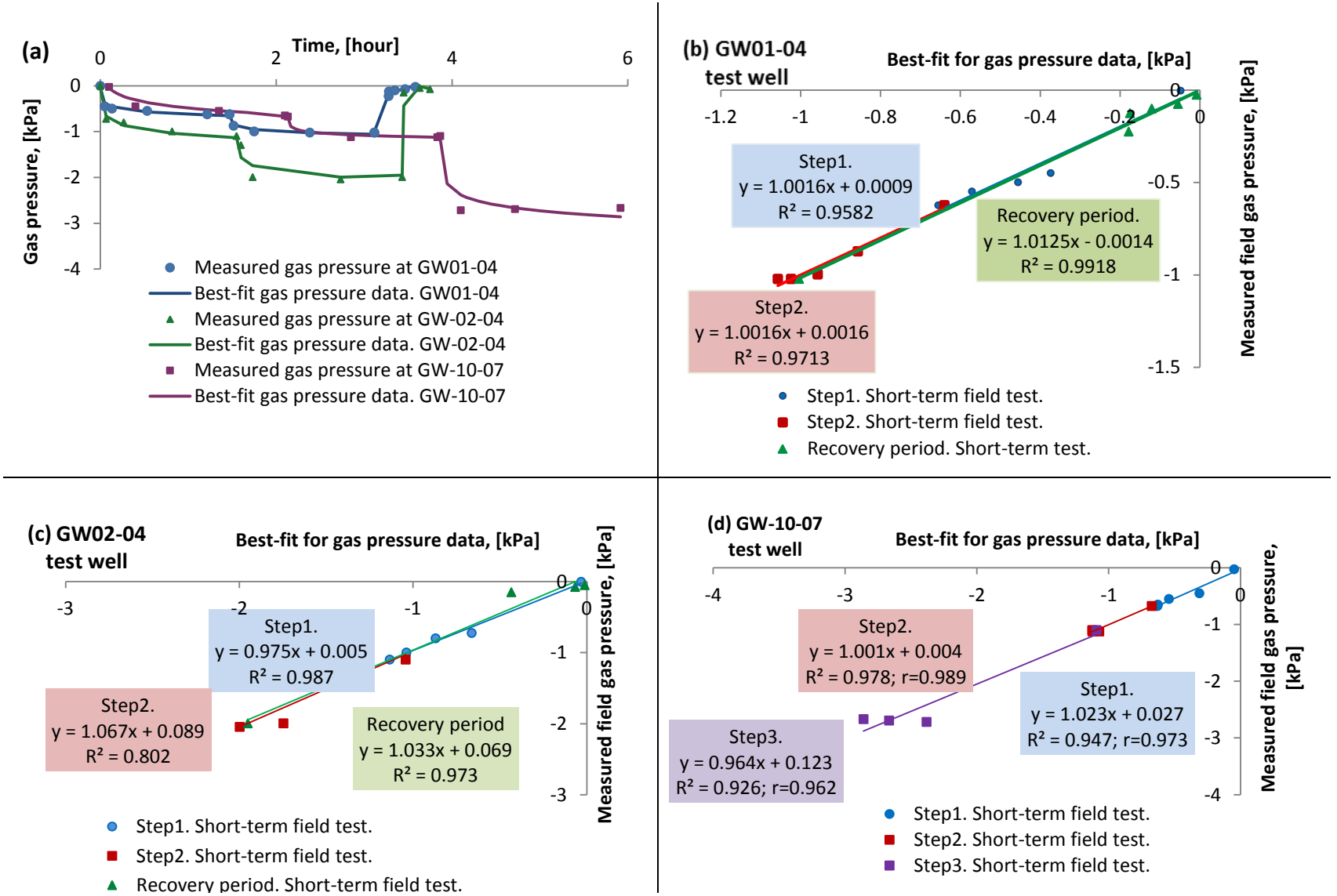

R^2 is the coefficient of determination; r_P is the Pearson's correlation coefficient.

Fig. 3. 4. Gas pressure: (a) Best-fit gas pressure P(t) for the measured gas pressure data during the short-term field test at GW01-04, GW02-04, and GW10-07, which were used as a boundary condition at a wellbore area in the models; (b), (c), and (d) goodness of fitting respectively for GW01-04, GW02-04, and GW10-07.

3.3.2. Material Properties

To simulate the models, the material properties must be assigned as well as other parameters. For a transient, two-phase flow model in AIR/W the following material properties must be defined:

- Material model
- Hydraulic properties:
    - Hydraulic conductivity function (which is the unsaturated hydraulic conductivity function estimated using the Van Genuchten method, with the input saturated hydraulic conductivity corresponding to the trial value of intrinsic permeability);
    - An anisotropy ratio (which is named in AIR/W as a conductivity ratio) and its direction;
    - Volumetric water content function (which is the moisture retention curve or soil-water characteristic curve);
    - Activation PWP (the initial pore-water pressure).
- Air properties:
    - Air conductivity function (which is the unsaturated conductivity function estimated using the Brooks-Corey equation, with the input saturated air conductivity corresponding to the trial value of intrinsic permeability);
    - Activation air pressure (the initial air pressure).

Since landfilled waste is unsaturated, the material was set to "Saturated/Unsaturated" for all three models. Hydraulic properties were assigned based on previous collected data described by Schmidt (2010). Thus the hydraulic conductivity values for the Saskatoon Spadina Waste Landfill Site for all simulations were varied in a range of $8.91*10^{-9}$[m/s] to $3.5*10^{-4}$[m/s], the porosity of MSW was defined as 0.4[m^3/m^3] and activation pore-water pressure as zero[kPa].

Typical relative permeability curves for non-wetting and wetting fluids are shown in Fig. 2.2 (Chapter 2). The relative permeability curves, used in AIR/W, for water (wetting fluid) and air (non-wetting fluid) are shown in Fig. 3.5. The relative permeability of air and water were estimated using Equations [2.3] and [2.4] (Section 2.2) with λ=2.9 (the Brooks-Corey index used in AIR/W).

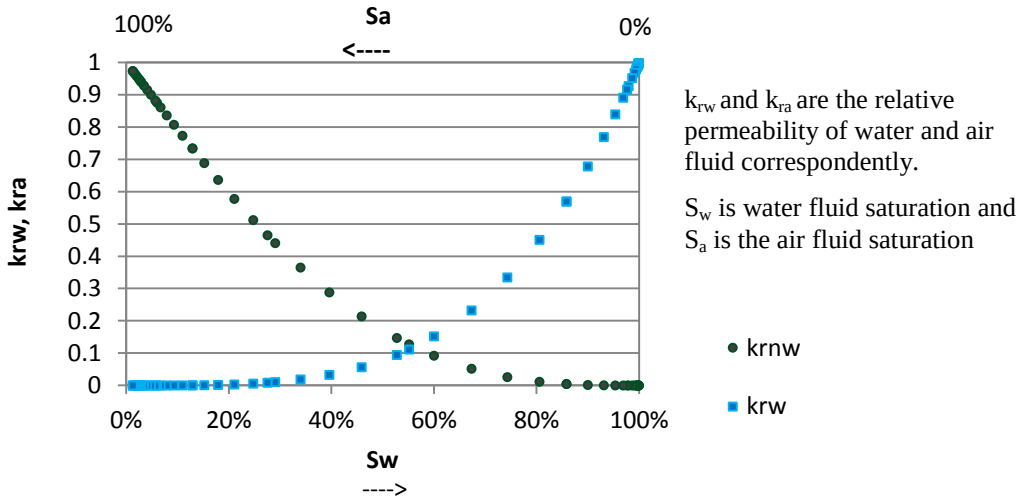

Fig. 3. 5. Relative permeability curves used in AIR/W.

The anisotropy ratio was varied from 1 to 10. The simulations and the results for all models are shown in Chapter 4 and the Appendices. AIR/W allows for heterogeneity to be incorporated into these models as well, but this was not done as there was insufficient data upon which to base such an interpretation. The initial air pressure was taken based on the collected gas pressure data in the field. Fig. 3.6 shows the moisture retention curves that Kazimoglu et al. 2006 determined for waste (i.e. the van-Genuchten parameters α = 1.4 and n=1.6) and the moisture retention curve (i.e. dual porosity) used in AIR/W.

Once the geometry, boundary conditions, and material properties for each case were defined, AIR/W models were run and the results were analyzed. The value for the intrinsic permeability was varied to fit the predicted flow rate for each "step" (constant-rate pumping) with the actually-measured flow rate measured for that particular pumping rate step in the field. A more detailed description of the modelling procedure is provided below and in the Appendices.

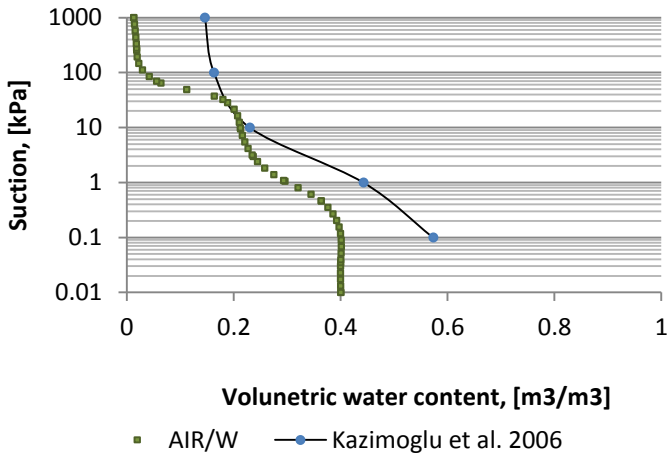

Fig. 3. 6. Moisture retention curves used in AIR/W and Kazimoglu et al. 2006.

3.3.3. Model Validation

A successful model simulation may be defined as achieving numerical convergence within a specified tolerance. According to Geo-Studio (2010), AIR/W solves the finite element equations by computing the air pressure at each node. In order to make the comparison between successive interactions, AIR/W does not use individual nodal matric pressures. Instead, the percent change in the vector norm is used, where a process considers all nodal matric pressures simultaneously.

The vector norm, *N*, is defined in AIR/W by the following equation (Geo-Studio 2010):

$$N = \sqrt{\sum_{i=1}^{n} (U_a - U_w)_i^2} \qquad [3.\ 1]$$

where *N* is the vector norm, *i* is a counter, *n* is the total number of nodes, U_a and U_w are respectively the air and the water pressures, and $(U_a\text{-}U_w)_i$ is the individual nodal matric pressure.

It is recommended that the convergence of the analysis be verified using an alternative method(s) (Barbour and Krahn 2004 and Geo-studio 2010). Convergence for the current study was determined by two different methods for each model. The first method was a vector norm versus iteration graph as provided by AIR/W (Geo-Studio 2010). In AIR/W, the first iteration uses the user-specified initial pressures to define the material

properties. The material properties were updated in subsequent iterations using the computed pressure from the previous iteration and the process continues until either the results satisfy the convergence criteria or the iteration number reaches the maximum number specified (Geo-Studio 2010). The second method was generated by plotting the hydraulic and the air conductivity values calculated by AIR/W against correspondently the input hydraulic and the air conductivity functions of all simulated models materials. Convergence has occurred when the calculated conductivities plot on or near the material ones. Both methods must meet the given tolerance to ensure complete convergence of the problem.

In AIR/W, the hydraulic function is estimated using the methods of either Fredlund and Xing (1994) or Van Genuchten (1980).

The first method (Fredlund and Xing 1994) consists of developing the unsaturated hydraulic conductivity function by integrating along the entire curve of the volumetric water content function. The governing equation, used in this method, is described in the following form (Geo-Studio 2010):

$$K_w^* = K_{sm} \cdot \frac{\sum_{i=j}^{N} \left(\frac{\Theta \cdot (e^y) - \Theta(\Psi^*)}{e^{y_i}} \right) \cdot \Theta' \cdot (e^{y_i})}{\sum_{i=1}^{N} \left(\frac{\Theta \cdot (e^y) - \Theta_S}{e^{y_i}} \right) \cdot \Theta' \cdot (e^{y_i})} \qquad [3.\ 2]$$

where K_w^* is the calculated hydraulic conductivity for a specified water content or negative pore-water pressure [m/s], K_{sm} is the measured saturated conductivity [m/s], Θ_s is the volumetric water content [m^3/m^3], e is the natural number *2.7183*, y is a dummy variable of integration representing the logarithm of negative pore-water pressure, i is the interval between the range of j to N, j is the least negative pore-water pressure to be described by the final function, N is the maximum negative pore-water pressure to be described by the final function, Ψ^* is the suction corresponding to the j^{th} interval, and Θ' is the first derivative of the equation.

The second method (Van Genuchten 1980), describes the hydraulic conductivity as a function of matric suction, proposed in Geo-Studio (2010) as the following closed form

solution:

$$K_w^{**} = K_S \cdot \frac{\left[1-a\cdot\left(\Psi^{(n-1)}\right)\cdot\left(1+\left[a\cdot\left(\Psi^n\right)\right]^{-m}\right)\right]^2}{\left\{\left[\left(1+a\cdot\Psi\right)^n\right]^{\frac{m}{2}}\right\}} \qquad [3.\ 3]$$

where K_s is the saturated hydraulic conductivity [m/s], *a,n,m* are the curve fitting parameters, *n* is equal to *n=1/(1-m)*, and Ψ is the required suction range.

Several simulations were run to check if the choice of method of estimation for hydraulic conductivity affected the obtained results.

No changes in the results for the simulated gas flow rates were found; i.e. the results obtained using the two formulations were the same (Fig. 3.7). The example of the gas

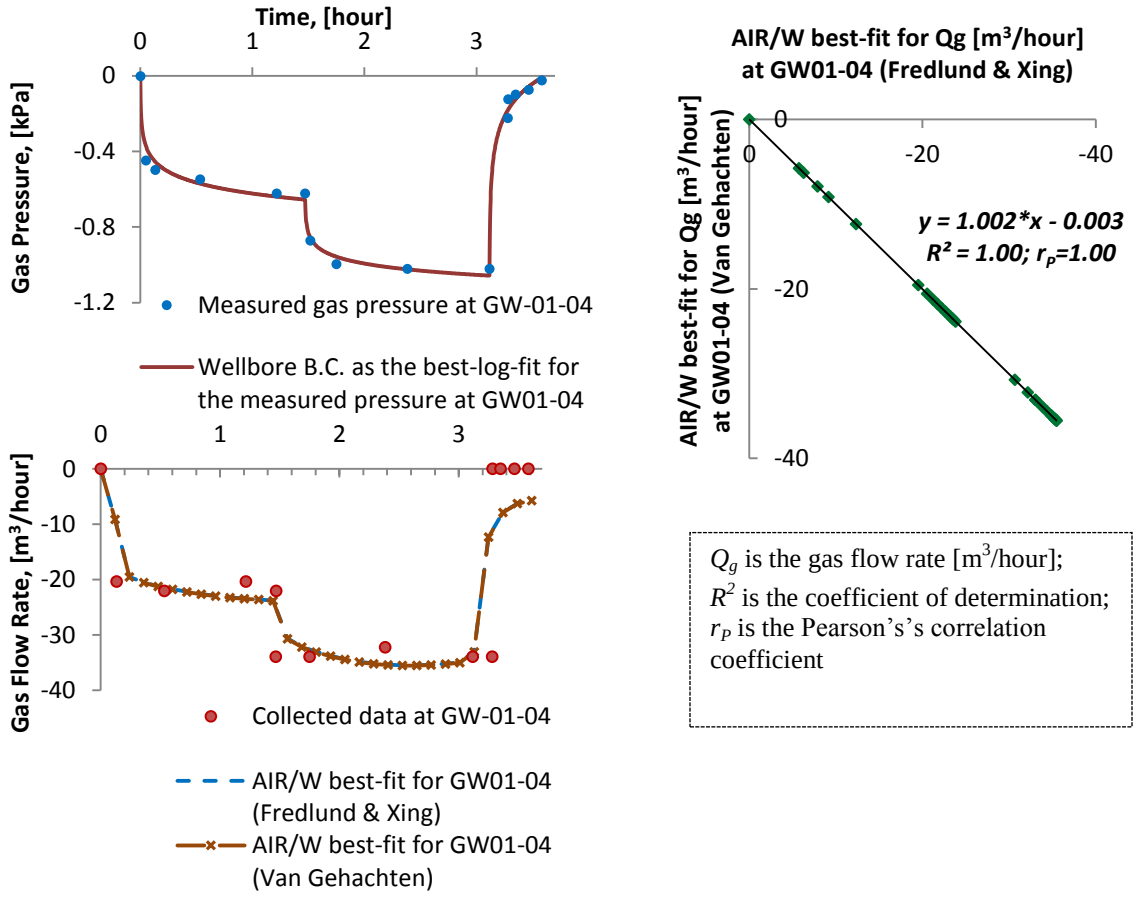

Fig. 3. 7. AIR/W model outputs for two different estimation methods of the input hydraulic conductivity function.

flow outputs, simulated in AIR/W for GW01-04, where either one of the methods were used in estimation of a hydraulic conductivity function shown graphically in Fig. 3.7.

After comparing both methods in numerous simulations and finding that there is no effect of using one method over the other for this particular research, the second estimation method (van Genuchten) was chosen for subsequent analyses as it is widely used and the van Genuchten parameters can easily be compared from material to material (van Genuchten 1980, Kazimoglu et al. 2005, 2006).

3.3.4. Parametric Study of the Effects of Anisotropy and Partial Penetration

The parametric study was designed to evaluate the combined effect of both partial penetration (P/P) and anisotropy on the AIR/W models' results.

Because the gas wells as actually constructed did not incorporate a screened section that encompassed the entire thickness of waste, it is evident that the effect of decreasing the vertical permeability while maintaining the horizontal permeability constant (i.e. to increase the anisotropy) would be to decrease the flow rate to the wellbore, all other things being equal.

Landva et al. (1998), Buchanan and Clark (2001), Kazimoglu et al. (2006), Beaven et al. (2008), and Hudson et al. (2009) reported laboratory and field tests as indicating that for landfilled MSW, the anisotropy ratio for hydraulic conductivity is less than ten, likely to be around six.

Another important consideration in the design of this parametric study was to enable comparison with the 1-D FD solution that was developed to evaluate the effect of simultaneous fluid flow and generation. Because the solution that was developed to evaluate the effect of non-conservation of fluid mass was formulated in one dimension only, the results of that approach (with the generation term set to zero) can be compared directly with the results from AIR/W only if the well is assumed to be fully penetrating and all flow is horizontal.

Accordingly, a parametric study was carried out to evaluate the magnitude of the

combined effect of anisotropy and partial penetration on the value of intrinsic permeability interpreted for each pumping test using AIR/W.

A fully penetrating model can be achieved either by increasing the screen length to the total depth of the model or by keeping the screen length as constant (i.e. as it was constructed in the field) and adjusting the total depth of the model. After comparing both methods in AIR/W simulations for GW01-04 test-well, it was found out that there is no noticeable effect of using one method verses another when estimation of intrinsic permeability takes place at the particular research model. Therefore, the method where the full penetration is reached by adjusting the total depth was chosen for the parametric study.

The anisotropy ratio (k_x/k_z) and the partial penetration (L_S/D_T) for all three models were varied according to the parametric study shown as flow charts in Fig. 3.8 and Fig.3.9.

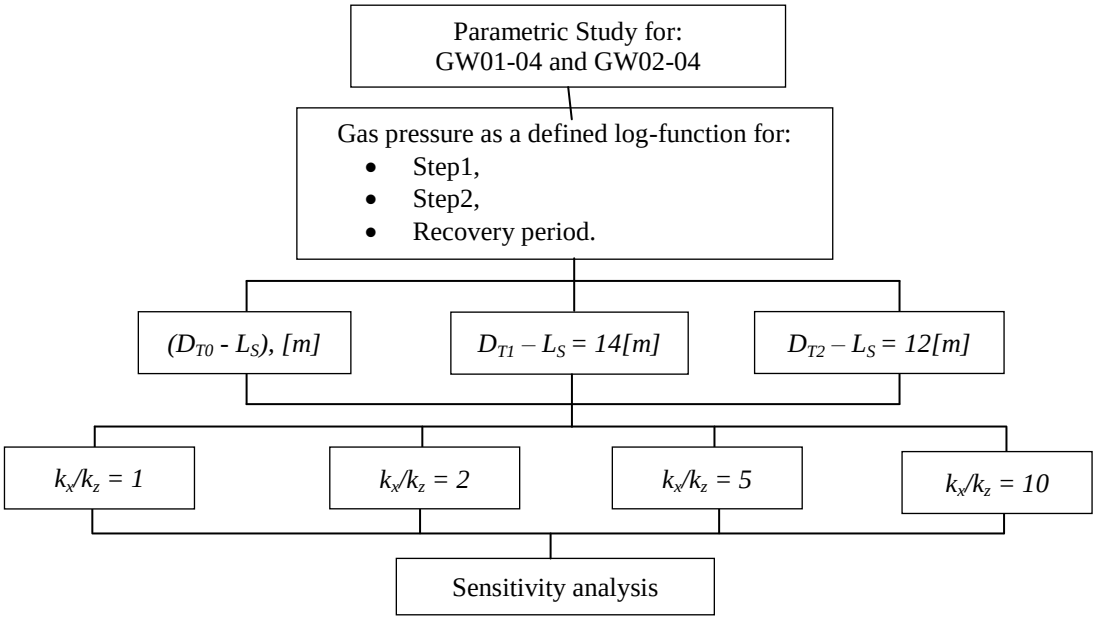

Where $D_{T0}=36[m]$ is the initial depth of the models, D_{T1} is the first cut of a model, where the models were cut at the top by "*x*"[m] depending on the test well, but $D_{T1} - L_S = 14[m]$ for all cases; D_{T2} is the second cut of a model, where the models were cut at the bottom by "*y*"[m] depending on the test well, but $D_{T2} - L_S = 12[m]$ for all cases.

Fig. 3. 8. Parametric Study for GW01-04 and GW02-04 AIR/W models.

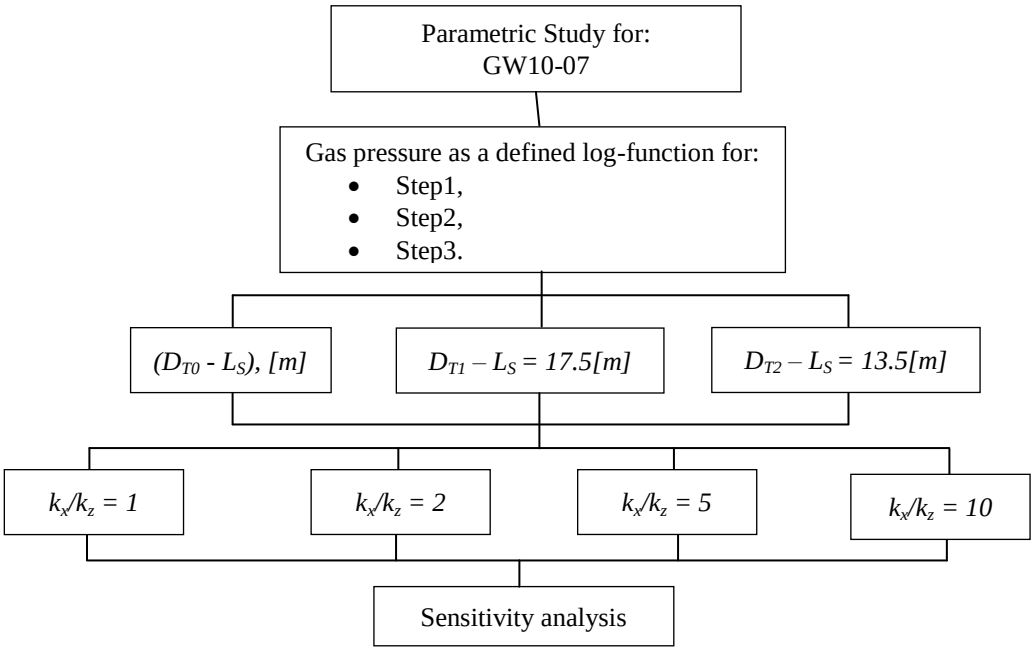

Where $D_{T0}=36[m]$ is the initial depth of the models, D_{T1} is the first cut of a model, where the models were cut at the top and the bottom by "*x=3*"[m] and $D_{T1} - L_S = 17.5[m]$; D_{T2} is the second cut of a model, where the models were cut at the top and the bottom by "*y=2*"[m] and $D_{T2} - L_S = 13.5[m]$.

Fig. 3. 9. Parametric Study for GW10-07 AIR/W model.

A sequential decrease in total depth of the models (D_T) from the initial 36[m] depth was implemented to approach as much as possible the partially penetrating models to the fully penetrating ones. This approach was intended to allow a comparison of the best-fit values from the fully-penetrated AIR/W models with those intrinsic permeability values estimated using the 1-D FD solution in which the anisotropy ratio is implicitly equal to one, the gas generation rate is set to zero ($R_g=0$), and the well is fully-penetrating. This was carried out step by step as following:

- First, the initial 36[m] axisymmetric models ($D_{T0,}$[m] model) were simulated for all anisotropy ratios starting with one (an isotropic material);
- Once all the anisotropy ratios were completed, the model depth was cut by *"x"*-metres, so the difference between the total model depth and the screen length *((D_{T1}-L_S),*[m]) were correspondently equal 14[m] for GW01-04 and GW02-04 and 17.5[m] for GW10-07;

- The D_{T1},[m] models were simulated for all the anisotropy ratios starting with one;
- Finally, the models were again cut by *"y"*-metres, so the difference between the total model depth and the screen length ($(D_{T2}$-$L_S)$,[m]) were correspondently equal 12[m] for GW01-04 and GW02-04 and 13.5[m] for GW10-07; and
- The last anisotropic study for the $D_{T2,}$[m] models was simulated following the same approach with an anisotropy ratio equal to ten.

The difference in cuts for GW01-04, GW02-04, and GW10-07 are based on their actual constructed geometry since their screen lengths (L_S) and depth to the screens (L_{DS}) are variable. However, after the models were cut the final distance from the screen bottom to the model bottom (L_{SB}) is equal 10[m] for all of them and the final depth to the screens (L_{DS}) was equal 2-3.5[m] depending on the models. Fig. 3.10 and Table 3.1 show the AIR/W models geometry used in the parametric study to evaluate the partial penetration and anisotropy effects.

Table 3. 1. Model geometry used to evaluate P/P and anisotropy.

Parameters	GW01-04 geometry		GW02-04 geometry		GW10-07 geometry	
	As actually constructed	AIR/W model	As actually constructed	AIR/W model	As actually constructed	AIR/W model
L_S,*[m]*	18.3		16.8		12.5	
L_{DS},*[m] at* D_{T0}	6.0		9.1		8.5	
D_{T0},*[m]*	36		36		36	
D_{T1},*[m]*	-	32	-	31	-	30
D_{T2},*[m]*	-	30	-	29	-	26
L_S / D_{T0},*[m/m]*	0.50		0.47		0.35	

Once the geometry, boundary conditions, and material properties for each case were defined, the AIR/W models were run and the results were analyzed. Time-steps ranged from 3.47[min] to 8.53[min] based on the time of the short-term test for each model (detailed model description is provided in Appendix B).

The pressure at the monitoring probes, GP01-04 to GP04-07, was measured during the pumping tests in the field (location of which shown in Fig. 3.1). These data were used to verify the models and their outputs. Results of the pressure monitoring data from the

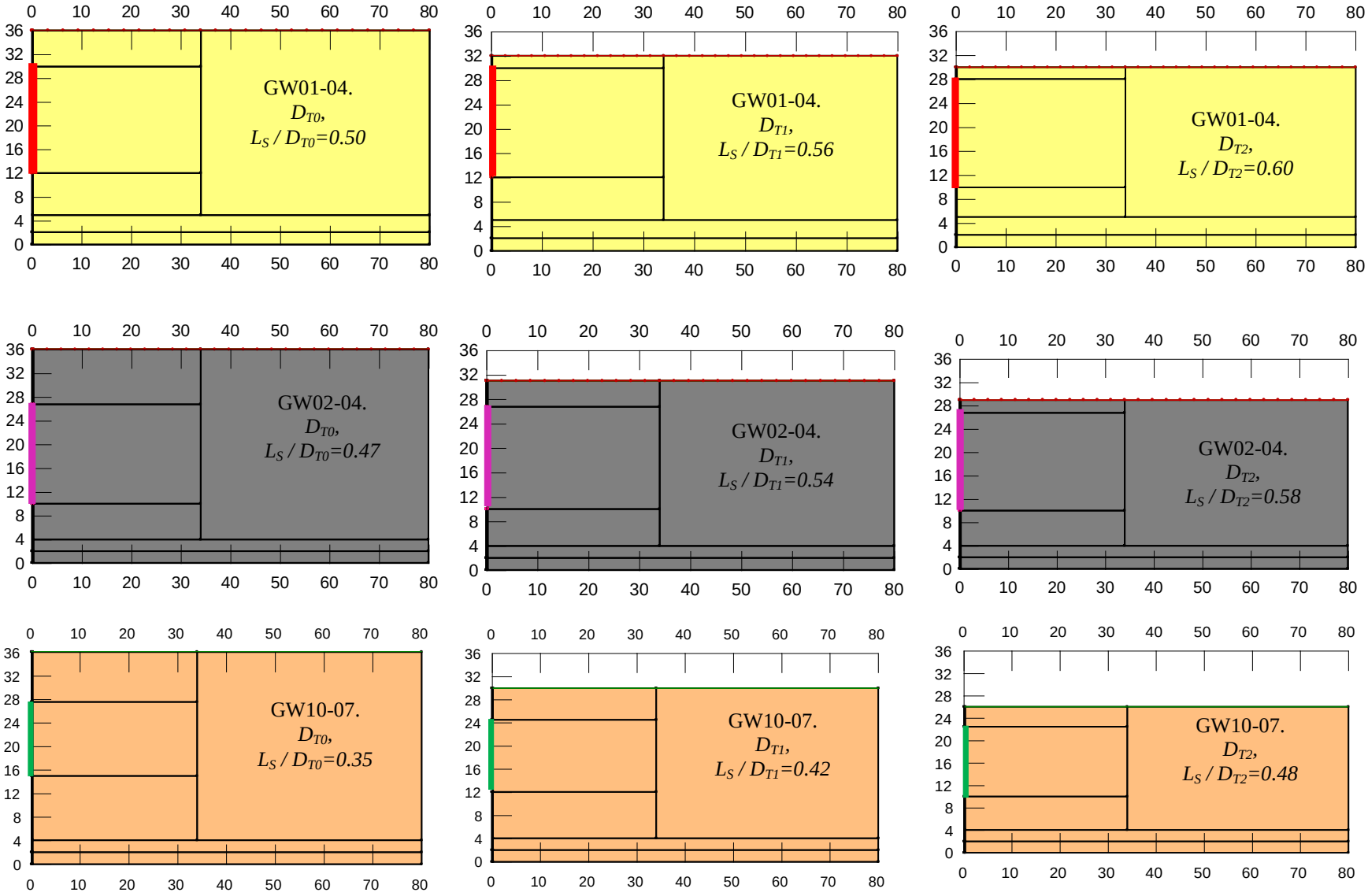

Fig. 3. 10. Changing the total AIR/W models depth (GW01-04, GW02-04, and GW10-07) for investigating P/P and anisotropy.

field show results that are comparable to the models outputs. The AIR/W simulated results for probes GP01-04 and GP02-04 that were carried to verify AIR/W results for GW01-04 test-well as an example provided in Fig.3.11. The purpose of Fig. 3.11 is to calibrate AIR/W outputs (i.e. for GW01-04 test well) rather than to find the best-fit for two monitoring probes, GP01-04 and GP02-04. GP01-04 is located at 34[m] from GW01-04 and GP02-04 at 38[m], where their screens are about at 3-6[m] below the surface.

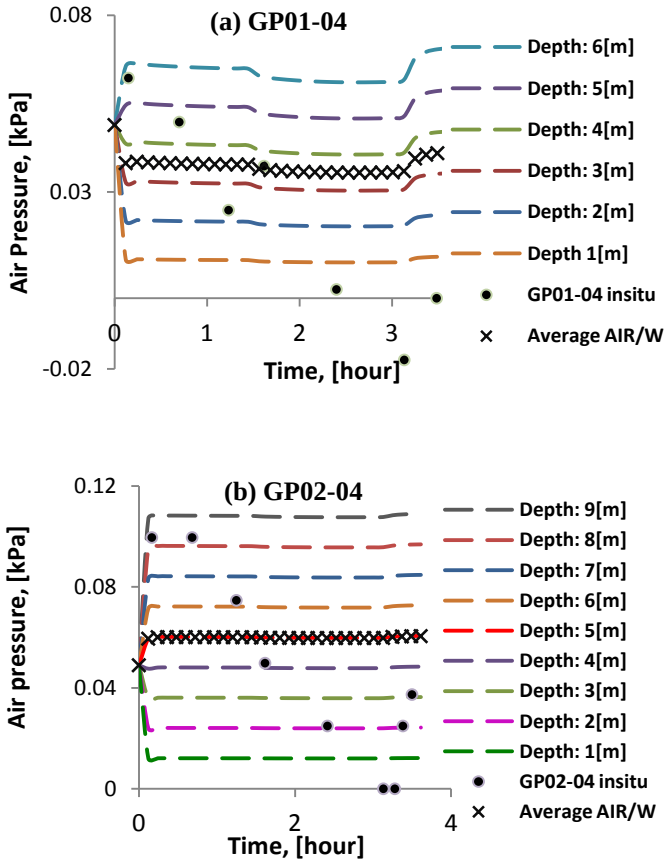

Fig. 3. 11. Monitoring pressure response measured in the field and AIR/W output pressure profile at different depths for (a) GP 01-04 and (b) GP 02-04.

Chapter 4, Chapter 5 and the Appendices provide additional explanation and simulation results for all three models built in AIR/W.

3.3.5. Non-Convergence and Initial Simulations

During the parametric study, issues with respect to convergence criteria and material properties proved to be critical. For example, due to sensitivity of the models to the value of intrinsic permeability, not all cases could be evaluated without changing the intrinsic permeability, and thereby the hydraulic conductivity and the air conductivity values. For example, given a certain value of intrinsic permeability (and thereby the hydraulic and air conductivities) successful simulations could not be completed for all of the anisotropy values. Thus it would be required to change the intrinsic permeability value to estimate the gas flow rate outputs. In other cases, changing the anisotropy or partial penetration would result in changing the water table line and submerging a well: such cases were considered to be failed simulations.

Moreover, changing the material porosity function which was set the same at all of the models would result in non-convergence. However, by doing so, the model is deviating from the real system being modelled based on the landfilled material properties and therefore an acceptable compromise needs to be done to keep the model solvable. On the other hand, by changing the porosity function the models would deviate from the real material porosity that exists in the landfill.

The iteration number in AIR/W was limited to 50 and the difference in results can be also controlled in the convergence data outputs. Thus when an iteration number for each time step reached its maximum the solution might be not found, the simulation was determined as non-convergent. Examples of converged and non-converged simulations are provided in Fig. 3.12. All of the AIR/W results that presented in this work passed the convergence criteria that outlined above, and more detailed information about convergence is provided in Section 3.3.3.

The main objective of the sensitivity study was to define which input parameters affected convergence the most and how to better manage these parameters to improve convergence. The key conclusions have been defined from the sensitivity study and outlined below.

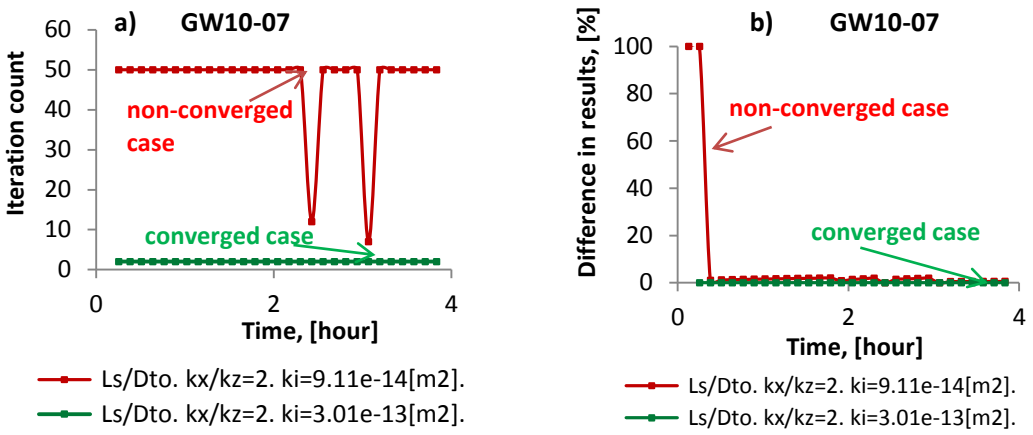

Fig. 3. 12. Convergence in result simulations: the red colour is shown for non-convergence and the green colour is for convergence.

- Numerical models are extremely sensitive to input parameters.
- The material properties assigned to the waste proved to be the most crucial factor governing the fit of the simulation to the measured pressures and flow rates as obtained from the field.
    - The intrinsic permeability range (and thereby the hydraulic and air conductivities) where the models are valid is quite narrow.
    - Decreasing the anisotropy ratio was found to be important since the simulations for all of the three pumping test-wells would fail if the anisotropy ratio, k_x/k_z, was assumed to be higher than 12. On the other hand, this value likely exceeds the typical anisotropy ratio of waste.
- The simulated thickness of waste above and below a well screen can be varied but with the following limitations:
        - At least 2 metres of material above the well screen should be left for GW01-04 and GW02-04 models and 3.5 metres of material for GW10-07,
        - At least 10 metres of material below the well screen should be left for all three models.

3.4 1-D finite difference solution to gas generation and flow in a homogeneous porous medium

3.4.1. Mathematical Approach and Model Geometry with Its Boundary Conditions

Reasonable fit to the field data was possible using AIR/W, and correspondingly estimates could be made for the intrinsic permeability of the waste. However, in reality these values overestimate the true average permeability of the waste because of the effect of the landfill gas generated during the pumping test within the zone of interest (i.e. rather than solely being subject to flow under a pressure gradient as it is inherently assumed in AIR/W or SEEP/W where conservation of mass is assumed). In these tests, it is estimated as discussed in Table 3.2 that the volume of gas generated during the pumping test steps ranged from 20% to 97% of the gas that was actually pumped from the well during the corresponding test step. Thus in order to identify the importance of this gas generation rate, a 1-D finite difference solution ("1-D FD") was developed for gas flow in a porous medium incorporating a gas generation term.

The 1-D FD solution to gas generation and flow in a homogeneous isotropic porous medium ($k_x/k_z=1$), was developed to compare its results with the measured field data and AIR/W built model outputs, and to determine if the total gas generation rate can reasonably be ignored in evaluating the results of landfill gas pumping tests and making estimates of intrinsic permeability.

Both equations, shown in Chapter 2, Equation [2.14], which describes a compressive gas flow in porous media, and Equation [2.17], which describes a multicomponent fluid system in porous media, can be modified and combined to describe a radial symmetric gas flow in a landfill, assumed to be a homogeneous porous medium, where MSW produces the generated gas, and expressed in the following form:

$$\left(\theta_g \cdot \frac{MW}{R \cdot T}\right)\frac{\partial P}{\partial t} + R_g = \frac{k_{ir}}{\mu_g} \cdot \left(\frac{MW}{R \cdot T}\right) \cdot \left[\frac{\partial^2 P^2}{\partial r^2} + \frac{1}{r}\frac{\partial P^2}{\partial r}\right] \qquad [3.4]$$

where R_g is the total gas generation rate [kg/(m^3·s)].

As it is mention in Chapter 2, the gas flow is compressible and it should not be ignored when the applied vacuum is large, more than 0.5[atm]; however, the applied vacuum in the particular MSW landfill was significantly lower, less than 0.05[atm]. Therefore, the gas flow compressibility effect is low in term of incorporating it for mathematical corrections. But Equation [3.4] is applicable for gas flow that can't be assumed incompressible as well, where a constant compressibility factor is $1/P_{atm}$ would need to be incorporated.

Fleming (2009) estimated the methane generation rate at the Spadina Landfill to be 3-5[m^3/Mg/year]. Given that the methane content of the landfill gas is about 55%, the total landfill generation gas is about 5-8[m^3/Mg/year].

In order to ensure consistent in units, the total gas generation rate, R_g, was developed as follows:

$$R_g = \frac{\left[\left(\frac{R_{CH_4}}{f_{CH_4}}\right)\cdot\left(\rho_{waste}^{app}\right)\cdot\rho_g\right]}{(3.1536\cdot 10^7)} \qquad [3.5]$$

where $R_{CH_4}$is the methane generation rate [m^3/Mg/year], f_{CH_4} is the methane fraction, ρ_{waste}^{app} is the apparent density of waste [Mg/m^3], and $3.1536\cdot10^7$ is the coefficient to convert one year to seconds [year/s].

Equation [3.4] can be reorganized and used in calculating pressure profile versus change in radius and time. Mathcad and Excel were used to implement the model. Therefore, the 1-D FD solution to gas generation and flow in a homogeneous, isotropic porous media that is saturated by a single phase can be expressed in the following form:

$$\frac{\partial P}{\partial t} = \frac{\frac{k_{ir}}{\mu_g}\cdot\left(\frac{MW}{R\cdot T}\right)\cdot\left[\frac{\partial^2 P^2}{\partial r^2}+\frac{1\partial P^2}{r\ \partial r}\right]-R_g}{\left(\theta_g\cdot\frac{MW}{R\cdot T}\right)} \qquad [3.6]$$

To run the 1-D FD solution the geometry, material air effective permeability (i.e. the unsaturated air conductivity at the ambient average volumetric water content), and the initial and boundary conditions must be defined. The 1-D FD solution, described by

Equations [3.4] or [3.5], allow solving the problem only for test wells implicitly assumed to be fully penetrating in material assumed to be homogeneous and isotropic.

The following typical geometry parameters must be set up:

- Radius of influence (*ROI*);
- Screen length (L_S);
- Well radius (r_w).

The 1-D FD solution model has the following initial and boundary conditions:

- The initial conditions are: $P(r,0) = P_{atm}$ at any distances from a well (r);
- Boundary conditions:
    - $\frac{\partial P}{\partial r} = 0$ for any time (t) at distance R(radius of influence);
    - Either: a defined gas pumping flow rate ($Q_g(t)$) at the well or a measured gas pressure during a short-term field test at the well ($P(t)$).

The main material properties and the data gathered in the field, listed below, were set up and calculated based on the previous collected data described in the following papers: Schmidt (2010) and Fleming (2009):

- Total gas generation rate in the landfill (R_g);
- Apparent density of waste (ρ_{waste}^{app});
- Molecular weight of gas (MW);
- Gas-filled porosity (θ_g);
- Gas pumping flow rate (Q_g);
- Temperature (T);
- Intrinsic permeability (k_i).

Fig. 3.13 illustrates the typical geometry and the initial and boundary conditions for the 1-D FD solution. Fig. 3.13 shows that a test well is fully penetrating thereby the screen length is equal to the total thickness of the 1-D FD solution model ($L_S / D_T = 1$).

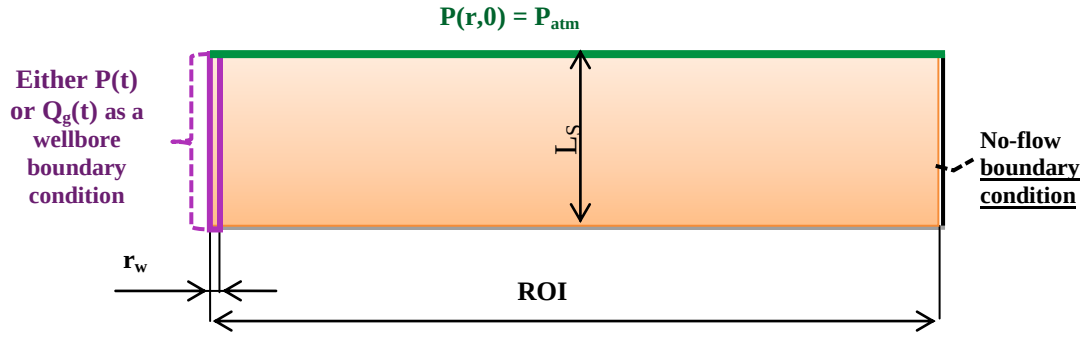

Fig. 3. 13. Typical geometry and its initial and boundary conditions for a 1-D FD solution.

The volume of waste that affected the measured data by producing landfill gas during the short-term pumping test and can be expressed in the following form:

$$V_{waste} = \pi \cdot (ROI)^2 \cdot D_{waste} - V_{screen} \qquad [3.\ 7]$$

where V_{waste} is the waste volume [m^3], D_{waste} is the entire depth of waste [m], and V_{screen} is the screen volume [m^3].Knowing the waste volume the volume of generated gas per hour can be calculated as:

$$£_{Rg} = (R_g^{**}) \cdot V_{waste} \qquad [3.\ 8]$$

where $£_{Rg}$ is the volume of gas generated per unit time [m^3/hour] and R_g^{**} is the total gas generation rate [m^3/m^3/hour].

To convert the total gas generation rate in units [m^3/m^3/hour] the following equation was used:

$$R_g^{**} = \frac{R_g}{\rho_g} \cdot 3600 \qquad [3.\ 9]$$

where *3600* is the coefficient to convert 1[s^{-1}] to an hour [s/hour].

Table 3.2 provides calculations for the four test wells showing that the estimated volume of gas generation during each pumping test ranges from 20% to 97% of the volume of gas actually pumped. Volume of gas generation did not come from storage rather than MSW.

Table 3. 2. Gas flow rate and generated gas flow within volume of influence*.

Test well data	Gas flow rate and generated gas flow, [m^3/hour]		
GW01-04	Step1	Step2	Recovery period
Q_g, [m^3/hour]	21.1	33.6	0
$£_{Rg}$, [m^3/hour]	20.5	29.5	29.5
$£_{Rg}/Q_g$, [%]	97%	88%	-
ROI, [m]	25	30	30
$V_{waste,}$ [m^3]	35931	51742	51742
GW02-04	Step1	Step2	Recovery period
Q_g, [m^3/hour]	19.4	35.3	0
$£_{Rg}$, [m^3/hour]	18.5	26.6	26.6
$£_{Rg}/Q_g$, [%]	95%	75%	-
ROI, [m]	25	30	30
$V_{waste,}$ [m^3]	32937	47430	47430
GW04-07	Step1	Step2	Step3
Q_g, [m^3/hour]	20	33	50.7
$£_{Rg}$, [m^3/hour]	5.2	7.2	10.1
$£_{Rg}/Q_g$, [%]	26%	22%	20%
ROI, [m]	23	27	32
$V_{waste,}$ [m^3]	9124	12573	17661
GW10-07	Step1	Step2	Step3
Q_g, [m^3/hour]	16.1	24.9	51
$£_{Rg}$, [m^3/hour]	12.7	19.8	27
$£_{Rg}/Q_g$, [%]	79%	80%	53%
ROI, [m]	24	30	35
$V_{waste,}$ [m^3]	22628	35357	48124

- $£_{Rg}$ was calculated based that R_{CH_4} = 4[m^3/Mg/year]

The example of ROI effect on intrinsic permeability estimates using the 1-D FD solution is shown in Fig. 3. 14, which was defined for the first drawdown pumping step at GW01-04 test-well (i.e. R_{CH4}=5[m^3/Mg/year]). In 1-D FD for the 1st pumping step, GW01-04, ROI was set as 25[m] (Table D.2). The ROI=25[m] is in agreement with the previous reported values by Fleming 2009 (Table A.3).

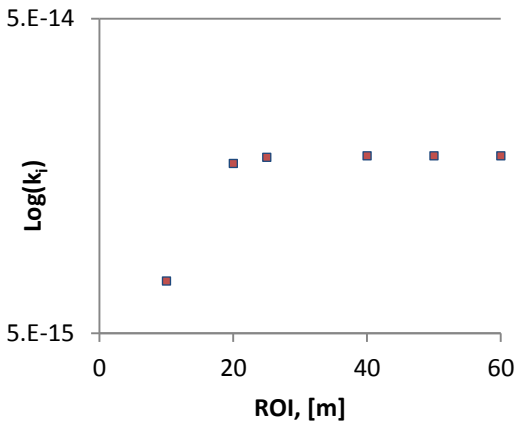

Fig. 3. 14. Log(k_i) versus radius of influence relationship for GW01-04 test-well.

3.4.2. Model Validation

One aspect of validation of the 1-D FD solution, involved comparing the two approaches to the wellbore boundary condition, to confirm that the same intrinsic permeability value can be reached with the same input parameters for the same test well.

Scenario I (1st approach): wellbore boundary condition is the defined gas pumping flow rate at GW01-04 well and the 1-D FD solution output was fitted with the measured gas pressure at well GW01-04.

Scenario II (2nd approach): wellbore boundary condition is the measured gas pressure during the short-term field test at GW01-04 well and the 1-D FD solution output was fitted with the measured gas flow rate at well GW01-04.

The main input parameters and the boundary conditions for the 1-D FD solution, used with the GW01-04 data-set, are provided in Table 3.3.

The 1-D FD solution for GW01-04 well for both scenarios was run for two drawdown steps and recovery period and its results are graphically shown in Fig. 3.15. The 1-D FD solution results for both Scenarios I and II, shown in Fig. 3.15, were obtained with the same geometric mean value of air effective permeability, which is $k_{ir}=5.8*10^{-15}[m^2]$.

Table 3. 3. Input parameters and boundary conditions for the 1-D FD solution (GW01-04).

Input parameters		1st step	2nd step	Recovery
Total gas generation rate, [kg/(m^3*s)]	R_g		1.76*10^{-7}	
Methane fraction, [%]	f_{CH4}		57	
Gas-filled porosity, [m^3/m^3]	θ_g		0.4	
Apparent waste density, [kg/m^3]	ρ_{APP}		700	
Temperature, [K]	T		40	
Time, [s]	τ	5292	5928	1680
Radius of influence, [m]	ROI	25	30	30
Screen length, [m]	L_S		18.3	
Well radius, [m]	r_w		0.1	
Scenario I. Wellbore boundary condition is the defined gas pumping flow rate.				
Pumping gas flow rate [m^3/hour]	$Q_g(t)$	20	34	0
Scenario II. Wellbore boundary condition is the fitted field gas pressure.				
Fitted field gas pressure, [Pa]	$P(t)$	$P(t)=a*Ln(t)+\beta$ *α and β are the fitting coefficient and vary for each step.*		

Several conclusions that were apparent after the simulations of both scenarios were completed.

- First of all, no difference in evaluating the air permeability was found by using Scenario I versus Scenario II in the 1-D FD solution.
- Since no difference between the two scenarios was found, Scenario I, the defined gas flow rate as the wellbore boundary conditions, was used in all future 1-D FD solution simulations.
- Finally, the results of 1-D FD solution can be compared with AIR/W results, which were set as for homogeneous isotropic case ($k_x/k_z=1$), where the maximum available fully-penetration in AIR/W models were achieved (L_S/D_{T2}), and the gas generation rate is set up to zero (R_g=0).

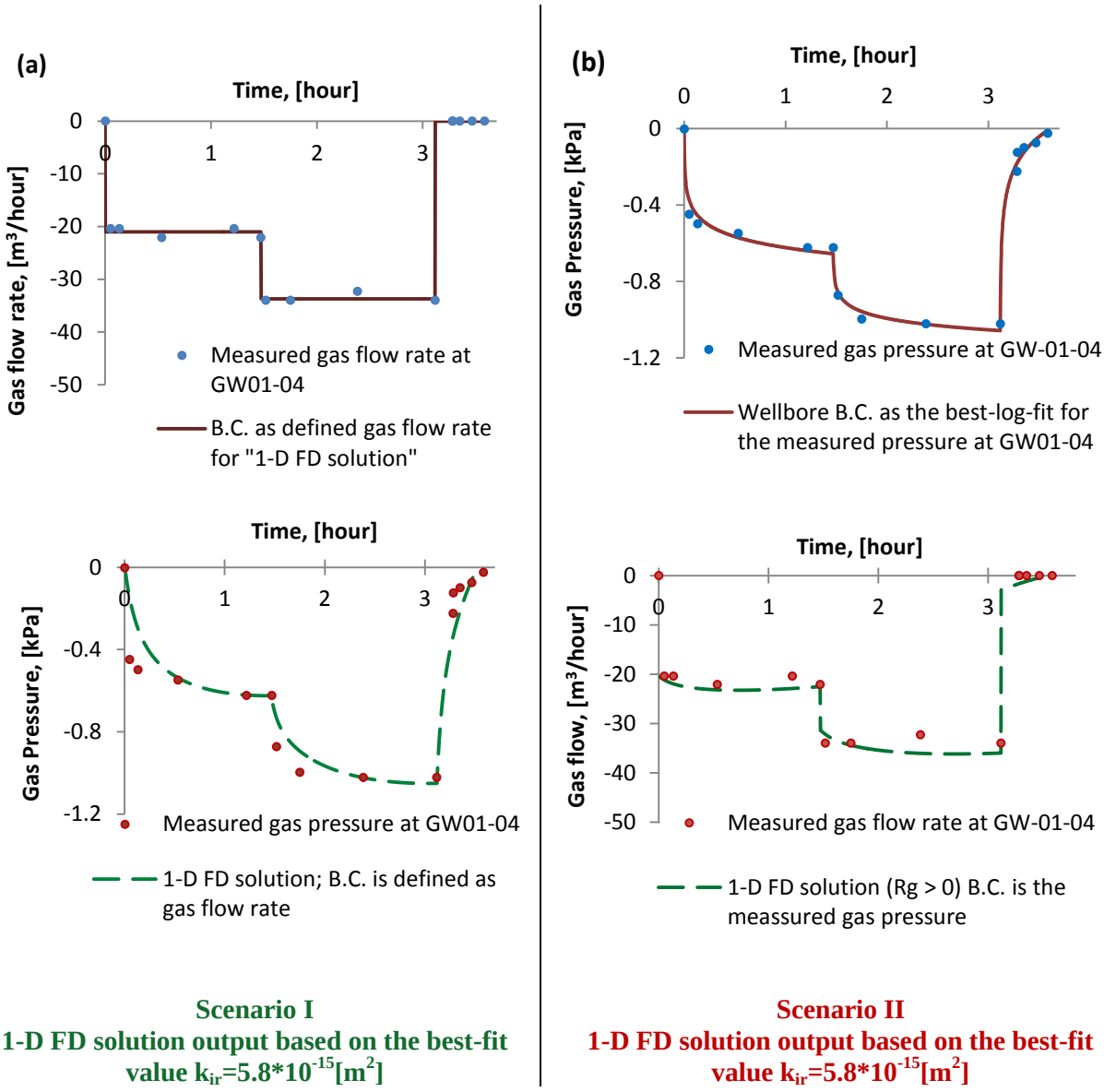

Scenario I
1-D FD solution output based on the best-fit value $k_{ir}=5.8*10^{-15}[m^2]$

Scenario II
1-D FD solution output based on the best-fit value $k_{ir}=5.8*10^{-15}[m^2]$

Fig. 3. 15. The 1-D FD solution: (a) Scenario I: boundary condition as the defined gas flow rate at GW-01-04 and the 1-D FD solution; (b) Scenario II: boundary condition as the measured gas pressure at the same well (GW-01-04) and the 1-D FD solution output.

To compare the results that were estimated using 1-D FD with AIR/W, the intrinsic permeability needed to be determined using equation [2.5] where the air effective permeability is the best-fit results of air permeability in 1-D FD and the relative permeability of air was estimated as 0.15 (k_{ra}=0.15 see Fig. 3.5).

Another aspect of 1-D FD model verification involved simulations in SEEP/W (i.e. 1-D axisymmetric). To verify if the same results can be reached using SEEP/W while the

models are set-up with the same geometry and input parameters for the same test well. Thereby, a finite element simulation was carried out using SEEP/W, where the geometry, the material properties, the initial and boundary conditions were defined exactly the same as in the 1-D FD solution (with $R_g=0$). The SEEP/W models were run using the first step pumping rates for each test-well; and their results graphically shown in Fig. 3.16. Both SEEP/W and 1-D FD results shown in Fig. 3.16, were obtained using the same values of intrinsic permeability respectively for each of the four test-wells; both of them showed good fit with field data. Therefore, SEEP/W can be alternatively used for simulating gas flow within unsaturated MSW. Additional information regarding these results is provided in Appendix D.

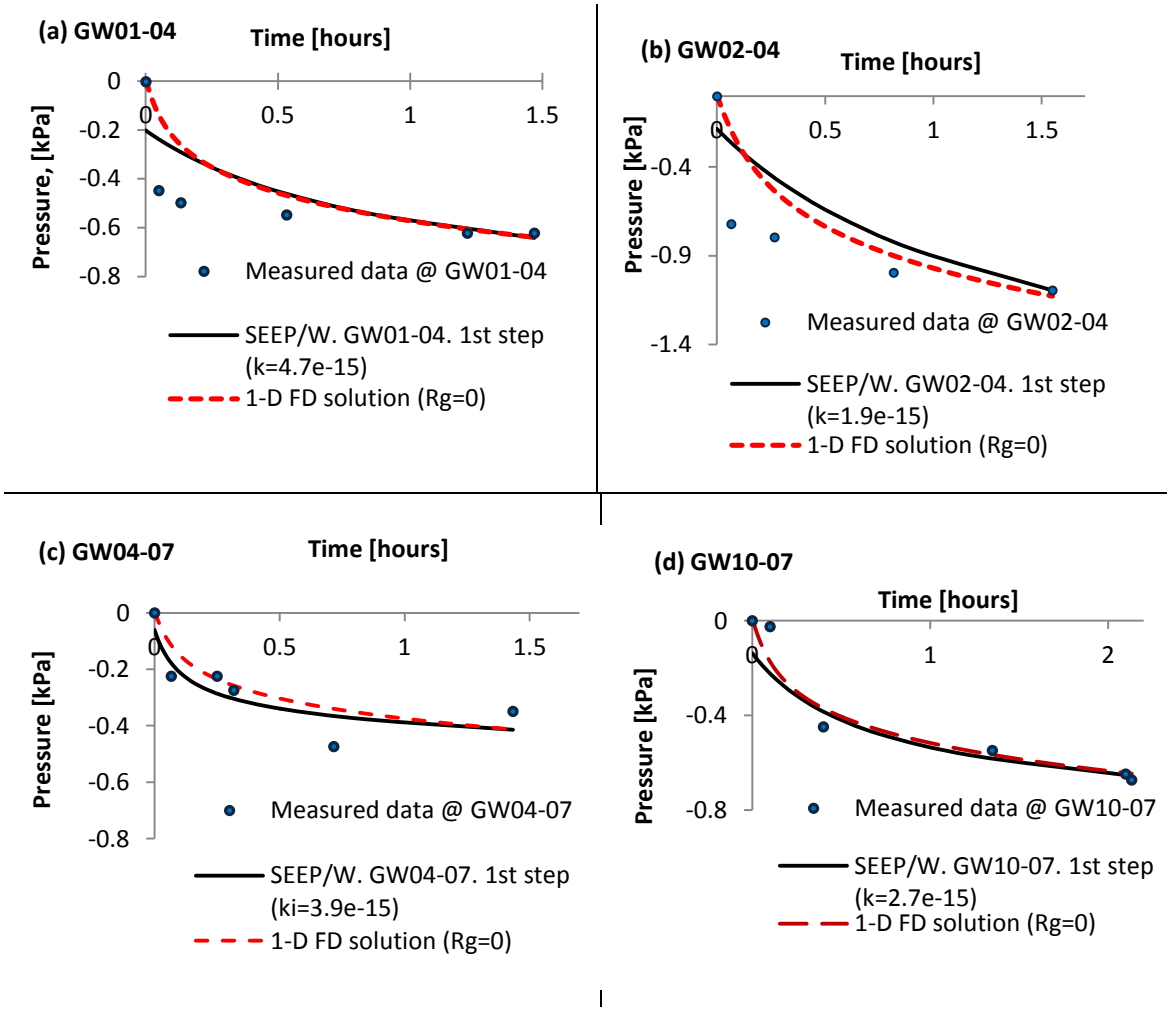

Fig. 3. 16. Measured gas pressure during the short-term field test at all four test wells and SEEP/W and 1-D FD solution outputs based on the same best-fit values of intrinsic permeability respectively.

3.4.3. Parametric Study of the Effect of Gas Generation

The parametric study was carried out to evaluate the extent to the gas generated within the landfill might affect the results. In order to evaluate the gas generation impact, the 1-D FD solution were run for the four test wells and the results (GW01-04, GW02-04, GW04-07, and GW10-07) are presented and discussed in Chapter 4, Chapter 5, and the Appendices. The parametric study for all four wells is shown as flow charts in Fig. 3.17 and Fig. 3.18.

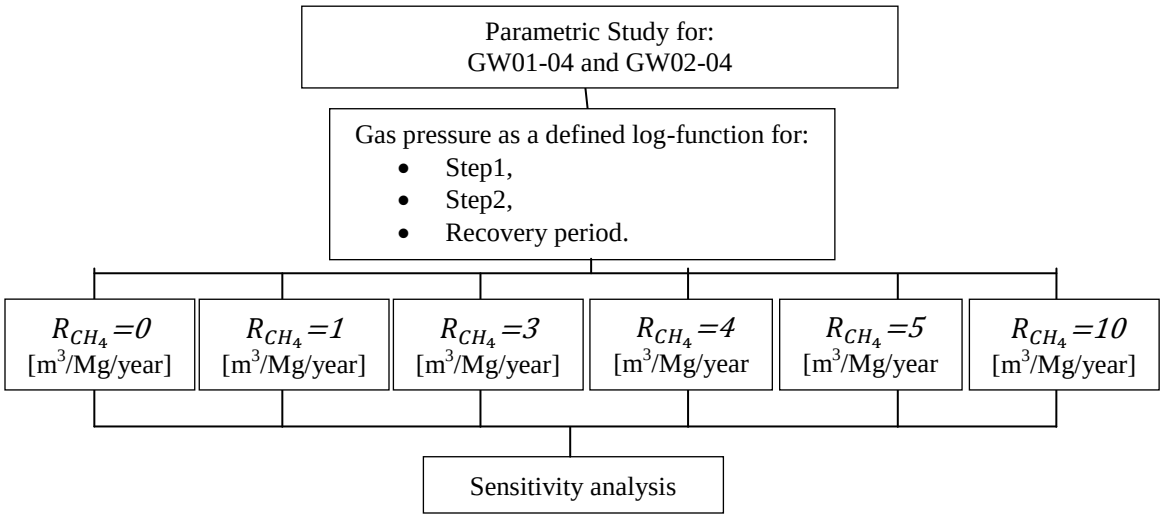

Fig. 3. 17. Parametric Study for 1-D FD solution for GW01-04 and GW02-04 wells.

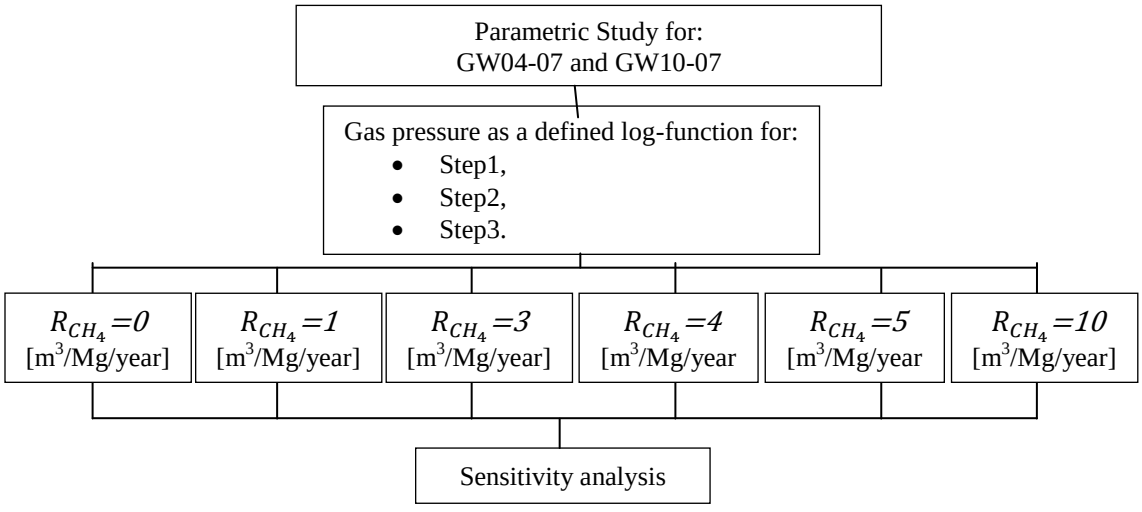

Fig. 3. 18. Parametric Study for 1-D FD solution for GW04-07 and GW10-07 wells.

As mentioned above, Fleming (2009) reported that the in-situ methane generation rate at the Spadina Landfill is 3-5[m^3/Mg/year]. Laboratory tests had indicated a stable methane generation rate of 10 to 20 [m^3/Mg/year], although it was expected that the gas generation rates determined from the laboratory tests may have overestimated the average in-situ rate as a result of more uniform moisture conditions etc. Accordingly, given this uncertainty, the methane generation rate (R_{CH4}) used in evaluation of the 1-D FD solution was varied from 0 to 10[m^3/Mg/year]. The methane fraction in R_g ranged from 50% to 60% depending on test well, to reflect actual field measurements.

The only difference in Fig. 3.17 and Fig. 3.18, which schematically describe the parametric study of the generated gas effect, is that:

- for the test wells GW01-04 and GW02-04 the short-term test data included two pumping steps and the recovery period;
- and for the test wells GW04-07 and GW10-07 the short-term test data included three pumping steps;
- In order to evaluate R_g, all "1-D FD" models were initially simulated for the gas generation rate set as zero;
- When R_g=0[m^3/Mg/year], there was no effect of gas generation included and results reflect fluid (gas) flow to a well in a homogeneous isotropic porous-media;
- Once all 1-D FD solution models for the case "R_{CH_4}=0[m^3/Mg/year]" were completed, systematic incremental changes were made for each of the 1-D FD solutions set up for each of the pumping tests respectively; and
- The value of R_g was progressively increased to approach the maximum predicted value of "R_{CH_4}=10[m^3/Mg/year]".

The results of the generation gas impact in evaluation of the intrinsic permeability for all four wells can be found in Chapter 4 and the Appendices.

CHAPTER 4
PRESENTATION OF RESULTS, ANALYSIS, AND DISCUSSION

4.1. Introduction

Chapter 4 presents the results of the modelling studies described in Chapter 3. Two approaches were taken to evaluate transient gas flow in two (axisymmetric) dimensions. First, saturated/unsaturated two-phase flow was studied using the finite element (FEA) computer program AIR/W (GeoStudio 2010). A parametric study was first carried out using AIR/W to evaluate the significance of partial penetration of the gas wells and anisotropy of the permeability of the landfilled waste. More than 300 simulations were completed in which the flow rate, well screen length, and material anisotropy were varied for three different pumped wells. The relevant simulations and the results are presented in this chapter and in the Appendices.

The second approach used a 1-D transient numerical solution which incorporated gas generation in-situ as well as radial gas flow. To verify the 1-D FD solution SEEP/W (GeoStudio 2010) was used as one aspect of validation. Using SEEP/W to model gas flow requires one to make an assumption that the porous medium is saturated by that single phase (i.e. the gas) and thus the permeability function is really just a single saturated value; thereby it is really just like the 1-D FD model (where $R_g=0$). In the 1-D FD solution, six different assumed values for the gas generation rate were used along with three step pumping rates for GW01-04 and GW02-04 test-wells and four step pumping rates for GW04-07 and GW10-07 test-wells for a total of 84 simulations.

The 1-D FD solution was used for two purposes. The principal purpose was to evaluate the degree to which accounting for the gas generation actually occurring in-situ would influence the best-fit value of intrinsic permeability determined for a particular pumping test. In addition, the 1-D FD solution was used as an alternative numerical solution and

was used to compare and help corroborate the results obtained from the AIR/W finite element method. The effect of in-situ gas generation was evaluated using the 1-D FD solution where the field data from the test-wells were analyzed. The description and the results for each of the four test-wells (GW01-04, GW02-04, GW04-07, and GW10-07) are presented in this chapter, Chapter 5, and the Appendices.

4.2. AIR/W Parametric Study of the Effects of Anisotropy and Partial Penetration

Transient numerical models were developed using AIR/W to stimulate stepped-rate pumping tests which had been carried out for the following test-wells: GW01-04, GW02-04, and GW10-07. Numerous simulations for these three data sets were carried out and results are shown in this chapter and in the Appendices.

Chapter 3 discussed the geometry and the boundary conditions of the models and the parametric study intended to evaluate the effect of partial penetration and anisotropy.

The intrinsic permeability values determined using AIR/W for the best-fit gas flow outputs were defined for each pumping test-wells subsequently the anisotropy ratio (k_x/k_z) and the partial penetration effect (L_S/D_T) for all tree models were varied according to the parametric study shown as flow charts in Fig. 3.8 and Fig. 3.9 (Chapter 3).

Prior carrying out any parametric study for two modelling approaches, the definition of a "successful simulation" needed to be defined. The initial simulation is considered to be the first case of the parametric study for each model:

- Total model height is $D_{T0}=36[m]$,
- Anisotropy ratio is $k_x/k_z=1$,
- Initial partial penetration ratios (as actually constructed in the Spadina Landfill) for:
    - GW01-04 model it is $L_S/D_{T0}=0.50[m/m];$
    - GW02-04 model it is $L_S/D_{T0}=0.47[m/m];$ and

- GW10-07 model it is $L_S/D_{T0}=0.35[m/m]$.

The examples of four successful simulations with their gas flow outputs for each initial 36[m]-model, GW01-04, GW02-04, and GW10-07, with $k_x/k_z=1$ with four different intrinsic permeability inputs shown in Fig. 4.1. The plots in Fig. 4.1 show how applying the wellbore vacuum boundary condition gives reasonable results for the simulated gas flow outputs with the intrinsic permeability value being the only input that was varied.

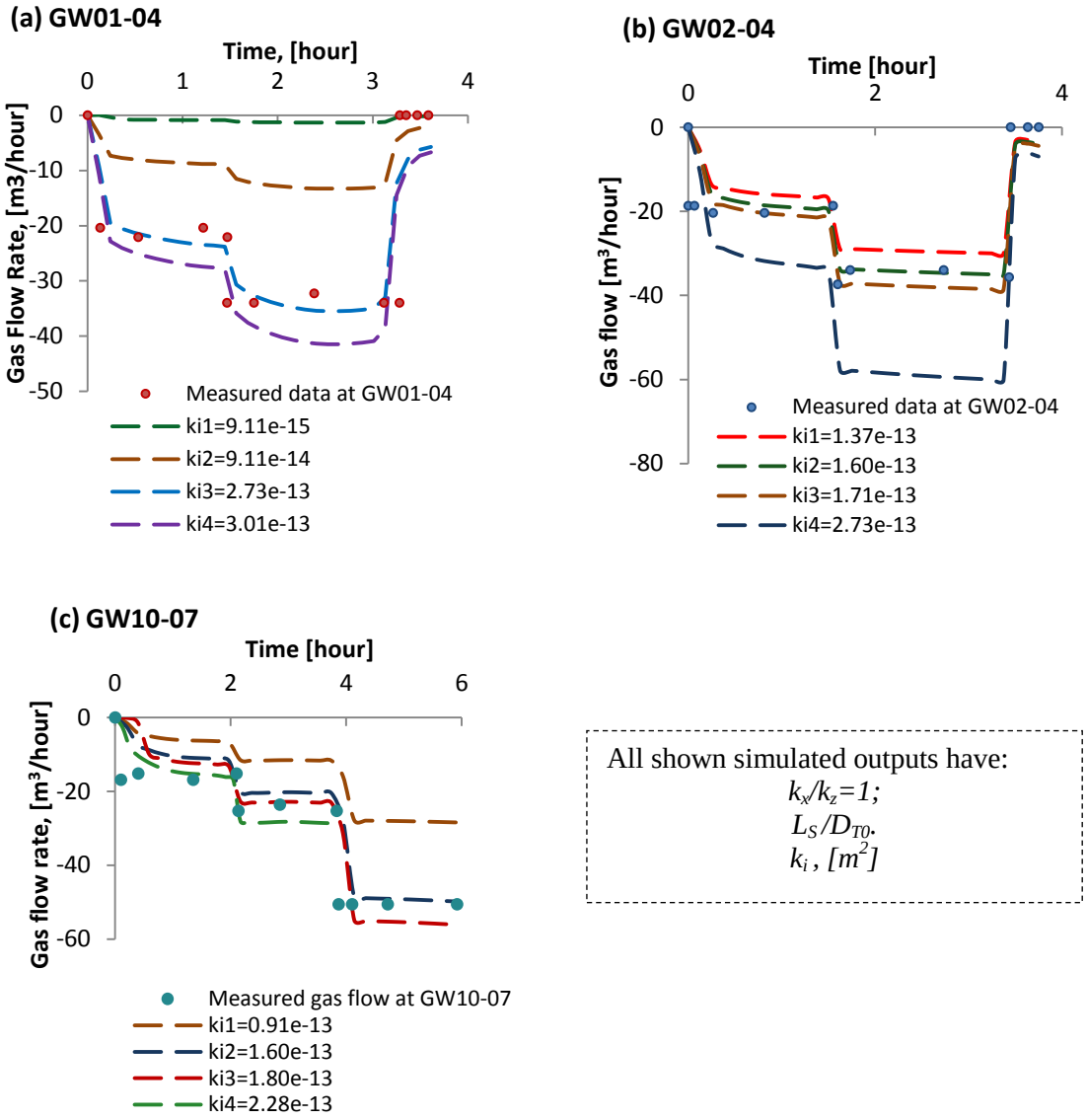

Fig. 4. 1. Three models with four simulated gas flow outputs made in the AIR/W for the initial 36[m] case: (a) GW01-04, (b) GW02-04, and (c) GW10-07.

The wellbore boundary condition plays a significant role in determining the intrinsic permeability value. When the stepped-rate pumping test was run as two drawdown steps and a recovery period (GW01-04 and GW02-04), the fitted measured field data was applied as a complex wellbore boundary pressure function (two steps and a recovery period) in order to define the best-fit value of intrinsic permeability (Fig. 4.1 (a) and (b)). When the short-term test was cared over three drawdown steps, like at GW10-07, the process of fitting data was somewhat more complex (Fig. 4.1 (c)).

Accordingly, it was found easier to consider each pumping step separately and define the best-fit intrinsic permeability value for each individual pumping rate using the respective portion of pressure drawdown function applied as the wellbore boundary condition.

The author believes that it is reasonable to expect some difference in the intrinsic permeability values that best fit each step of the pumping tests, given the complex heterogeneous nature of MSW, and because higher gas flow rates have higher radius of influences, and thereby cover a bigger area of MSW, and thereby potentially include material with a different intrinsic permeability.

The models were not varied to try reflecting potential variations of material properties at different radii from the pumped wells, as the objective of this work was not to perfectly match the field data, but rather to investigate the importance of the gas generation term (R_g).

Once best-fit gas flow AIR/W outputs for measured gas pressure data at a particular well were used to generate corresponding best-fit intrinsic permeability values, the parametric study was run. The starting point was the following best-fit intrinsic permeability values, which were determined using the initial 36[m]-models (i.e. as they were actually constructed in the field with k_x/k_z=1 and L_S/D_{T0} as actually constructed):

- for GW01-04: $k_i=2.73*10^{-13}[m^2]$;
- for GW02-04: $k_i=1.60*10^{-13}[m^2]$; and
- for GW10-07: $k_i=2.24*10^{-13}[m^2]$.

The parametric study was simulated according to the flow charts, shown in Fig. 3.6 and Fig. 3.7 and the gas flow outputs were correspondently compared with the field gas pumping rate data measured at GW01-04, GW02-04, and GW10-07. During the parametric study, the intrinsic permeability values were varied ranging from $8.1*10^{-16}[m^2]$ to $3.2*10^{-11}[m^2]$, which were calculated based on the reported values of unsaturated hydraulic conductivity for the Saskatoon Spadina Waste Landfill Site by Schmidt (2010) and Fleming (2011). The accuracy of fitting gathered through AIR/W models' simulations were checked with the following statistics: the Pearson's correlation coefficient (r_P) and the coefficient of determination (R^2) details of which were discussed in Appendix E.

The best-fit intrinsic permeability values, used for the various simulations and carried out for these parametric studies, are presented in Table C.1 (Appendix C).

The effect of the partial penetration ratio on the GW01-04 AIR/W gas flow outputs with an anisotropy ratio $k_x/k_y=1$ is shown in Fig. 4.2. Thus based on the modelling results for GW01-04 test-well, a 17% decrease in the total model thickness (i.e. from L_S/D_T *=0.5 to 0.6* and $k_x/k_z=1$) results in a decrease of the best-fit intrinsic permeability value of approximately 6.6%.

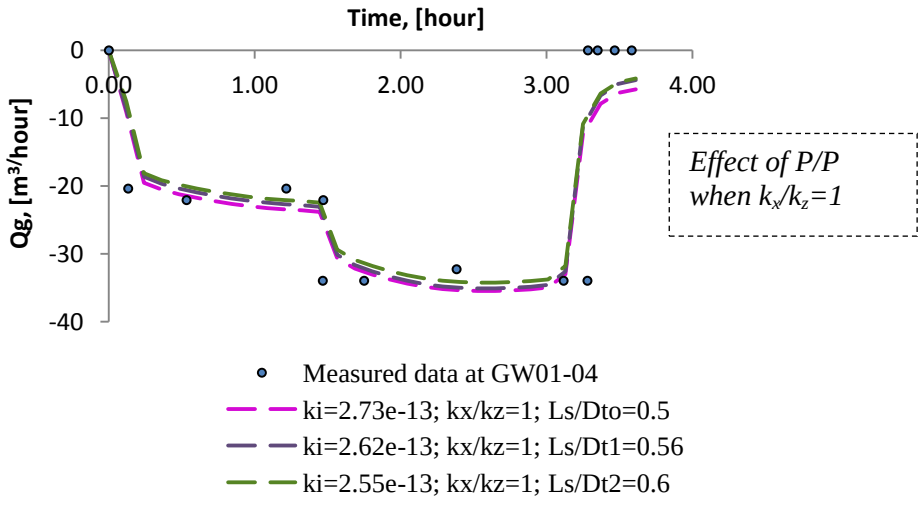

Fig. 4. 2. Gas flow rate measured during the short-term field test at GW01-04 and AIR/W results based on the best-fit values of $k_i[m^2]$ with different P/P ratio and anisotropy to be equal one in GW01-04 AIR/W model.

In comparison when the thickness of the initial 36[m] GW01-04 model was 36 metres (i.e. the actual case, with the true partial penetration ratio of 0.5) and only an anisotropy effect was evaluated, the best-fit intrinsic permeability value increased by approximately 40% when the anisotropy ratio rises from 1 to 10 (Fig. 4.3, Table C.1).

For GW02-04 AIR/W model, a decrease of 19% in the total model thickness results in a decrease of 6.3% in the best-fit intrinsic permeability value. Similarly, for the total model thickness at 36[m] and an increase in the anisotropy ratio from 1 to 10 suggest a change of 36% in the best-fit intrinsic permeability value (Fig. 4.3, Table C.1).

For GW10-07 AIR/W model, a 28% decrease in total model thickness results in a 4.5% decrease of the best-fit intrinsic permeability value. For 36[m] constant model thickness, changing the anisotropy ratio from 1 to 10 suggest a change of 41% in the best-fit intrinsic permeability (Fig. 4.3, Table C.1).

Thereby independent analyses of the both effects anisotropy and partial penetration (for each of the three test-wells) has been evaluated and the following conclusions were made:

- when the total thickness of the models is cut by about 17%-28% (or L_S/D_T varies for: GW01-04 from 0.5 to 0.6; GW02-04 from 0.47 to 0.58; and for GW10-07 from 0.35-0.48[m/m] and for all cases with the anisotropy ratio is constant, k_x/k_z=1) results in only a 4.5%-6.6% decrease in the best-fit intrinsic permeability value, and
- when the anisotropy ratio is changed from 1 to 10 (or k_x/k_z=1 to k_x/k_z=10 with the constant total model thickness D_T=36[m] for all three models), the best-fit intrinsic permeability value is increased by 36%-41%.

Fig. 4.3 shows the intrinsic permeability values which were used in parametric study to best fit AIR/W gas flow model outputs with the measured gas flow rate at GW01-04, GW02-04, and GW10-07. It is evident that the effect of partial penetration is less pronounced than that of anisotropy and that in general, the effect of anisotropy is reduced if the well screen is closer to fully penetrating. None of these findings are

unexpected; however, this aspect of the study has served to quantify (approximately) the magnitude of error that could be introduced if the effect of partially penetration and anisotropy are not properly captured (as is necessarily the case for the 1-D FD solution, for example).

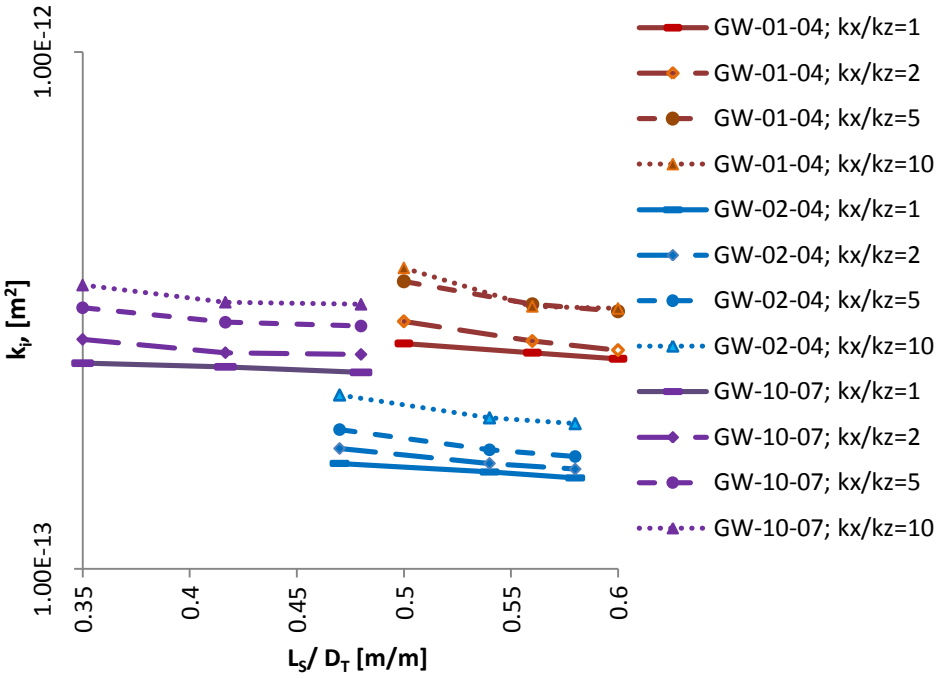

- Orange lines for GW01-04, blue for GW02-04, and purple for GW10-07

Fig. 4. 3. Intrinsic permeability values used for the best-fit AIR/W models' outputs.

Fig. 4.3 and the discussion of the results together with the information in Appendix C (Table C.1, Fig. C.1, Fig. C.2, and Fig. C.3) illustrate that the effect of partial penetration exist, but are not as influential as the anisotropy.

Accordingly, an "intrinsic permeability ratio", I_k, was defined, for each of the various pumping tests evaluated as shown below in Equation [4.1]:

$$I_k = \frac{k_i^{F/P}}{k_i^{initial}} \qquad [4.\ 1]$$

where I_k is the intrinsic permeability ratio [dimensionless], $k_i^{F/P}$ is the best-fit value of intrinsic permeability determined using the AIR/W model assuming a geometry that is closest to a fully-penetrated well screen, within the constants of convergence described

above [m^2], and $k_i^{initial}$ is the best-fit value of intrinsic permeability using the AIR/W model with the actual partially-penetrating geometry of each well as actually constructed [m^2].

This intrinsic permeability ratio is compared in Fig. 4.4 to the partial penetration ratio.

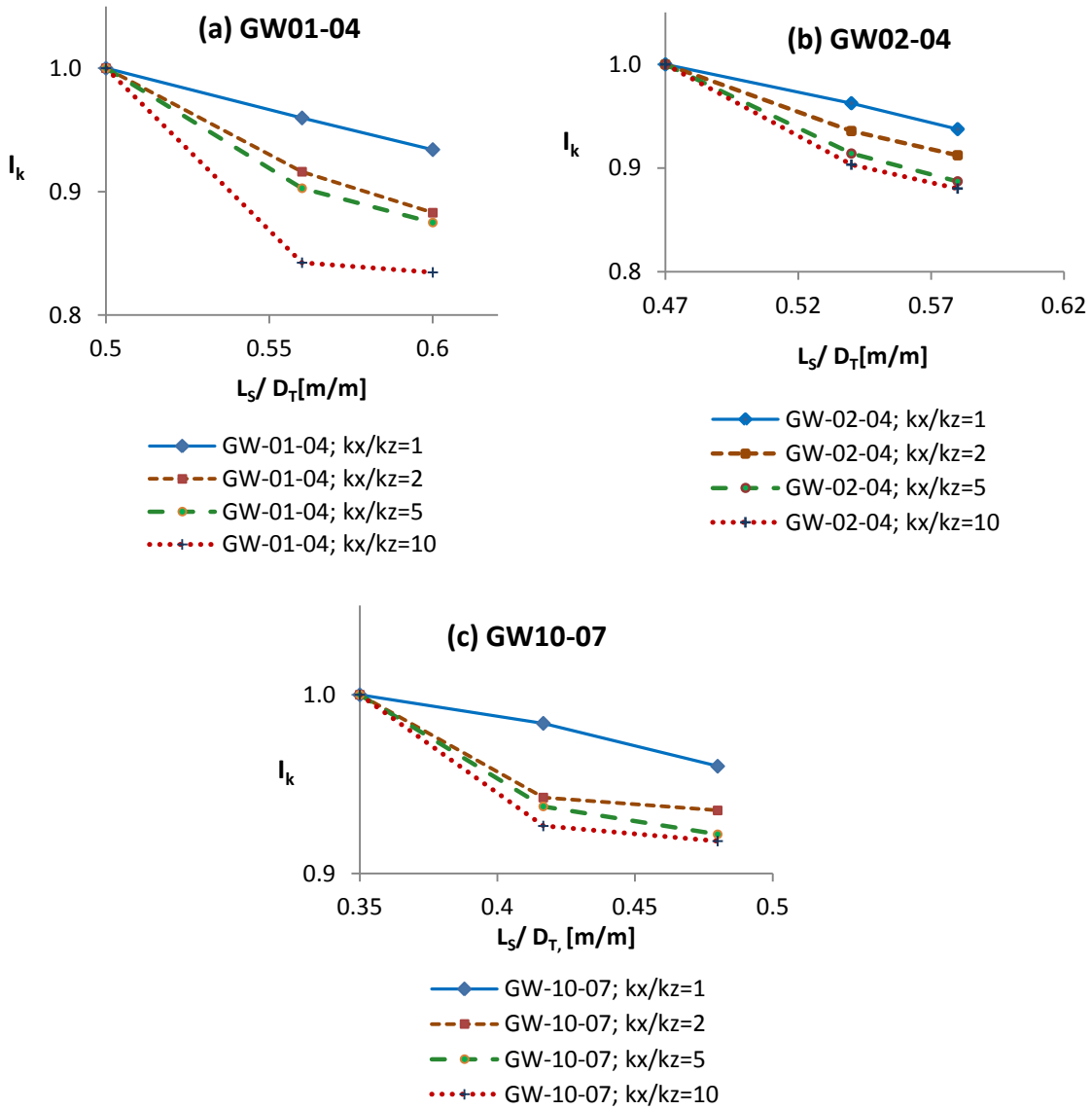

Fig. 4. 4. The intrinsic permeability ratio verses the partial penetration ratio for the AIR/W models for (a) GW01-04, (b) GW02-04, and (c) GW10-07.

These results clearly show that the combined effects of partial penetration and anisotropy are such that the best-fit value of intrinsic permeability would be interpreted from a 1-D analysis of a pumping test (in which partial penetration and anisotropy are

inherently ignored) should change by only a small amount, corresponding to a correction factor, close to or greater than 0.9.

The parametric studies demonstrated that the effect of partial penetration influence the results of the best-fit intrinsic permeability input values but much less than the change in anisotropy ratio. All results of the best-fit intrinsic permeability obtained through the parametric studies for the three pumped test wells under consideration fall inside of the defined intrinsic permeability range for the particular site of investigation.

Fig. 4.5 displays the range of intrinsic permeability values, calculated based on the reported values of hydraulic conductivity for the Saskatoon Spadina Waste Landfill Site by Schmidt (2010), and the intrinsic permeability values obtained through the parametric studies for all three models built in AIR/W.

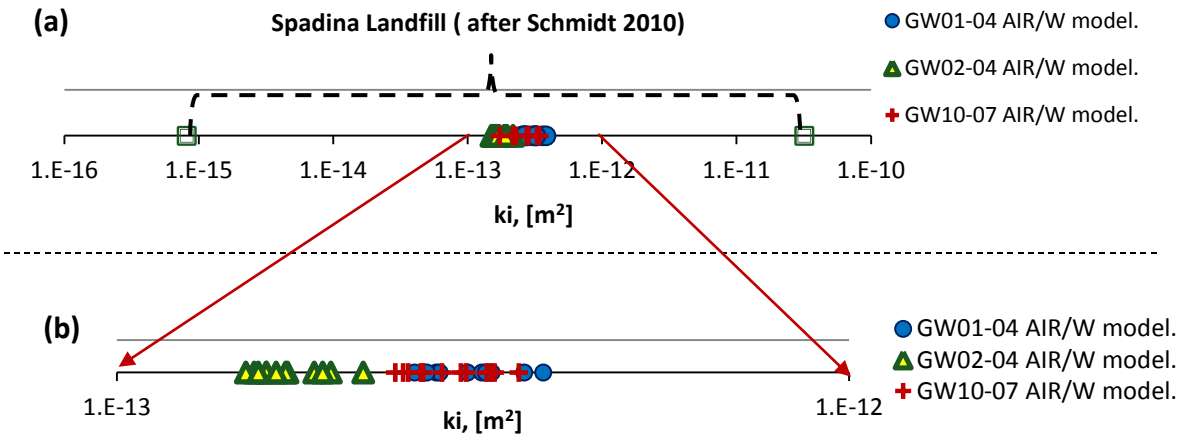

Fig. 4. 5. Parametric study results for the best-intrinsic permeability values: (a) the AIR/W intrinsic permeability inputs compare to the previously defined values in the field (after Schmidt 2010) and (b) the AIR/W intrinsic permeability inputs.

Based on the best-fit AIR/W models results for pumping tests at three test-wells (and ignoring the effect of gas generation) it can be concluded that the intrinsic permeability of the landfilled waste at the Spadina Landfill varies from 10^{-13}[m^2] to 10^{-12}[m^2], based only on an analysis of porous media flow (Fig. 4.5 and Table C.1).

The AIR/W results for the cases with k_x/k_z=1 and L_S/D_T is as large as possible (fully-penetrating) are comparable with those from the 1-D FD solution (R_g) later in this chapter.

4.3. Comparing the AIR/W modes and 1-D FD solution (R_g=0) results

The results that were obtained during the parametric studies using both AIR/W and the 1-D FD solution ($R_g=0$) are presented here and in the Appendices. The intrinsic permeability values from AIR/W were compared with those from 1-D FD using field data from the three test wells (GW01-04, GW02-04, and GW10-07). The intrinsic permeability values for the 1-D FD solution were determined using the best-fit air permeability values obtained using 1-D FD for $R_g=0$, corrected to intrinsic permeability using the relative permeability of air at the average ambient water content.

The range of estimated intrinsic permeability values for the Spadina Landfill is presented in Fig. 4.6 (a) based on the best-fit 1-D FD solution and AIR/W model results (i.e. parametric study). Thus, all of these estimates of intrinsic permeability obtained using both approaches are within the range which was reported by Schmidt (2010) and Fleming (2011).

The intrinsic permeability estimates defined using the 1-D FD solution and the AIR/W computer package are displayed in Fig. 4.6 (b) and in Table D.2, for cases where the simplifying assumptions allow a direct comparison to be made. Thus for these analyses it was assumed that gas generation may be ignored, there is no anisotropy ($k_x/k_z=1$) and the well fully penetrate the waste thickness, the intrinsic permeability values differ approximately by 2% to 5%. This difference in results can be possibly attributed to the following considerations:

- the 1-D FD solution considers only single phase (“saturated”) gas flow rather than the 2-phase water and gas system considered by AIR/W, thus the pneumatic conductivity determined using 1-D FD can relate to an intrinsic k value only for an estimated constant average volumetric water content (and thus a single point on the relative permeability function);
- in AIR/W, the volumetric gas and water contents are not constant spatially and localized zones of high VWC would exhibit lower relative air permeability –

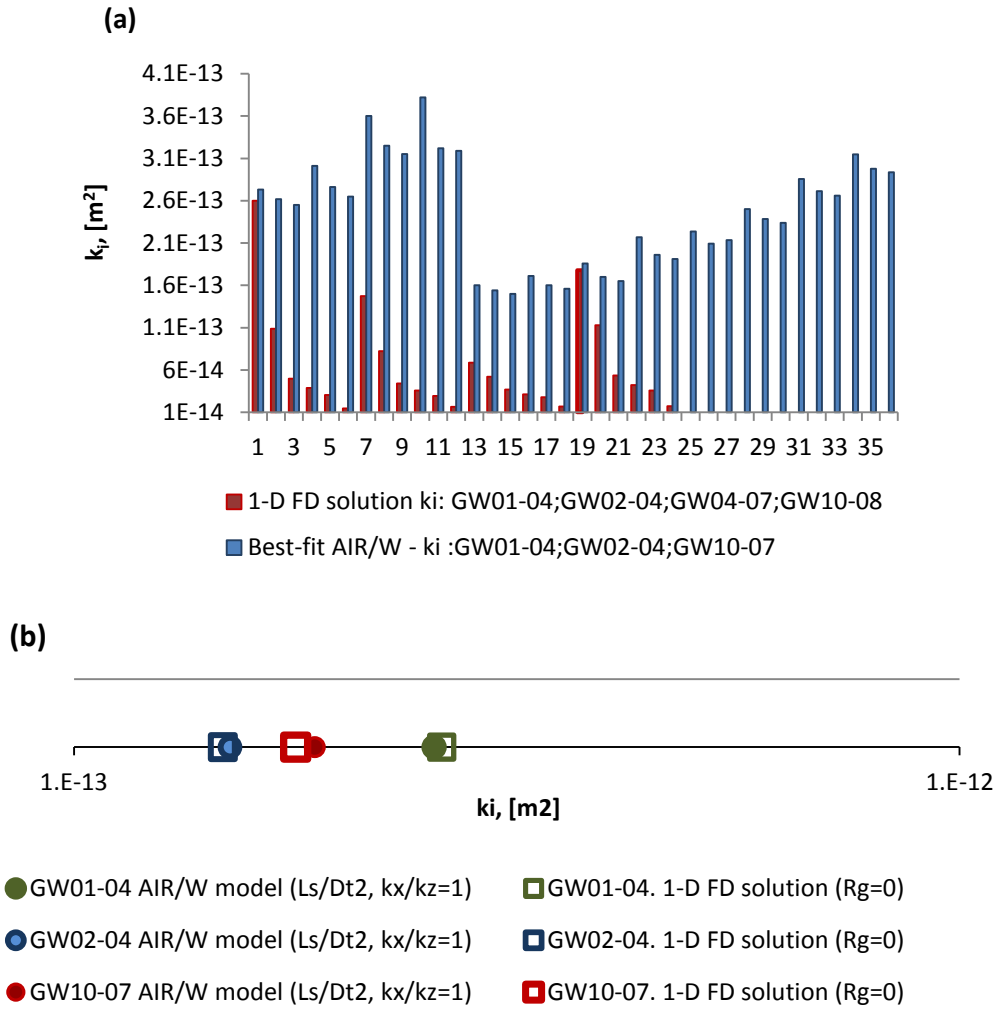

Fig. 4. 6. Defined intrinsic permeability values based on the obtained results from AIR/W and 1-D FD solution: (a) 1-D FD solution and AIR/W results from parametric studies; (b) AIR/W and 1-D FD comparable results.

thus the effect of such lower zones is to decrease the harmonic mean conductivity value that controls the relationship between wellhead vacuum and flow. Stated simply, simple harmonic mean arithmetic requires that the situation with non-constant VWC would have a lower harmonic mean K value than the corresponding situation with a constant, average value of VWC. Alternatively stated, in order to match the same dataset of flow and wellhead vacuum, an higher intrinsic permeability value would be required where the relative permeability is spatially varying, because of the inherent dominance of the harmonic mean K value by the zones of lower relative permeability. Thus it is

entirely expected that the best-fit spatially-invariate value of intrinsic permeability determined using AIR/W should be somewhat higher than would be determined using a spatially-invariate average pneumatic conductivity value as is done using 1-D FD;

- Fig. 4.7 schematically shows the major difference in defining the gas permeability by the two approaches. In the 1-D FD solution the degree of gas saturation is constant and in AIR/W since there is two-phase flow the degree of water saturation affects the relative permeability curve of gas fluid (more detailed description of two-phase flow is provided in Chapter 2);
- "full-penetration" was not actually possible using AIR/W for the models, GW01-04, GW02-04, and GW10-07. Convergence could not be reached for cases where the total thickness would be equal to the screen length ($L_S/D_T=1$) as discussed in Section 3.3.5.

The results obtained within the first approach, AIR/W, implicitly incorporate a requirement for conservation of mass – this is inherent in the formulation of the computer package and thereby the gas generation occurring within the landfill was ignored ($R_g=0$). Therefore, the defined intrinsic permeability results in AIR/W should be corrected.

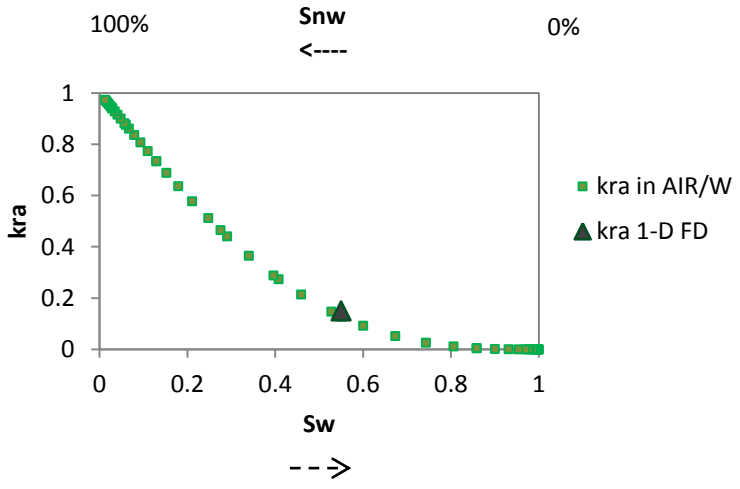

Fig. 4. 7. Typical difference in relative permeability curves of gas in AIR/W and 1-D FD solutions.

4.4. The 1-D FD Solution

4.4.1. Initial Results

In total, the 1-D FD solution was set up for four test-wells, GW01-04, GW02-04, GW04-07, and GW10-07. The effect of in-situ gas generation on the relationship between flow, wellhead vacuum and best-fit permeability was evaluated for all four test wells following the approach outlined in the flow charts shown in Fig. 3.17 and Fig. 3.18. Chapter 3 discussed the main aspects of the 1-D FD solution such as the mathematical basis, the boundary conditions, a typical geometry, and the material properties.

The 1-D FD solution is significantly easier and faster than the 2-D unsaturated FEA using AIR/W. Potential problems with numerical stability that are inherent in FD methods can be avoided by adjusting the relative value of the increments of time and radius. It was found for the step drawdown tests, a time increment of 10 to 20[s] and radius increment of 0.2 to 0.3[m] worked well, depending on the test-well. For the recovery period when the gas generation is ignored it was found that the time increment must be much smaller, approximately 1.5 to 2[s]. Since the most noticeable effect of the gas generation occurs during the recovery period when the gas pumping rate is equal to zero, it was found that the value of this parameter was also important in defining the appropriate time increment for assurance of numerical stability.

4.4.2. Parametric Study of the Gas Generation Effect

The analysis of the effect of the gas generation rate on the interpreted value of intrinsic permeability for all four test-wells (GW01-04, GW02-04, GW04-07, and GW10-07) was completed according to the flow charts provided in Fig. 3.17 and Fig. 3.18.

Results for all four test-wells show how changes in the gas generation rate would affect the predicted gas pressure if all the inputs and boundary conditions were to stay the same. From Fig. 4.8 it is evident that the gas generation rate influences the gas pressure outputs.

Importantly, when gas pumping tests are analyzed under the assumption that the landfill can be treated as a porous medium and thereby ignore the gas generation rate (i.e. $R_g=0$), the best-fit intrinsic permeability values are overestimated. It is important to understand that landfills continuously generate landfill gas.

The 1-D FD results, shown in Fig. 4.8 also show that assuming the same material properties (i.e. the best-fit permeability for the case of no gas generation), including gas generation up to $1.4*10^{-3}[m^3/(m^3*hour)]$ results in a significant decrease in the

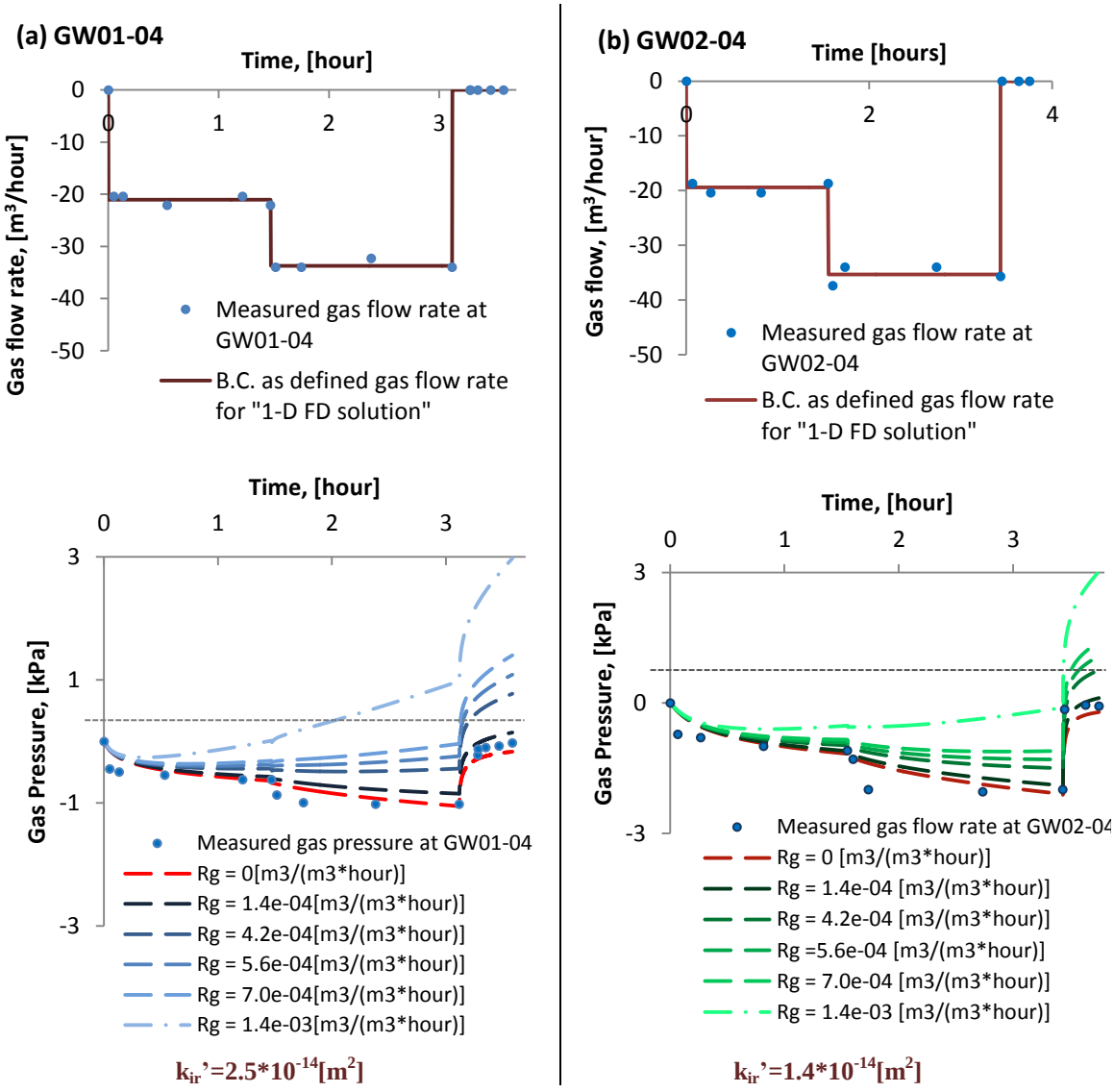

Fig. 4. 8. Effect of assumed gas generation on predicted wellbore vacuum under pumping rates and air permeability value best-fit from zero-gas generation scenario for following test-wells: (a) GW01-04, (b) GW02-04, (c) GW04-07, and (d) GW10-07.

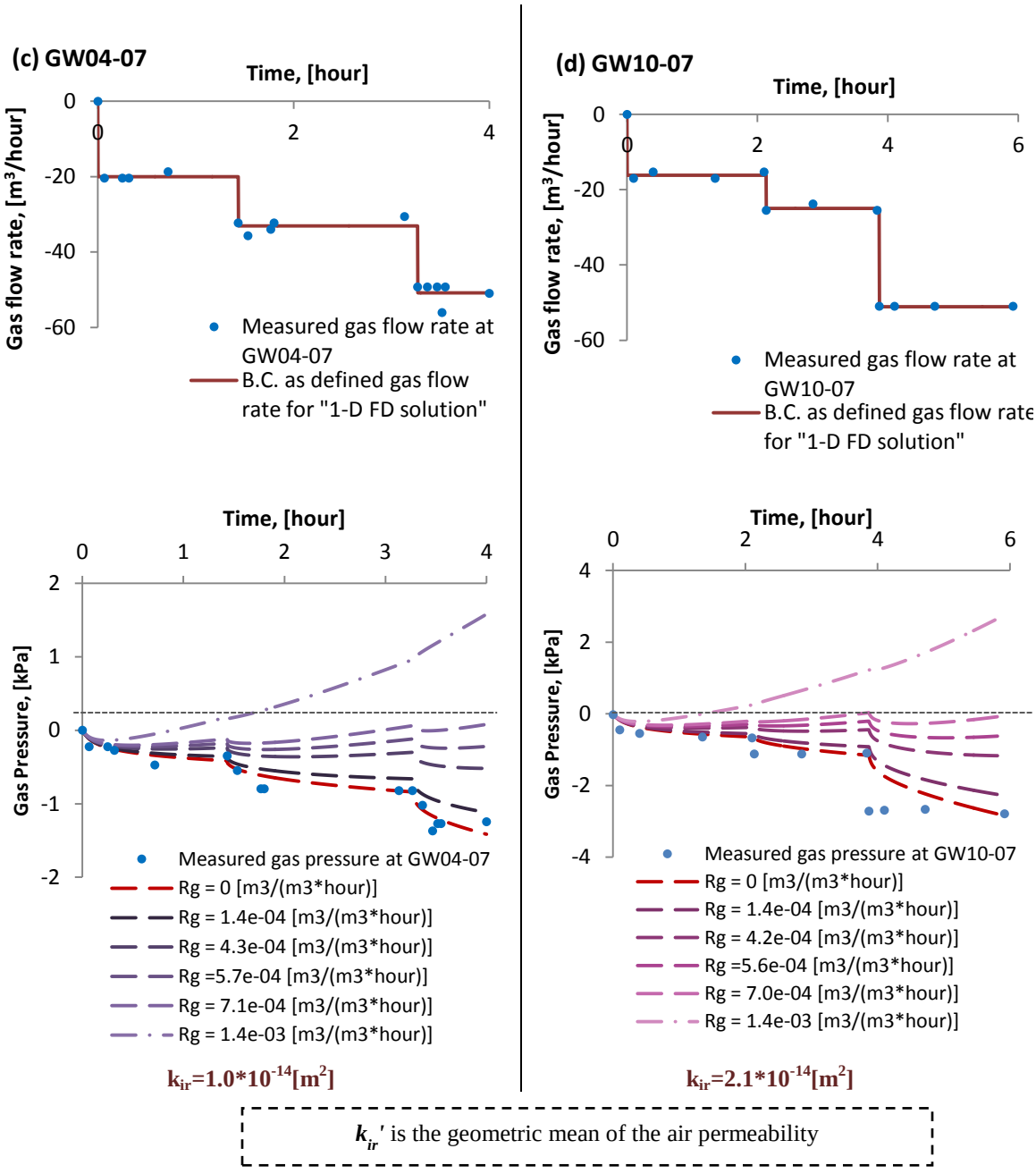

Fig. 4. 8 (continued).

predicted wellhead vacuum. This reflects the fact that with gas generation more than zero, significantly less wellhead vacuum needs to be applied in order to reach the same gas flow pumping rate.

The gas pressure outputs are shown in Fig. 4.8 with the negative sign signifying that the negative gas pressure drives gas flow toward the well and therefore when the predicted

gas pressure is not negative, no wellhead vacuum is required since the generated gas creates enough pressure to force the gas to the well at the observed flow rate.

A more direct investigation of the gas generation effect was carried out by varying the intrinsic permeability to find a best-fit set of values for each of the measured data sets (i.e. a set of R_g and k_{ir} values that together yield a best fit to the field data). Several 1-D FD solution outputs for each of the four different test-wells are shown in Fig. 4.9 and all other results are provided in Appendix D.

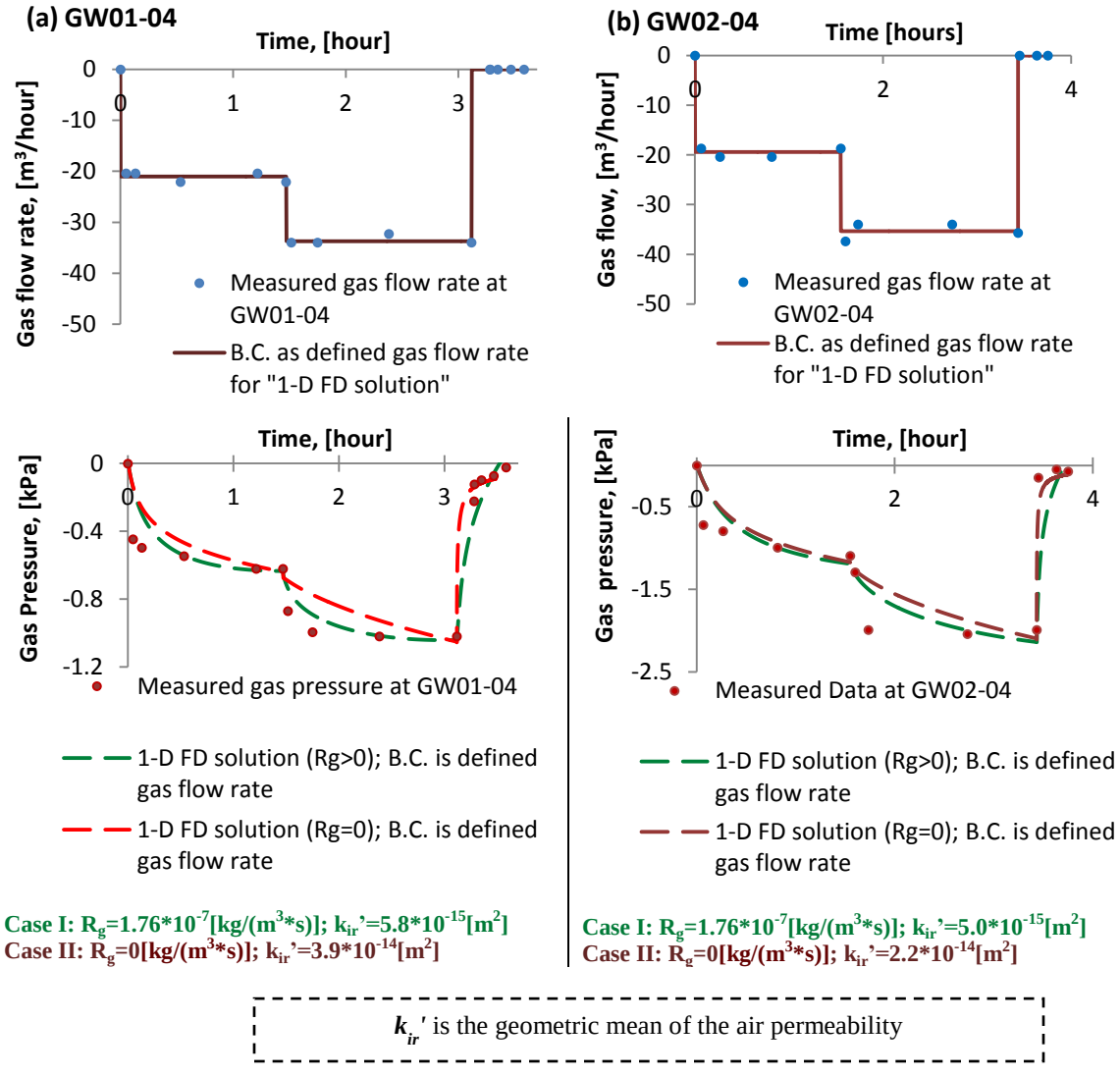

Fig. 4. 9. The 1-D FD solutions for both settings where the total gas generation is taken in account and where it is ignored with their boundary condition as the defined gas flow rate at the wellbore area and the 1-D FD solution outputs based on the best-fit value k_{ir} for each of the four test-wells: (a) GW01-04, (b) GW02-04, (c) GW04-07, (d) GW10-07.

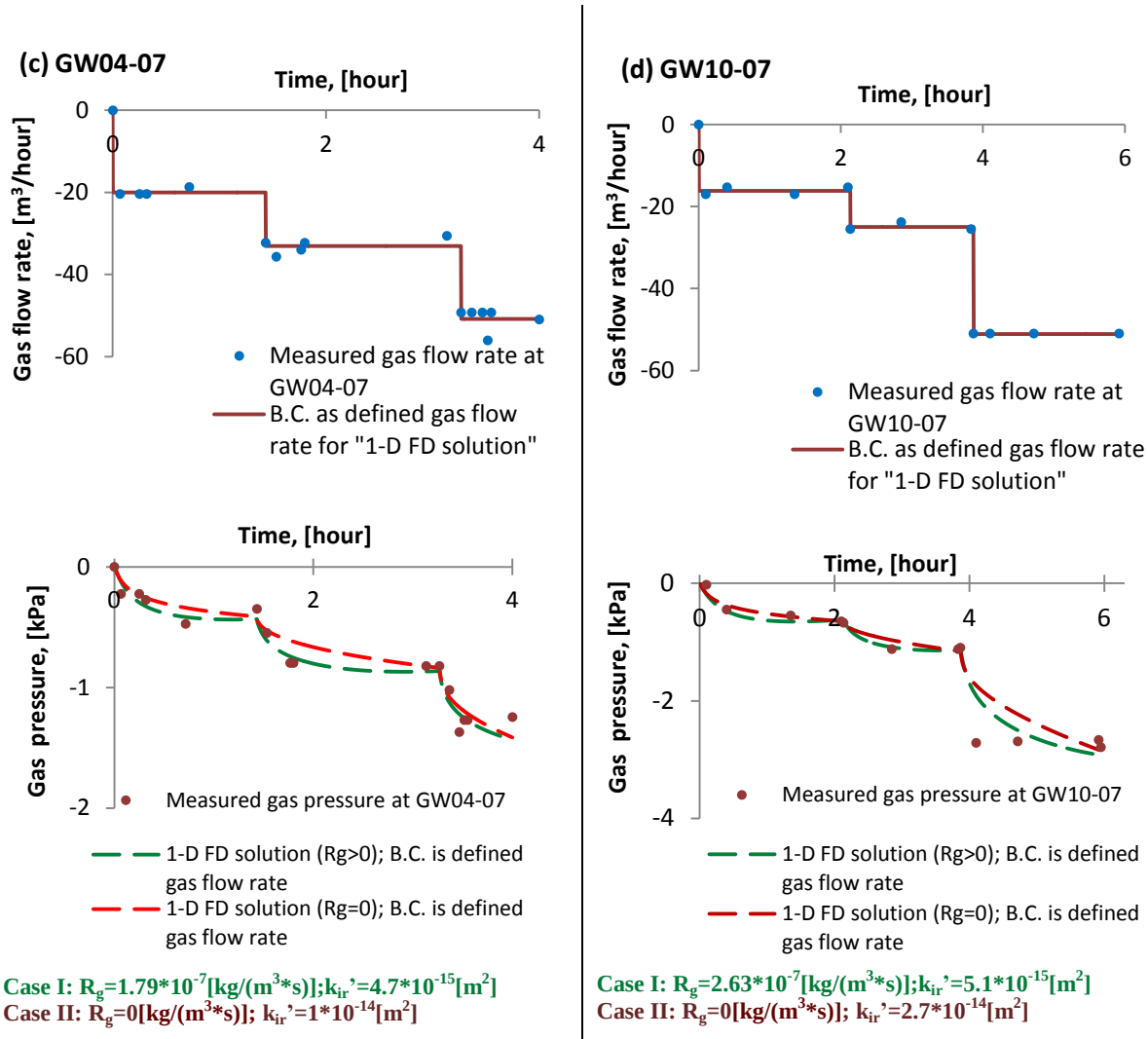

Case I: R_g=1.79*10^{-7}[kg/(m^3*s)];k_{ir}'=4.7*10^{-15}[m^2]
Case II: R_g=0[kg/(m^3*s)]; k_{ir}'=1*10^{-14}[m^2]

Case I: R_g=2.63*10^{-7}[kg/(m^3*s)];k_{ir}'=5.1*10^{-15}[m^2]
Case II: R_g=0[kg/(m^3*s)]; k_{ir}'=2.7*10^{-14}[m^2]

k_{ir}' is the geometric mean of the air permeability

Continue Fig. 4. 9.

The 1-D FD solution outputs shown in Fig. 4.9 illustrate the importance of the gas generation rate for the following two cases:

- Case I: "*1-D FD solution (R_g>0)*" is the air permeability value that best-fits the 1-D FD solution estimates of wellbore pressure to the measured data from the field assuming that the total gas generation is greater than zero and varies accordingly the flow charts provided in Fig. 3.16 and Fig. 3.17; and
- Case II: "*1-D FD solution (R_g=0)*" is the air permeability value that provided a best-fit between the 1-D FD solution - derived estimates of wellbore pressure

with the measured field data assuming that there is no gas generation occurring within the waste.

It is clear that the 1-D FD solution outputs provide a better degree of fit when the gas generation rate is taken into account (Fig. 4.10). The accuracy of fitting gathered through 1-D FD models' simulations were checked with the following statistics: the Pearson's correlation coefficient (r_P) and the coefficient of determination (R^2). Fig. 4.10 shows examples of these statistics for GW01-04 (i.e. 1st and 2nd short term test) for Cases I and II.

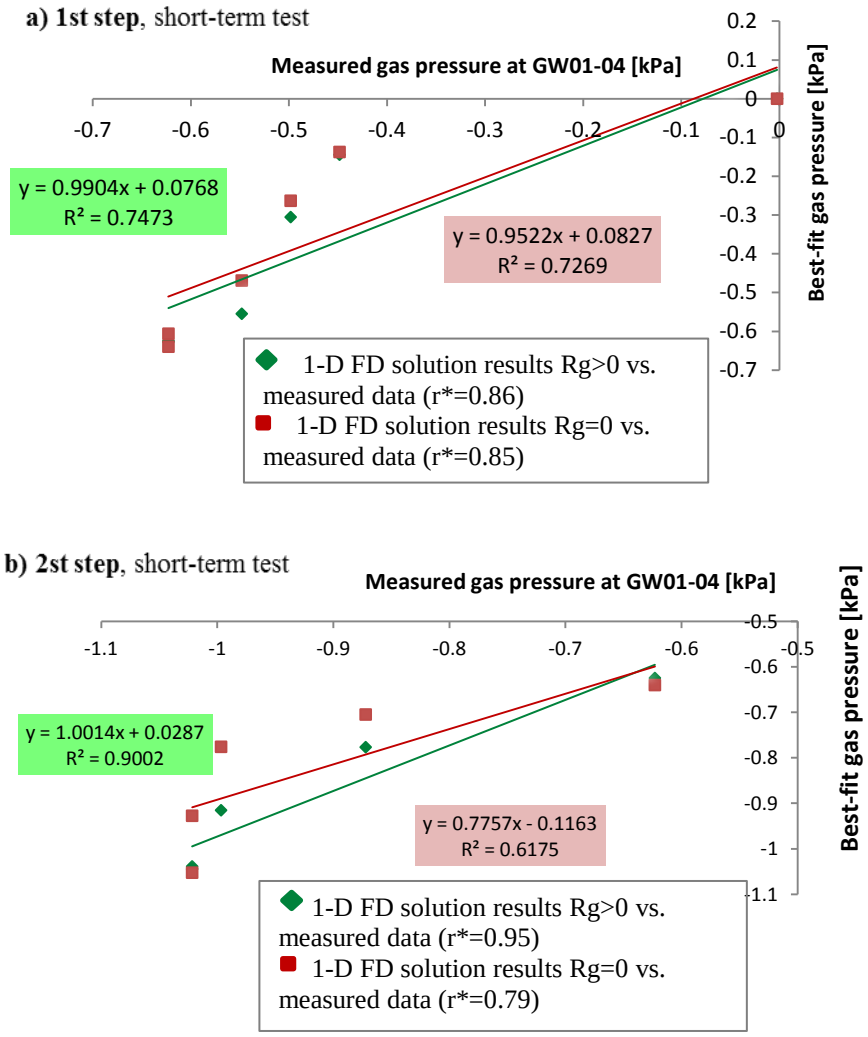

Fig. 4. 10. Statistics for best-fit data using 1-D FD defined for GW01-04: (a) 1st drawdown step and (b) 2nd step.

The results of a parametric study using the 1-D FD solution are provided in Fig. 4.11, in which the best-fit k_{ir} values are shown for various assumed values of R_g. More details are provided in Appendix D. The air permeability values shown in some figures as the geometric means of k_{ir}, were used only to simplify the visual interpretation of the 1-D FD results. Therefore, based on the best-fit 1-D FD solution results shown in Fig. 4.11, it can be concluded the air permeability of landfilled waste at the Spadina Landfill is $2.2\text{x}10^{-15}$ to $3.9\text{x}10^{-14}$[m^2].

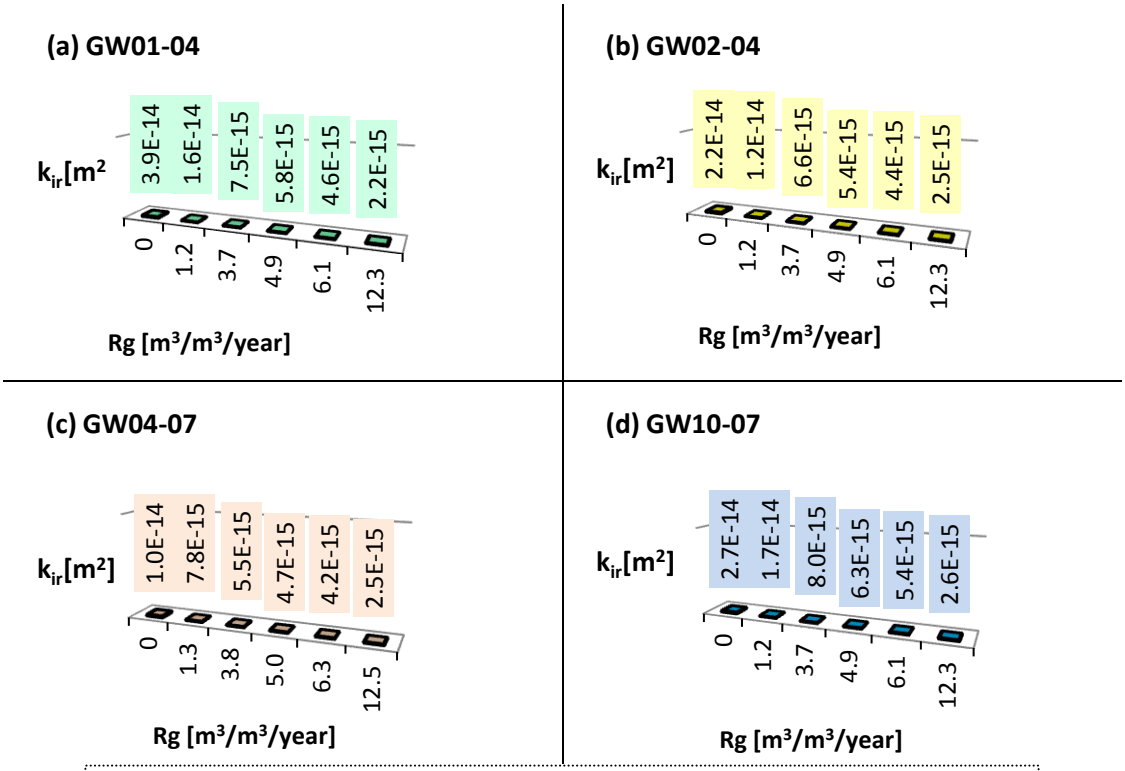

(R_g; k_{ir}) is the data points in the charts represent the values of the total generation rate and the geometric mean of the air permeability in radial direction, found through the parametric study in the 1-D FD solution.

Fig. 4. 11. The geometric mean of the air permeability values obtained through 1-D FD solution within the parametric studies.

The best-fit intrinsic permeability values and correspondently assumed gas generation rates are compiled and plotted in Fig. 4.12. The log(k_i) versus R_g (total gas generation rate) relationship is strong, with the goodness of fitting expressed by R^2=81% and r_p=90%. Thus, from Fig. 4.12 the intrinsic permeability ranges from $1.5\text{x}10^{-14}$ to $2.6\text{x}10^{-13}$ [m^2] (Table D.1, and Table D.2).

Based on this initial analysis and the unsurprising determination that the gas generation rate affects the interpreted value of intrinsic permeability, two additional correction factors are proposed, which may be applied to the calculated intrinsic permeability to account for the effect of the gas generation rate (R_g) relative to the pumping rate of the well and the intrinsic permeability (k_i).

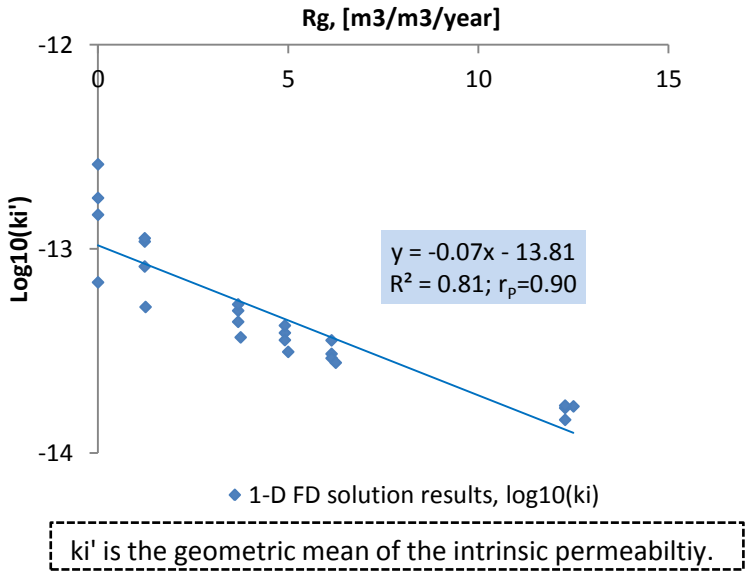

Fig. 4. 12. 1-D FD solution outputs. Logarithm to the base ten of the intrinsic permeability verses the total gas generation rate.

By using an intrinsic permeability correction factor due to gas generation, φ_{kR}, a two-step procedure is proposed for analysis of LFG pumping test data (equation [4.2]). First, best-fit intrinsic permeability values may be easily determined from a pumping test analysis using software such as GeoStudio that requires conservation of mass (i.e. R_g=0). The results of such analysis can then be adjusted for gas generation and thereby a more accurate intrinsic permeability value can be determined for a landfill where the gas generation rate is non-zero. Perhaps equally importantly, this approach may be used with relatively short-term pumping test data to yield an estimate (by simultaneous best fit of k and R_g), not only of the permeability of the waste, but also the gas generation rate within the landfill, although it must be acknowledged and recognized that such an approach cannot yield a unique best-fit solution for both simultaneously.

The proposed intrinsic permeability correction factor due to gas generation was defined by the following equation:

$$\varphi_{kR} = \frac{k_i^*}{k_i^o} \quad [4.\ 2]$$

where φ_{kR} is the intrinsic permeability correction factor due to gas generation [dimensionless], k_i^* is the intrinsic permeability determined using the 1-D FD solution with the total gas generation rate included ($R_g>0$) [m^2], and k_i^o is the intrinsic permeability determined using the 1-D FD solution but where the total gas generation rate was ignored ($R_g=0$) [m^2].

The gas ratio was defined as the total gas generation rate produced by one cubic metre of waste divided by the gas pumping rate in the landfill by the following equation:

$$\Lambda_{waste} = \frac{R_g^{**}}{Q_g} \quad [4.\ 3]$$

where Λ_{waste} is the gas ratio [$1/m^3$].

The results of Fig. 4.12 were modified to incorporate these effects, thus the intrinsic permeability correction factor due to gas generation (φ_{kR}) versus the gas ratio for a defined gas flow pumping rate were plotting as shown in Fig. 4.13. Where the accuracy of each function based on two statistics are: the Pearson's coefficient: r_P=98.6% to 99.9% and the coefficient of determination R^2=97.2% to 99.8%. More details about this are presented in Fig. D.1 and Table D.3.

The relationship between the intrinsic permeability correction factor due to gas generation and the gas ratio for a defined gas flow rate was found to be:

$$\varphi_{kR} = a \cdot ln(\Lambda_{waste}) + b \quad [4.\ 4]$$

where *a* and *b* are the fitting parameters.

Fig. 4.13 illustrates 5 lines that were built based on the 1-D FD solution results and the reported data from the following test-wells: GW01-04, GW02-04, GW04-07, and GW10-07. It was established that the relationship between the intrinsic permeability correction factor due to gas generation and the gas ratio for various values of gas

pumping rate can be described by a series of logarithmic functions (Equation [4.4]). The statistical analysis of these plotted functions is shown in Appendix D.

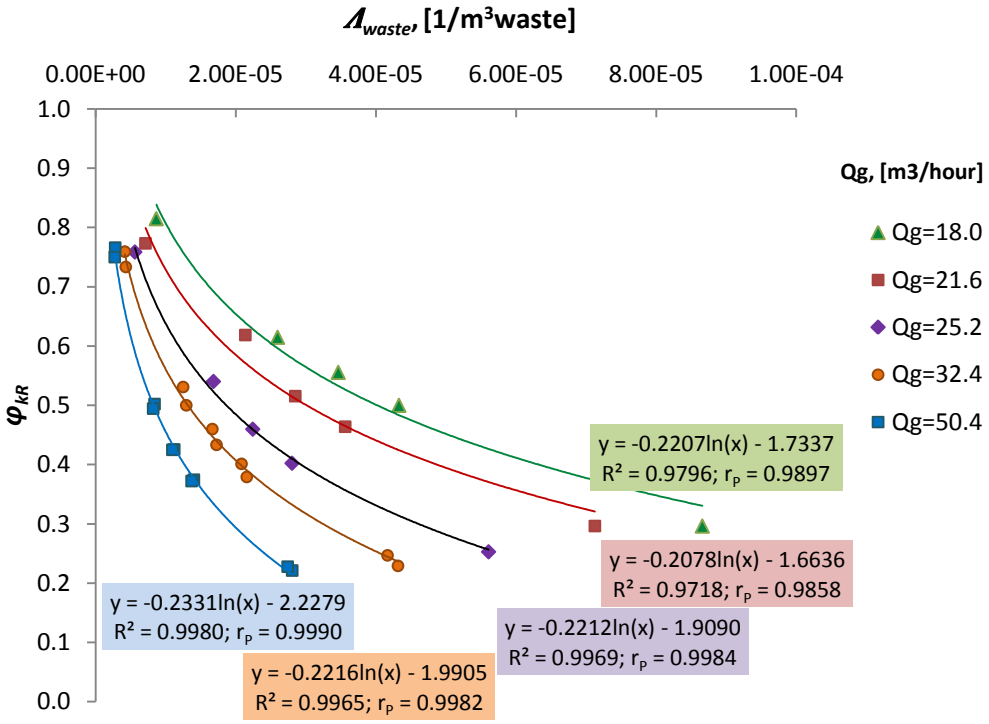

Fig. 4. 13. The functions of the intrinsic permeability correction factor due to gas generation and the gas ratio based on the data sets from the following test-wells: GW01-04, GW02-04; GW04-07; and GW10-07.

To conclude, the intrinsic permeability correction factor due to gas generation can be used to correct the defined intrinsic permeability values in AIR/W, so the values would be adjusted to reflect the gas generation and thereby more realistically describe the landfill material properties. More details of the parametric studies for both approaches are provided in Appendices C and D. Summary, conclusions, and recommendations will be shown in Chapter 5.

4.5.Worked example

It has been demonstrated in this thesis the software package AIR/W can be used for simulating two-phase flow occurring in the landfill; however the best-fit intrinsic permeability value should be corrected to account for the gas generation term.

In general, the method outlined herein may be used with pumping test data to develop improved estimates of the gas generation term.

To simplify understanding of the proposed method, one worked example of using it is provided below.

Step 1. Take a data-set from a pumping test and run AIR/W to determine a best-fit intrinsic permeability value using a reasonable assumed anisotropy ratio and the actual partial penetration. The resulting value of intrinsic permeability would account for the conditions within the landfill such as two-phase flow, partial penetration and anisotropy, but not the gas generation term.

- Actual pumping pressure data from GW01-04 test-well;
- Actual measured flow rate for the pumping step is Q_g= 32.4[m^3/hour];
- The estimated gas generation rate is $R_g = 2.19 \cdot 10^{-7} \left[\frac{kg}{m^3 \cdot s}\right]$ (i.e. methane generation rate $R_{CH4} = 5 \left[\frac{m^3}{Mg \cdot year}\right]$)

$$R_g = \frac{\left[\left(\frac{R_{CH_4}}{f_{CH_4}}\right) \cdot \left(\rho_{waste}^{app}\right) \cdot \rho_g\right]}{(3.1536 \cdot 10^7)} = \frac{\left[\left(\frac{5\ [m^3/Mg/year]}{0.57}\right) \cdot \left(0.7 \left[\frac{Mg}{m^3}\right]\right) \cdot 1.127 [\frac{kg}{m^3}]\right]}{\left(3.1536 \cdot 10^7 \left[\frac{s}{year}\right]\right)}$$

$$= 2.19 \cdot 10^{-7} [kg/(m^3 \cdot s)]$$

- Assumed anisotropy ratio k_x/k_z=10;
- Actual partial penetration L_S/D_T=0.50[m/m]; then
- The best-fit value of intrinsic permeability from an AIR/W simulation is $k_i^{initial}$=1.86*10^{-13}[m^2].

Step 2. Determine the correction factor for gas generation, $\varphi_{kR,}$ to adjust the previously estimated value of intrinsic permeability (from the AIR/W simulation).

If R_g is assumed as explained above, Λ_{waste} is equal 2.16*10^{-5}[1/m^3];

$$R_g^{**} = \frac{R_g}{\rho_g} \cdot 3600 = \frac{2.19 \cdot 10^{-7} \left[\frac{kg}{m^3 \cdot s}\right]}{1.127 \left[\frac{kg}{m^3}\right]} \cdot 3600 \left[\frac{s}{hour}\right] = 7 \cdot 10^{-4} \left[\frac{m^3}{m^3 \cdot hour}\right]$$

$$\Lambda_{waste} = \frac{R_g^{**}}{Q_g} = 7 \cdot 10^{-4} \left[\frac{m^3}{m^3 \cdot hour}\right] / 32.4 \left[\frac{m^3}{hour}\right] = 2.16 \cdot 10^{-5} \left[\frac{1}{m^3}\right]$$

Fig. 4.14 schematically shows how φ_{kR} was defined using the estimated value of Λ_{waste} (i.e. Q_g=*32.4[m^3/hour]* and R_{CH4} =*5[m^3/Mg/year]*). Using Fig. 4.14, φ_{kR}=0.4 for Q_g=32.4[m^3/hour]:

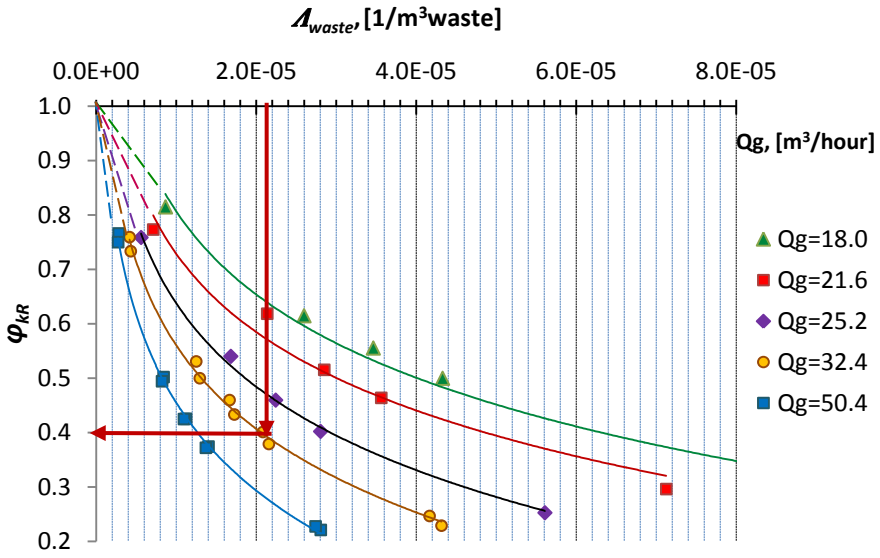

Fig. 4. 14. Use of correction φ_{kR} to estimate the gas generation rate using pumping test data.

Based on a value of φ_{kR}=*0.4*:

- $k_i = k_i^{F/P} \cdot \varphi_{kR}$ =*1.86*10^{-13}[m^2]*0.4 =7.44*10^{-14}[m^2]*, where the estimated value of k_i incorporated the gas generation term of R_g= 2.2*10^{-7}[kg/(m^3*s)] (i.e. the methane generation rate R_{CH4} =5[m^3 /Mg/year].

In other words, an average intrinsic permeability value of 7.4*10^{-14}[m^2] rather than 1.9*10^{-13}[m^2] would better fit the test data since it incorporate the gas generation term for the landfill. It is easy to see only from this example that if the intrinsic permeability

were determined using AIR/W and thereby ignoring gas generation, its value would be overestimated by a factor of 2.5.

The example above (as well as all others described in this thesis) shows that the gas generation term is relatively more significant than partial penetration and anisotropy in terms of affecting the results:

- in this thesis, the correction factor for the combined effect of partial penetration and anisotropy was defined to be around 0.9; and
- the correction factor for the gas generation term, on the other hand, was equal to 0.4 (and in cases with a higher gas generation rate, may be less than 0.2).

It must be emphasized that the gas generation rate in the Spadina landfill is relatively low compared to many landfills. For a landfill with a higher gas generation rate, the effect of ignoring gas generation would be greater.

CHAPTER 5
SUMMARY, CONCLUSIONS, AND RECOMMENDATIONS

5.1. Introduction

To date, little rigorous research has been published regarding the simultaneous generation and flow of gasses within MSW landfills. The properties of MSW are highly complex, anisotropic and likely to vary with depth and over time as a result of aging and degradation. This research was intended to provide a simply-applied correction to readily-available tools for analysis of gas pumping tests in unsaturated porous media, so as to more realistically and accurately represent the intrinsic permeability value for MSW in the case when gas is being generated in-situ as well as moving through the porous medium in response to pressure gradients. Ultimately, this thesis demonstrated that the gas generation term should not be ignored when the gas flow is evaluated for MSW.

The numerical analysis of gas flow within MSW is described in the previous chapters of the thesis. The conceptual model was implemented mathematically by defining the governing equations and solving using both FEA and FD methods. Transient numerical modelling for three test-wells was completed with the finite element computer package (AIR/W) as the first model solution. Simulations were carried out using pumping test data from the following test-wells: GW01-04, GW02-04, and GW10-07 using this two-dimensional axisymmetric saturated/unsaturated two-phase flow modelling software. A second transient solution was developed using a simple 1-dimentional finite difference solution that incorporated the gas generation effect which actually occurs in landfills. This 1-D FD solution was applied to pumping test results from the following test-wells: GW01-04, GW02-04, GW04-07, and GW10-07.

To compare the results of two approaches, AIR/W and the 1-D FD solution, the data from three test-wells were used (i.e. GW01-04, GW02-04, and GW10-07). To evaluate

the effect of gas generation, one additional test-well, GW04-10, in the 1-D FD solution was used. In addition, to verify the 1-D FD results, the SEEP/W package (GeoStudio) was used as well. This chapter summarizes what has been learned from the problems faced within the model set-ups, the parametric study, the development of the 1-D FD solution, and an example of the proposed methodology for estimating the intrinsic permeability of MSW using LFG pumping test data.

5.2.Summary and Conclusions

The results of the AIR/W test-well models illustrated the complexity of unsaturated flow in the porous medium, where it was assumed that the effect of the gas generation present in the landfill can be ignored. This assumption may not be reasonable; however, it represents a practical approach given the features and limitations of the widely available software. The evolution of a simple solution starting from initial simulations using AIR/W and increasing in complexity provided valuable insight into the problem also a basis for future studies.

From the sensitivity analysis, it was determined that the AIR/W test-well models are highly sensitive to the input parameters. The intrinsic permeability range at which the gas flow moves to the well and thereby can be pumped varied by about two orders of magnitude in average for all three AIR/W test-well models. The parametric study of anisotropy, which was varied from 1 to 10 for the initial 36-metre models (representing conditions as actually constructed in the Spadina landfill), showed that it affected the best-fit intrinsic permeability values by at most 40% for the three well pumping tests. The parametric study of the partial penetration ratio where the anisotropy ratio equals to one (k_x/k_y=1) demonstrated that the best-fit intrinsic permeability results changed by approximately 6.5%; in other words the partial penetration effect may be considered less important in affecting the results compared with the effect of anisotropy. However, the assumption of full penetration ($L_S/D_T=1$) cannot be used for flow models in AIR/W due to boundary condition and convergence issues. On the one hand, the features and capability of AIR/W allows for the development of models even for a relatively complicated input gas pressure function over time that may incorporate three drawdown

steps as the wellbore boundary condition. However, increasingly complicated wellbore gas pressure functions, such as those which incorporated (as the wellbore boundary condition) more than three-drawdown steps plus recovery were found to be time-consuming and somewhat more difficult in terms of the process of finding the permeability value that would best fit the observed field data.

A solution with its best-fit intrinsic permeability value was ultimately defined for each pumping step for all three test wells. Unfortunately, while GeoStudio's AIR/W program is powerful and widely available, the effect of gas generation cannot be evaluated as this capability has not been incorporated in the software; accordingly, an alternative approach was developed to evaluate its effect and provide a simple correction for results obtained using the widely-available GeoStudio software suite.

The 1-D FD solution was developed to evaluate the gas generation effect and to determine whether or not it can be ignored when determining an intrinsic permeability value using flow rate and wellhead pressure data measured during a LFG pumping test. The results of simulations made using the 1-D FD solution for all four test-wells suggested that gas generation significantly affects the best-fit intrinsic permeability values. Based on the analysis of these results, the following effects of gas generation on the best-fit values of intrinsic permeability were observed:

- The gas generation rate has a greater effect on the best-fit values of intrinsic permeability during the recovery period;
- The effect of the gas generation rate is greater where the estimated best-fit values of the intrinsic permeability are lower;
- In general, better fit to measured gas pressure flow rate data were realized when the gas generation rate was taken into account; and
- There was a consistent relationship between the intrinsic permeability corrections.

From the pumping test data, best-fit values of intrinsic permeability were determined for the case of zero gas-generation using both approaches (i.e. AIR/W and the 1-D FD

solution). Similarly, for the case in which the gas generation was included, the best-fit permeability value was determined using the 1-D FD solution. These respective best-fit values were then compared to develop a correction factor to account for this effect. Since it has been determined that the effect of partial penetration is much less significant than that of anisotropy, the results obtained from AIR/W simulations for the case with L_S/D_{T2} and k_x/k_y=1 were compared with the 1-D FD solution results where the total gas generation was set equal to zero.

For all three pumping test datasets, the range of best-fit intrinsic permeability values was $1.9x10^{-13}$ to $3.8x10^{-13}$[m^2] using AIR/W. Using the 1-D FD solution, on the other hand, the best-fit intrinsic permeability values were found to be $1.5x10^{-14}$ to $2.6x10^{-13}$ [m^2]. Comparing these results (i.e. 1-D FD and AIR/W for comparable cases), it was found that they differ by 2% to 5%. The reasons for this difference are:

- -the major factor is the non-constant volumetric gas content in AIR/W, because it simulates two-phase flow and pore-water flow is also induced together with gas flow during each simulation; and
- -the partial penetration seems to be relatively insignificant, but still, convergence of a simulation incorporating "fully-penetrating" wells was not achieved using AIR/W.

By following the methodology for numerical analysis outlined in Chapter1 and Chapter3, the numerical models were developed and simulations completed. Based on the results obtained from both approaches, the following main lessons have been learned:

- both approaches can be used to define the intrinsic permeability values; and
- gas generation should not be ignored.

5.3.Significance of the findings

The ability to accurately determine the properties of the landfilled waste is potentially important in well-field design. In order to complete a rigorous network analysis of a wellfield, the wellhead pressure and flow rates must be known, in addition to the spacing of the wells and diameter of the header pipes. All of these will affect the

efficiency of gas extraction; excessive wellhead vacuum in certain locations may not only be inefficient from the perspective of gas capture, but may also induce air ingress and provoke the risk of underground fire.

For the City of Saskatoon Landfill, the methane generation rate is 3 to 5 [m^3/Mg/year], thus it may be shown that during the pumping tests carried out at the site, the landfilled waste within the zone of influence (ROI) generated a volume of gas between 20% and 97% of the total volume extracted from the well during gas pumping, depending on the test-well location (Fleming 2009).

The research, described in this thesis thus represents an incremental improvement for the analysis of landfill gas pumping tests, thus potentially improving technical and economic performance of LFG collection.

5.4.Need for further research

This study investigated the gas generation effect using a simple 1-D axisymmetric solution to evaluate the influence of the gas generation in terms of estimating an intrinsic permeability value for the landfilled waste.

In general, it was found that the computer package, AIR/W, is a powerful tool for simulation a wide range of two-phase flow problems. The current study showed that AIR/W might be used to analyze the transient two-phase unsaturated flow in a landfill. Since the gas generation term cannot be incorporated using this software, an approximate method has been developed to enable the intrinsic permeability as determined using AIR/W to be adjusted using a correction factor for gas generation, determined through the 1-D FD solution.

In addition, the author suggests that incorporating the ability to apply a gas flow rate, rather than only gas pressure, as a boundary condition at the wellbore area would make AIR/W simpler and more intuitive for application to this type of problem. The ability to incorporate non-conservation of fluid mass (such as a gas generation rate produced by a landfill) as an input parameter in AIR/W would render this software even more flexible for use with a wider range of problems.

Further investigation of the gas generation effect would be beneficial for both future efficient design and for optimizing existing facilities in terms of environmental impact, improved sustainability and enhanced economics of LFG utilization for owners.

LIST OF REFERENCES

Amro, M.M. 2004. Treatment Techniques of Oil-Contaminated. Soil and Water Aquifers. Petroleum Engineering Department. King Saud University. Saudi Arabia. Available from www.psipw.org/English_PDF/2_Dry/E2-8.pdf [Accessed on 19 March 2010].

Barbour, S.L. and Krahn, J. (2004). Numerical Modelling – Prediction or Process. Canadian Geotechnical News, December: 44-52.

Barbour, S.L., 2010.Advanced hydrogeology. Course notes for CE 871. Department of Civil Engineering. University of Saskatchewan. Canada.

Barenblatt, G. I., Zheltov, I. P., and Kochina, I. N. 1960. Basic concepts in the theory of seepage of homogeneous liquids in fissured rocks. Journal of Applied Mathematics and Mechanics (Engl. Transl.), **24(5):** 1286-1303.

Barenblatt, G. I. and Zheltov, I. P. 1960. Fundamental equations of filtration of homogeneous liquids in fissured rocks. Doklady Akademii Nauk SSSR, **132(3):** 545-548.

Bear, J. 1972. Dynamics of Fluids in Porous Media. Dover Publications, Inc., New York.

Bear, J. and Bachmat, Y. 1990. Introduction to Modeling of Transport Phenomena in Porous Media. © Kluwer Academic Publishers. Dordrecht. The Netherlands.

Beaven, R. P., Cox, S. E., and Powrie, W. 2007. Operation and performance of horizontal wells for leachate control in a waste landfill. Journal of Geotechnical and Geoenvironmental Engineering: 1040-1047. doi: 10.1061/(ASCE)1090-0241(2007)133:8(1040).

Beaven, R. P., Powrie, W., and Zardava, K. 2008. Hydraulic properties of MSW. Geotechnical Characterization, Field Measurement, and Laboratory Testing of Municipal Solid Waste. Ed. by Zekkos, D., Geotechnical Special Publication, **209:** 1-43.

Bleiker, D.E., Farquhar, G., and McBean, E. 1995. Landfill settlement and the impact on site capacity and refuse hydraulic conductivity. Waste Management and Research, **13(6):** 533-554. doi: 10.1177/0734242X9501300604.

Bravo, M.C., Araujo, M., and Lago, M.E. 2007. Pore network modeling of two-phase flow in a liquid-(disconnected) gas system. Physica A, **375(1):** 1-17.

Brooks, R.H. and Corey, A.T. 1964. Hydraulic properties of porous media. Hydrological Papers No 3. Colorado State University. Fort Collins, Collorado.

Buchanan, D., Clark, C.F., Ferguson, N.S., and Kenny, N.J. 2001. Hydraulic characteristics of wet-pulverized municipal waste. J. CIWEM, March: 14-20.

Collazos, O.M., Bowders, J.J., and Bouazza, M. 2002. Prefabricated vertical drains for use in soil vapor extraction applications transportation research record 1786. Paper No. 02-2984. ISSN: 0361-1981: 104-111.

Corey, A.T. 1954. The interrelation between gas and oil relative permeabilities. Produce Monthly, **Nov.:** 39-41.

Corey, A.T., Rathjens, C.H., Henderson, J.H., and Wyllie, M.R.J. 1956. Three-phase relative permeability. Journal of Petroleum Technology, **8(11):** 63-65. doi: 10.2118/737-G.

El-Fadel, M., Findikakis, A.N., and Leckie, J.O. 1997a. Gas simulation models for solid waste landfills. Critical Reviews in Environmental Science and Technology, **27(3):**237-283. doi: 10.1080/10643389709388500

El-Fadel, M., Findikakis, A.N., and Leckie, J.O. 1997b. Modeling leachate generation and transport in soil waste landfills. Environmental Technology, **18(7):** 669-686. doi: 10.1080/09593331808616586.

Falta, R.W. 1996. A program for analyzing transient and steady-state soil gas pump tests. Ground Water, **34(4):** 750-755.

Fatta, D., Naoum, D., and Loizidou, M. 2002. Integrated environmental monitoring and simulation system for use as a management decision support tool in urban areas. Journal of Environmental Management, **64(4):** 333-343. doi:10.1006/jema.2001.0485

Fetter, C.W. 2001. Applied Hydrogeology. 4th Ed. Prentice-Hall, Inc. Upper Saddle River, New Jersey.

Fleenor, W.E. and King, I.P. 1995. Identifying limitations on use of the HELP model. Geotechnical Special Publication, **53:** 121-138.

Fleming, I.R. 2009. Evaluation of retrofitting rapid stabilization and gas collection in older landfills. Final report. Waste management and geoenvironmental engineering laboratory. Department of Civil and Geological Engineering. University of Saskatchewan. Canada.

Fleming, I.R. 2011. Indirect measurements of field-scale hydraulic conductivity of waste from two landfill sites. Waste Management, **31(12)**: 2455-2463. PMID: 21903374

Fredlund, M.D., Fredlund, D.G., and Wilson, G.W. 2000. An equation to represent grain-size distribution. Canadian Geotechnical Journal, **37(4):** 817-827.

Fredlund, D.G. and Rahardjo, H., 1993. Soil Mechanics for Unsaturated Soils. John Wiley & Sons, Inc.

Fredlund, D. G., and Xing, A. 1994. Equations for the soil-water characteristic curve. Canadian Geotechnical Journal, **31:** 521-532.

Fredlund, M.D., Wilson, G.W., and Fredlund, D.G. 2002. Use of the grain-size distribution for estimation of the soil-water characteristic curve. Canadian Geotechnical Journal, **39(5)**: 1103-1117. doi: 10.1139/T02-049.

Gee, J. 1984. Predicting leachate generation in landfills: a new method. Proceedings of Mid-Atlantic-Industrial Waste Conference: 548-567.

GeoStudio. 2010. Air Flow Modeling with AIR/W 2007. An Engineering Methodology, 4th Ed. © 2010 by GEO-SLOPE International, Ltd.

Guiguer, N., Franz, T. and Zaidel, J. (1995) AIRFLOW/SVE Version 1, Axisymmetric Vapor Flow and Transport Simulation Model. Waterloo Hydrogeologic Software, Sept. 1995.

Huang, M., Fredlund, D.G., and Fredlund, M.D. 2010. Comparison of measured and PTF predictions of SWCCs for loess soils in china, Geotechnical and Geological Engineering, **28(2):** 105-117.

Hudson, A.P., White, J.K., Beaven, R.P., and Powrie,W. 2004. Modelling the compression behaviour of landfilled domestic waste. Waste Management, **24(3):** 259–269.

Hudson, A.P., Beaven, R.P., and Powrie,W. 2009. Assessment of vertical and horizontal hydraulic conductivities of household waste in a large scale compression cell. In: Proceeding of the 12th Waste Management and Landfill Symposium Sardinia 2009, Ed. By Cossu, R., Dial, L.F., and Stegman, R. CISA, S. Marherita di Pula, Italy. 641-642.

Jain, P., Powell, P., Townsend, T.G., and Reinhart, D.R. 2005. Air permeability of waste in a municipal solid waste landfill. Journal of Environmental Engineering, **131(11):** 1565-1573. doi: 10.1061/(ASCE)0733-9372(2005)131:11(1565).

Jennings, A.A. 1997. A vapor extraction teaching module based on AIRFLOW/SVE. Environmental Modelling and Software, **12(4):** 335-353. doi:10.1016/S1364-8152(97)00028-5.

Kazimoglu, Y.K., McDougall, J.R., and Pyrah, I.C. 2005. Moisture retention and movement in landfilled waste. Proc. GeoProb2005 Int'l. Conf. Problematic Soils, Eastern Mediterranean University. North Cyprus. Ed. Bilsel, H.: 307-314.

Kazimoglu, Y.K., McDougall, J.R., and Pyrah, I.C. 2006. Unsaturated hydraulic conductivity of landfilled waste. Unsaturated Soils 2006, Proc. 4th Intl. Conf. Unsaturated Soils, Arizona, 2006, eds. Miller, Zapata,Houston & Fredlund, ASCE Geotechnical Special Publication, **147:** 1525-1534.

Kindlein, J., Dinkler, D., and Ahrens, H. 2006. Numerical modelling of multiphase flow and transport processes in landfills. Waste Management and Research, **24(4):** 376-387. doi: 10.1177/0734242X06065506.

Knudsen, H.A., Hansen, A. 2002. Relation between pressure and fractional flow in two-phase flow in porous media. Physical Review E, **65(5):** 1-10. doi:10.1103/PhysRevE.65.056310.

Korfiatis, G. P., Demetracopoulos, A. C., Bourodimos, E. L., and Nawy, E. G. 1984. Moisture transport in a solid waste column. Journal of Environmental Engineering, **110(4):** 789-796.

Lanvda, A.O., Pelkey, S.G., and Valsangkar, A.J. 1998. Coefficient of permeability of municipal refuse. Environmental Geotechnics, **1(4):** 63-67.

McCreanor P.T. and Reinhart D.R. 2000. Mathematical modelling of leachate routing in a leachate recirculating landfill. Water Research, **34(4):** 1285–1295.

McDougall, J.R., Pyrah, I.C. and Yuen, S.T.S. 2004. Extended phase relations and load effects in MSW. Waste Management, **24(3):** 251–257.

McDougall, J. 2007. A hydro-bio-mechanical model for settlement and other behavior in landfilled waste, Computers and Geotechnics, **34(4):** 229–246. doi:10.1016/j.compgeo.2007.02.004.

Nastev, M. 1998. Modeling landfill gas generation and migration in sanitary landfills and geological formations. PhD thesis, Universite´Laval, Que´bec.

Nastev, M., Therrien, R., Lefebvre, R., and Gelinas, P. 2001. Gas production and migration in landfills and geological materials. Journal of Contaminant Hydrology, **52(4):** 187–211.

Nastev, M., Lefebvre, R., Therrien, R., Gelinas, P. 2003. Numerical modeling of lateral landfill gas migration. Journal of Solid Waste Technology and Management, **29 (4):** 265-276.

Osiensky, J.L. and Williams, R.E. 1997. Potential lnaccuraciees in MODFLOW simulations involving the SIP and SSOR methods for matrix solution. Ground Water, **35(2):** 229-232.

Oweis I. S., Smith D. A., Ellwood R. B. and Greene D. 1990. Hydraulic characteristic of municipal refuse. Journal of Geotechnical Engineering, **116(4):** 539-553.

Oweis, I.S. and Khera, R.P. 1998. Geotechnology of Waste Management.2nd ed. Boston, MA: PWP Publishing Company.

Powrie, W., Beaven, R. 1999. Hydraulic properties of household waste and implications for landfills. Proceedings of the Institution of Civil Engineers: Geotechnical Engineering, **137(4)**: 235-247.

Powrie, W., Beaven, R., Hudson, A. 2005. Factors affecting the hydraulic conductivity of waste. International workshop "Hydro-Physico-Mechanism of Landfills". LIRIGM, Grenoble 1 University, France, March 21-22, 2005. Available from

www.infogeos.com/files/news/document/01-Powrie.pdf [Accessed on 19 May 2010].

Powrie, W. 2008. Landfill Hydrogeology: impact and challenges. 28 February 2008 Conference. University of Southampton. School of Civil Engineering and Environment. United Kingdom. Available from www.geolsoc.org.uk/webdav/site/GSL/shared/pdfs/specialist%20and%20regional%20groups/POWRIE.pdf [Accessed on May 28th, 2010]

Powrie, W., Beaven, R., Hudson, A. 2008. The influence of landfill gas on the hydraulic conductivity of waste. Geotechnical Special Publication No. 177**.** GeoCongress 2008. GeoTechnics of Waste Management and Remediaton, March 9, 2008. New Orleans, Louisiana: 264–271.

Pruess, K. 1987. TOUGH User's Guide, Nuclear Regulatory Commission Report NUREG/CR-4645; also Lawrence Berkeley Laboratory Report LBL-20700.

Pruess, K. 1991. TOUGH2 - A General Purpose Numerical Simulator for Multiphase Fluid and Heat Flow, Lawrence Berkeley Laboratory Report LBL-29400, Berkeley, CA.

Pruess, K., Oldenburg, C., and Moridis, G. 1999. TOUGH2 User's Guide, Version 2.0. Earth Sciences Division, Lawrence Berkeley Laboratory, University of California, Berkeley, California 94720.

Richards, L.A. 1931. Capillary Condition of Liquids through Porous Mediums. Physics, **1(5):** 318-333. doi: 10.1063/1.1745010.

Saskatoon waste and recycling plane. October 2007. Saskatoon. SK. Available from: http://www.saskatoon.ca/DEPARTMENTS/Utility%20Services/Environmental%20Services/Waste%20Minimization/Documents/swrp.pdf. [Accessed on Jan.14th, 2011]

Schroeder, P. R., Gibson, A. C., and Smolen, M. D. 1984. The hydrologic evaluation of landfill performance (HELP) model (1984b). Volume II. Documentation for version 1. Technical Resource Document EPA/530-SW-84-010. US Environmental Protection Agency. Cincinnati. OH.

Schroeder, P. R., Dozier, T.S., Zappi, P. A., McEnroe, B. M., Sjostrom, J. W., and Peyton, R. L. 1994. The Hydrologic Evaluation of Landfill Performance (HELP) Model: Engineering Documentation for Version 3. EPA/600/R-94/168b, September 1994, U.S. Environmental Protection. Agency Office of Research and Development, Washington, DC.

Schmidt, P. M. 2010. Evaluation of capacitance moisture sensors for use in municipal solid waste. MS Thesis. Department of Civil and Geological Engineering. University of Saskatchewan. Canada.

Simms, P.H. and Yanful, E.K. 2004. Estimation of soil-water characteristic curve of clayey till using measured pore-size distributions. Journal of Environmental Engineering, **130(8):** 847-854.

Strack, O.D.L. 1989. Ground Water. Prentice-Hall, Inc.

Stevens, D.W. 2012. An empirical analysis of gas well design and pumping tests for retrofitting landfill gas collection. MS thesis. Department of Civil Engineering. University of Saskatchewan. Canada.

Suthersan, S.S. 1999. Soil Vapor Extraction. Remediation engineering: design concepts. © CRC Press LLC.

Taylor, G.R. 2005. Integrating Quantitative and Qualitative Methods in Research. 2nd Ed. © University Press of America, ® Inc.

Tseng, P-H., Sciortino, A., and Genuchten, M.T. 1995. A partitioned solution procedure for simulating water flow in a variably saturated dual-porosity medium. Advances in Water Resources, **18(6):** 335-343.

US EPA. Soil Vapor Extraction. 1994. How to Evaluate Alternative Cleanup Technologies for Underground Storage Tank Sites: A Guide for Corrective Action Plan Reviewers. Chapter II. (EPA 510-B-94-003; EPA 510-B-95-007; and EPA 510-R-04-002). Available from http://www.epa.gov/oust/pubs/tum_ch2.pdf [Accessed on 10 February 2010].

van Genuchten, M. T. 1980. A closed-form equation for predicting the hydraulic conductivity of unsaturated soils. Soil Science Society of America Journal, **44:** 892-898.

Vigneault, H., Lefebvre, R., and Nastev, M. 2004. Numerical simulation of the radius of influence for landfill gas wells. Vadose Zone Journal, **3:** 909-916.

White, J., Robinson, J., and Ren, Q. 2004. Modelling the biochemical degradation of solid waste in landfills. Waste Management, **24(3):** 227-240.

White, J.K., Beaven, R.P., Powrie, W., and Knox, K. 2011. Leachate recirculation in a landfill: Some insights obtained from the development of a simple 1-D model. Waste Management and Research **31(6):** 1210-1221.

Zekkos, D. P. 2005. Evaluation of Static and Dynamic Properties of Municipal Solid Waste. PhD thesis. Department of Civil and Environmental Engineering. University of California. Berkeley.

Zekkos, D., Bray, J.D., Kavazanjian, E., Matasovic, N., Rathje, E.M., Riemer, M.F., and Stokoe, K.H. 2006. Unit weight of municipal solid waste. Journal of Geotechnical and Geoenvironmental Engineering **132(10):** 1250-1261. doi: 10.1061/(ASCE)1090-0241(2006)132:10(1250).

APPENDICES

APPENDIX A. TEST-WELLS GEOMETRY AND LANDFILLED DATA

The major parameters of test-wells geometry, GW01-04, GW02-04, GW04-07, and GW10-07, shown in Table A.1 as they were actually constructed in the Spadina Landfill (Fleming 2009).

Table A. 1. Test-wells geometry as were constructed in the field.

LFG Well	Screen length (L_S)	Screen diameter	Depth of screen (L_{DS})	Pipe length (drilling depth)	Pipe diameter	Hole diameter	Gravel pack
GW01-04	ft 60.0 m 18.3	inch 6.0 m 0.2	Ft 20.0 m 6.1	ft 80.0 m 24.4	inch 2.0 m 0.1	inch 152.0 m 3.8	Yes
GW02-04	ft 55.0 m 16.8	inch 6.0 m 0.2	ft 30.0 m 9.1	ft 85.0 m 25.9	inch 2.0 m 0.1	inch 152.0 m 3.8	Yes
GW04-07	ft 18.0 m 5.5	inch 8.0 m 0.2	ft 22.0 m 6.7	ft 40.0 m 12.2	inch 2.0 m 0.1	inch 152.0 m 3.8	Yes
GW10-07	ft 41.0 m 12.5	inch 8.0 m 0.2	ft 28.0 m 8.5	ft 69.0 m 21.0	inch 4.0 m 0.1	inch 152.0 m 3.8	Yes

The measured field data, used in this work for analysis, during the short-term pumping tests at each of the four test-wells (GW01-04, GW02-04, GW04-07, and GW10-07) are provided in Table A.2 in the following two pages.

Table A. 2. Measured field data during the short-term pumping tests at GW01-04, GW02-04, GW04-07, and GW10-07.

LFG test-well	Time	Hrs Passed	CH4	CO2	O2	Balance	Adj. Flow	Init. Flow	Temp	Adj. Static Pressure	Init. Static Pressure	Adj. Differential Pressure	Init. Differential Pressure	System Pressure	DRWDN
			%	%	%	%	Scfm	Scfm	degF	in H2O	in H2O	in H2O	in H2O	in H2O	in H2O
GW01-04	13:20:00	0.00	57.6	42.0	0.0	0.4	12	6	0	-1.4	0.5	0.037	0.007	-48.82	1.8
	13:28:00	0.13	-	-	-	-	12	11	75	-1.4	-1.3	0.031	0.032	-48.75	2.0
	13:52:00	0.53	-	-	-	-	13	10	80	-1.5	-1.5	0.036	0.030	-48.78	2.2
	14:33:00	1.22	-	-	-	-	12	10	75	-2.2	-1.7	0.036	0.027	-48.19	2.5
		1.47					13				-2.0				2.5
	14:48:00	1.47	-	-	-	-	20	15	70	-3.3	-2.0	0.102	0.056	-44.03	3.5
		1.75					20				-3.0				4.0
	15:43:00	2.38	-	-	-	-	19	18	70	-3.5	-3.5	0.090	0.079	-44.26	4.1
	16:27:00	3.12	-	-	-	-	20	19	80	-3.6	-3.6	0.099	0.095	-44.76	4.1
		3.28					20				-3.6				0.9
	16:37:00	3.28	-	-	-	-	0	0	0	-0.2	-0.4	0.305	0.370	-0.27	0.5
	16:41:00	3.35	-	-	-	-	0	0	0	0.0	0.00	-0.053	-0.041	-0.06	0.4
	16:48:00	3.47	-	-	-	-	0	0	0	0.1	0.1	-0.103	-0.060	0.17	0.3
	16:55:00	3.58	-	-	-	-	0	0	0	0.2	0.2	-0.161	-0.090	0.25	0.1
GW02-04	13:08:00	0.00	57.7	41.2	0	1.09	11	0	16	-3	0.3	0.031	0.011	-52.22	0
	13:12:00	0.07	-	-	-	-	11	10	50	-3	-2.6	0.034	0.027	-52.24	2.9
	13:24:00	0.27	-	-	-	-	12	8	61	-3.7	-2.9	0.037	0.02	-48.71	3.2
	13:57:00	0.82	-	-	-	-	12	11	68	-4.2	-3.7	0.037	0.033	-48.61	4
	14:41:00	1.55	-	-	-	-	11	9	69	-4.9	-4.1	0.031	0.021	-47.62	4.4
	14:44:00	1.60	-	-	-	-	22	13	71	-8.1	-4.9	0.125	0.042	-45.53	5.2
	14:52:00	1.73	-	-	-	-	20	21	79	-7.7	-7.7	0.102	0.117	-43.48	8
	15:52:00	2.73	-	-	-	-	20	20	79	-7.6	-7.9	0.106	0.108	-44.21	8.2
	16:34:00	3.43	-	-	-	-	21	20	79	-7.8	-7.7	0.109	0.101	-44.71	8
	16:35:00	3.45	-	-	-	-	0	0	80	-0.2	-0.3	0.32	0.395	-0.17	0.6
	16:46:00	3.63	-	-	-	-	0	0	0	0	0.1	-0.172	-0.16	0.13	0.2
	16:53:00	3.75	-	-	-	-	0	0	0	0	0	-0.175	-0.13	0	0.3

Continue Table A. 1.

LFG test-well	Time	Hrs Passed	CH4	CO2	O2	Balance	Adj. Flow	Init. Flow	Temp	Adj. Static Pressure	Init. Static Pressure	Adj. Differential Pressure	Init. Differential Pressure	System Pressure	DRWDN
			%	%	%	%	Scfm	Scfm	degF	in H2O	in H2O	in H2O	in H2O	in H2O	in H2O
GW04-07	12:26:00	-0.07	-	-	-	-	0	0	0	0.2	0.2	0.006	0.007	-33.04	0
	12:30:00	0.00	-	-	-	-	12	11	0	-0.7	-0.7	0.035	0.029	-31.5	0.9
	12:41:00	0.18	-	-	-	-	12	7	80	-0.9	-0.7	0.037	0.014	-31	0.9
	12:45:00	0.25	55.4	42.3	0.1	2.19	12	9	57	-1.2	-0.9	0.037	0.022	-30.66	1.1
	13:09:00	0.65	-	-	-	-	11	13	0	-1.2	-1.7	0.03	0.038	-30.65	1.9
	13:52:00	1.37	-	-	-	-	19	10	63	-1.7	-1.2	0.093	0.025	-28.89	1.4
	13:58:00	1.47	55.9	41.8	0	2.29	21	19	67	-2	-2	0.101	0.087	-28.87	2.2
	14:12:00	1.70	-	-	-	-	20	20	0	-3	-3	0.089	0.09	-28.74	3.2
	14:14:00	1.73	-	-	-	-	19	20	68	-3	-3	0.091	0.096	-28.71	3.2
	15:34:00	3.07	56.7	42	0	1.29	18	17	67	-3.2	-3.1	0.077	0.069	-28.42	3.3
	15:42:00	3.20	-	-	-	-	29	19	68	-3.4	-3.1	0.211	0.096	-26.6	3.3
	15:48:00	3.30	-	-	-	-	29	28	70	-5.2	-3.9	0.212	0.192	-25.45	4.1
	15:54:00	3.40	-	-	-	-	29	32	71	-4.1	-5.3	0.212	0.254	-26.38	5.5
	15:57:00	3.45	-	-	-	-	33	32	0	-4.8	-4.9	0.232	0.222	-26.41	5.1
	15:59:00	3.48	-	-	-	-	29	30	71	-4.8	-4.9	0.212	0.222	-26.48	5.1
	16:26:00	3.93	-	-	-	-	30	30	71	-4.8	-4.8	0.218	0.219	-26.52	5
GW10-07	10:02:00	0.10	-	-	-	-	10	3	66	-1.6	0.3	0.026	0.002	-29.84	0
	10:20:00	0.40	-	-	-	-	9	9	70	-2.1	-1.5	0.023	0.024	-29.49	1.8
	11:17:00	1.35	-	-	-	-	10	8	75	-2.2	-1.9	0.026	0.018	-28.52	2.2
	12:02:00	2.10	-	-	-	-	9	8	78	-2.3	-2.3	0.024	0.019	-28.22	2.6
	12:04:00	2.13	-	-	-	-	15	10	78	-4.1	-2.4	0.06	0.028	-27.15	2.7
	12:47:00	2.85	-	-	-	-	14	15	82	-4.2	-4.2	0.054	0.057	-27	4.5
	13:46:00	3.83	-	-	-	-	15	14	82	-4.1	-4.2	0.057	0.054	-26.8	4.5
	13:48:00	3.87	-	-	-	-	30	13	82	-10.2	-4.1	0.224	0.048	-23.05	4.4
	14:02:00	4.10	-	-	-	-	30	29	86	-10.5	-10.6	0.228	0.216	-23.06	10.9
	14:39:00	4.72	-	-	-	-	30	29	85	-10.5	-10.5	0.223	0.219	-23.2	10.8
	15:51:00	5.92	-	-	-	-	30	29	86	-10.8	-10.4	0.229	0.222	-23.02	10.7

Table A.3 presents ROI values, reported by Fleming 2009, for the range of pumping rates tested for all four test-wells.

Table A. 3. Radius of influence (ROI) for test-wells (after Fleming 2009).

LFG Well	GW01-04	GW02-04	GW04-07	GW10-07
		[m3/s]		
Pumping rate	0.0057 & 0.0189	0.0095	0.0095 & 0.213	0.0142
		[scfm]		
	12 & 40	20	20 & 45	30
Minimum ROI [m]	17 & 25	< 37	21 & 23	24
Maximum ROI [m]	31 & 43	< 37	38 & 38	40

APPENDIX B. MODEL INPUTS FOR BOTH AIR/W AND 1-D FD SOLUTION

The increments of time and radius that were used in 1-D FD solution for all four test-wells shown in Table B.1 including time length (steps).

Table B. 1. Time and radius increment used in the 1-D FD and step-by-step time length used in 1-D FD, AIR/W.

LFG Well	Δr (radius increment), [m]			Δτ (time increment),[s]			Time length, [s]			Total time length, [s]
	Step 1	Step 2	Recovery	Step 1	Step 2	Recovery	Step 1	Step 2	Recovery	
GW01-04	0.25	0.30	0.30	9.9	11.9	8.4	5292	5928	1680	12900
GW02-04	0.25	0.30	0.30	10.4	13.6	5.7	5580	6780	1140	13500
	Step 1	Step 2	Step 3	Step 1	Step 2	Step 3	Step 1	Step 2	Step 3	
GW04-07	0.23	0.27	0.32	9.6	13.2	13.2	5160	6600	2640	14400
GW10-07	0.24	0.30	0.35	14.4	12.5	19.4	7680	6240	7380	21300

APPENDIX C. AIR/W MODEL RESULTS

Table C.1 below provides the intrinsic permeability values that were used for input parameters, the hydraulic conductivity and the air conductivity within the parametric study of the AIR/W models, GW01-04, GW02-04, and GW10-07.

Table C. 1. AIR/W input intrinsic permeability values within the parametric study analysis.

Test data	L_S / D_{T0}	L_S / D_{T1}	L_S / D_{T2}	1-D FD solution (Rg=0	L_S / D_{T0}	L_S / D_{T1}	L_S / D_{T2}	L_S / D_{T0}	L_S / D_{T1}	L_S / D_{T2}	L_S / D_{T0}	L_S / D_{T1}	L_S / D_{T2}
GW01-04	GW-01-04; kx/kz=1				GW-01-04; kx/kz=2			GW-01-04; kx/kz=5			GW-01-04; kx/kz=10		
k_{ir}	2.73E-13	2.62E-13	2.55E-13	3.90E-14	3.01E-13	2.76E-13	2.65E-13	3.60E-13	3.25E-13	3.15E-13	3.82E-13	3.22E-13	3.19E-13
L_S/D_T	0.5	0.56	0.6		0.5	0.56	0.6	0.5	0.56	0.6	0.5	0.56	0.6
GW02-04	GW-02-04; kx/kz=1				GW-02-04; kx/kz=2			GW-02-04; kx/kz=5			GW-02-04; kx/kz=10		
k_{ir}	1.60E-13	1.54E-13	1.50E-13	2.21E-14	1.71E-13	1.60E-13	1.56E-13	1.86E-13	1.70E-13	1.65E-13	2.17E-13	1.96E-13	1.91E-13
L_S/D_T	0.47	0.54	0.58		0.47	0.54	0.58	0.47	0.54	0.58	0.47	0.54	0.58
GW10-07	GW-10-07; kx/kz=1				GW-10-07; kx/kz=2			GW-10-07; kx/kz=5			GW-10-07; kx/kz=10		
Step1	2.50E-13	2.46E-13	2.40E-13		2.78E-13	2.62E-13	2.60E-13	3.20E-13	3.01E-13	2.95E-13	3.54E-13	3.28E-13	3.25E-13
Step2 k_{ir}	2.00E-13	1.95E-13	1.90E-13		2.25E-13	2.17E-13	2.10E-13	2.55E-13	2.45E-13	2.40E-13	2.80E-13	2.70E-13	2.65E-13
Aver.	2.24E-13	2.09E-13	2.14E-13	2.70E-14	2.50E-13	2.38E-13	2.34E-13	2.86E-13	2.71E-13	2.66E-13	3.15E-15	2.98E-13	2.93E-13
L_S/D_T	0.35	0.42	0.48		0.35	0.42	0.48	0.35	0.42	0.48	0.35	0.42	0.48

The sensitivity cases results (parametric study) for GW01-04, GW02-04, and GW10-07 models are shown in Fig. C.1, Fig. C.2, and Fig. C.3.

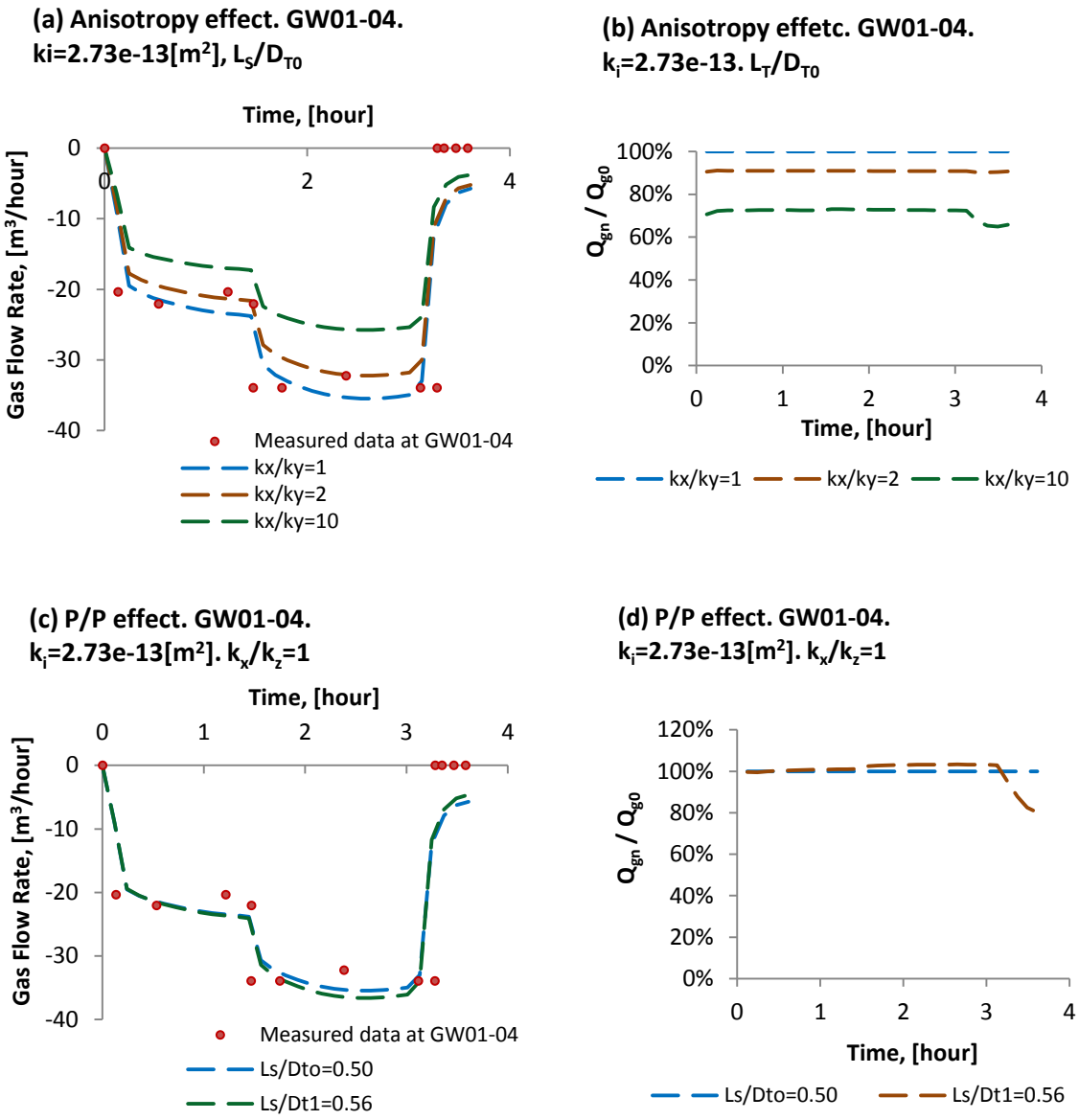

where Q_{gn} is the simulated gas flow in AIR/W for any case of parametric study, except the initial one, and Q_{g0} is the simulated gas flow in AIR/W for the initial case of parametric study ($k_x/k_y=1$ and L_S/D_{T0})

Fig. C. 1. Several simulated gas flow outputs that show the partial penetration and anisotropy effects in GW01-04 AIR/W model.

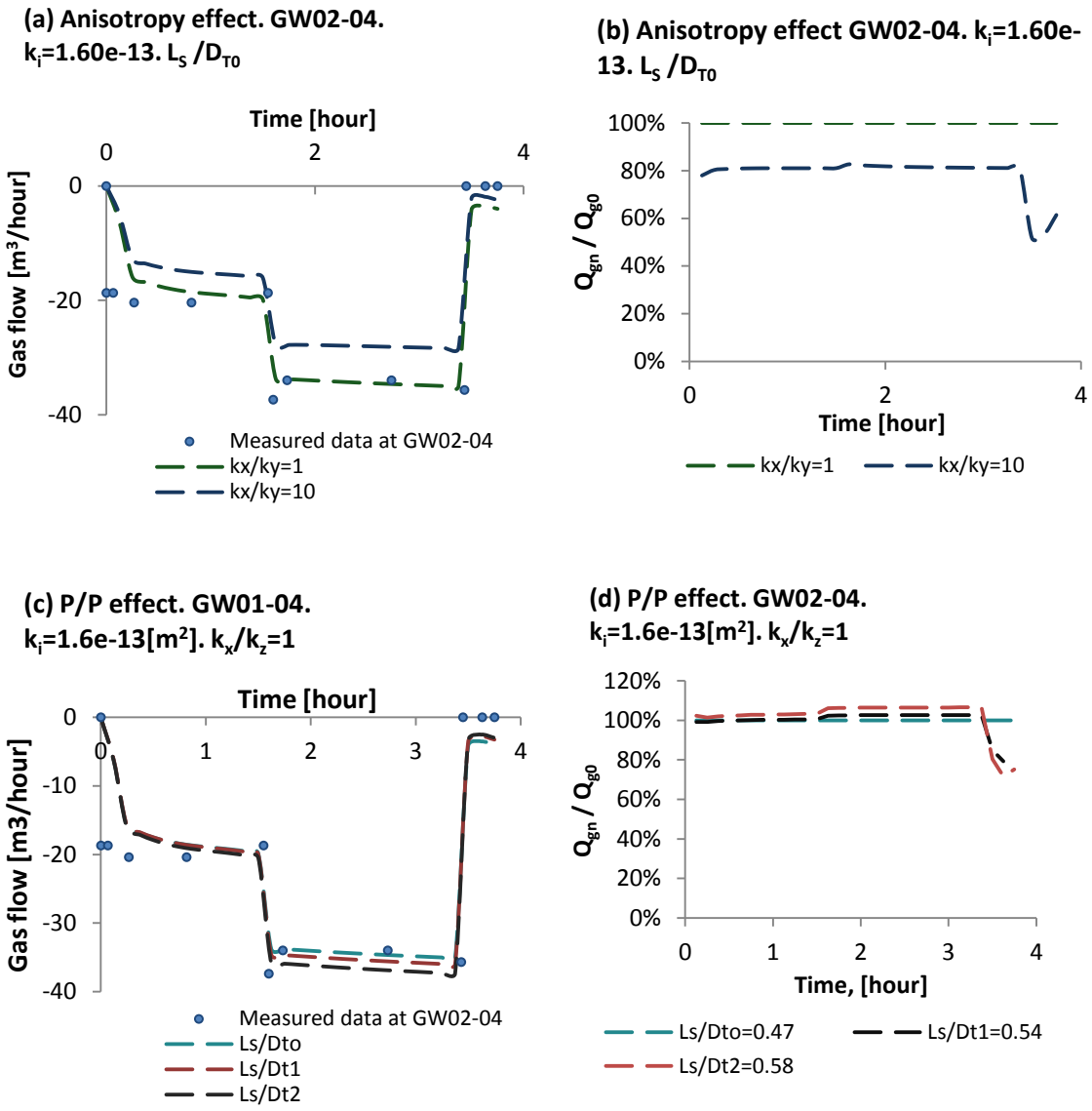

where $\boldsymbol{Q_{gn}}$ is the simulated gas flow in AIR/W for any case of parametric study, except the initial one, and $\boldsymbol{Q_{g0}}$ is the simulated gas flow in AIR/W for the initial case of parametric study ($k_x/k_y=1$ and L_S/D_{T0})

Fig. C. 2. Several simulated gas flow outputs that show the partial penetration and anisotropy effects in GW02-04 AIR/W model.

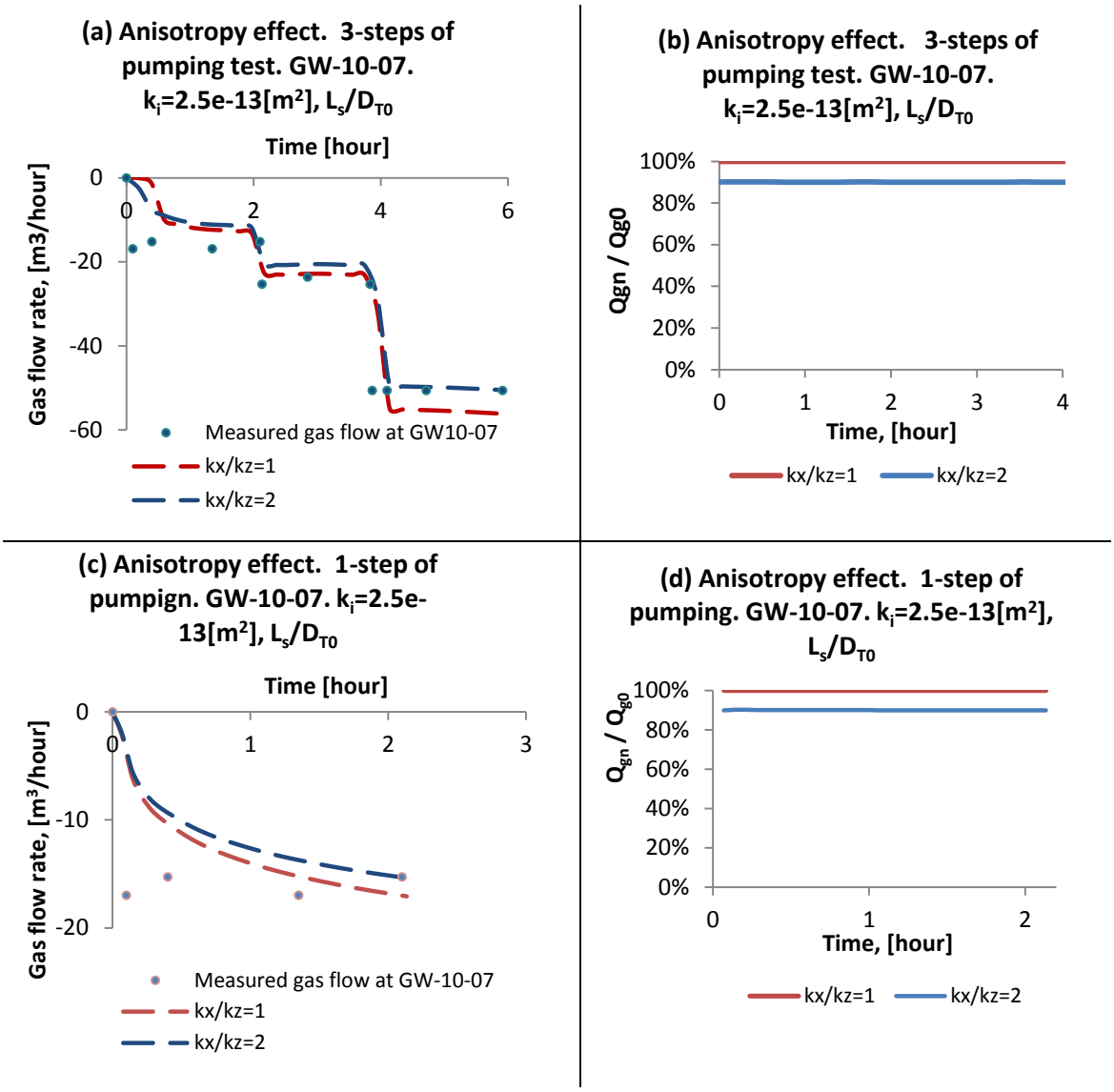

Fig. C. 3. Several simulated gas flow outputs that show the anisotropy effects in GW10-07 AIR/W model.

The example of the statistical analysis, Fig. C.4 shows its statistical results for the GW01-04 simulated gas flow output in AIR/W for the initial case of the parametric study where *kx/ky=1* and $L_S/D_{T0.}$

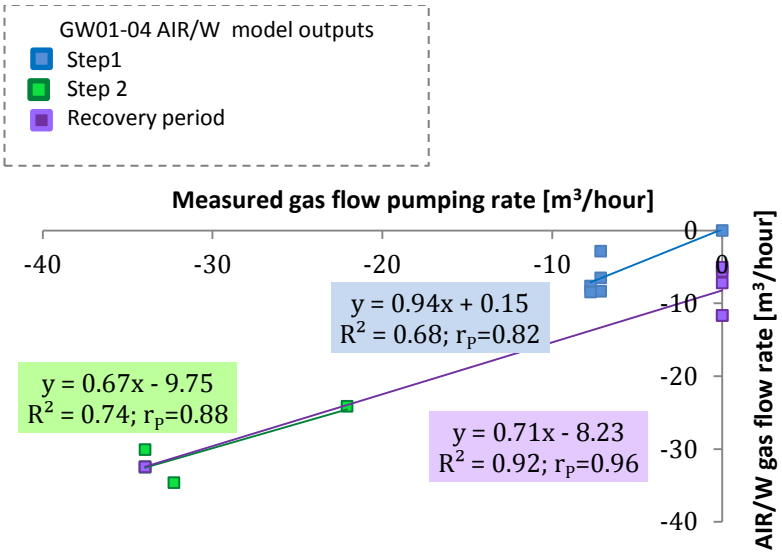

Fig. C. 4. Gas flow rate during the short-term field test at GW-01-04 vs. AIR/W output based on a best-fit value $k_{ir}=2.73*10^{-13}[m^2]$ (initial case *kx/ky=1* and L_S/D_{T0}).

APPENDIX D. 1-D FD SOLUTION RESULTS

The results of few SEEP/W simulations that were used as an alternative way to verify the 1-D FD solution show in Fig. D.2. The SEEP/W model was built as finite element where the geometry, material properties, initial and boundary conditions were defined exactly the same as in 1-D FD solution (with R_g=0). The SEEP/W results, shown in Fig. D.2, were obtained based on the same values of intrinsic permeability as in 1-D FD solution respectively to each of the four test-wells.

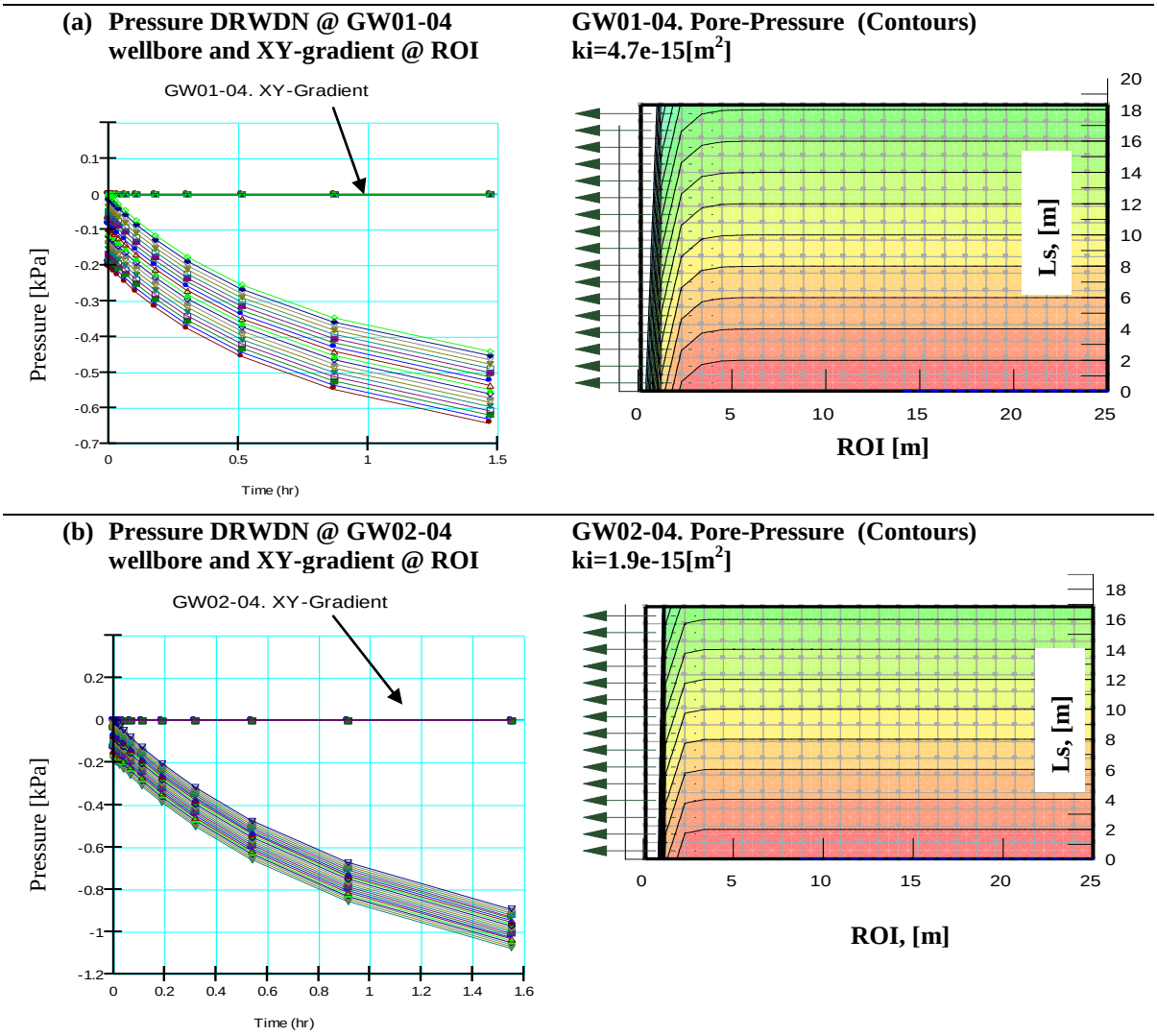

Fig. D. 1. SEEP/W simulation results respectively for each test-well.

(c) Pressure DRWDN @ GW04-07 wellbore and XY-gradient @ ROI

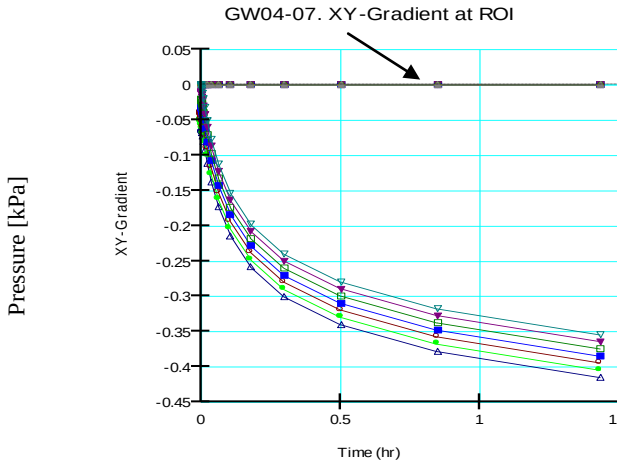

GW04-07. Pore-Pressure (Contours) ki=3.9e-15[m^2]

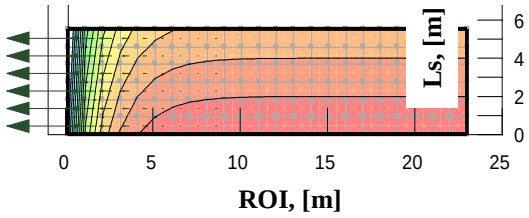

(d) Pressure DRWDN @ GW10-07 wellbore and XY-gradient @ ROI

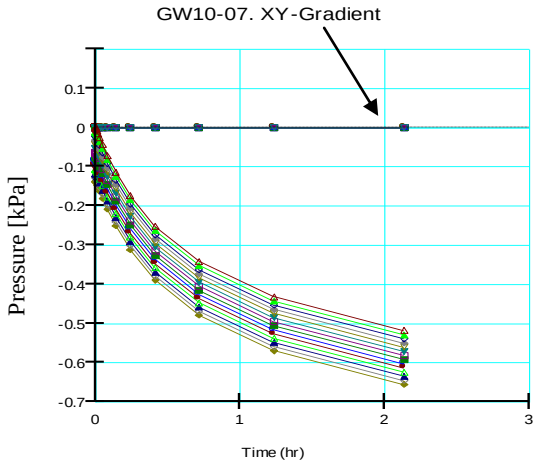

GW10-07. Pore-Pressure (Contours) ki=2.7e-15[m^2]

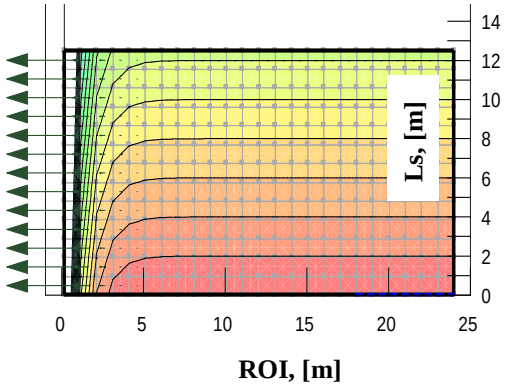

Continue Fig. D.1.

To verify the 1-D FD results, the 1-D FD solution (with R_g=0) and SEEP/W model were run for the first drawdown step and their results graphically shown in Fig. D.3. Both SEEP/W and 1-D FD results, shown in Fig. D.3, were obtained based on the same values of intrinsic permeability respectively to each of the four test-wells. Fig. D.3. also presents the difference in fitting the SEEP/W and the 1-D FD results (i.e R_g term is on ($R_g>0$) and turns off ($R_g=0$)) with the measured field data.

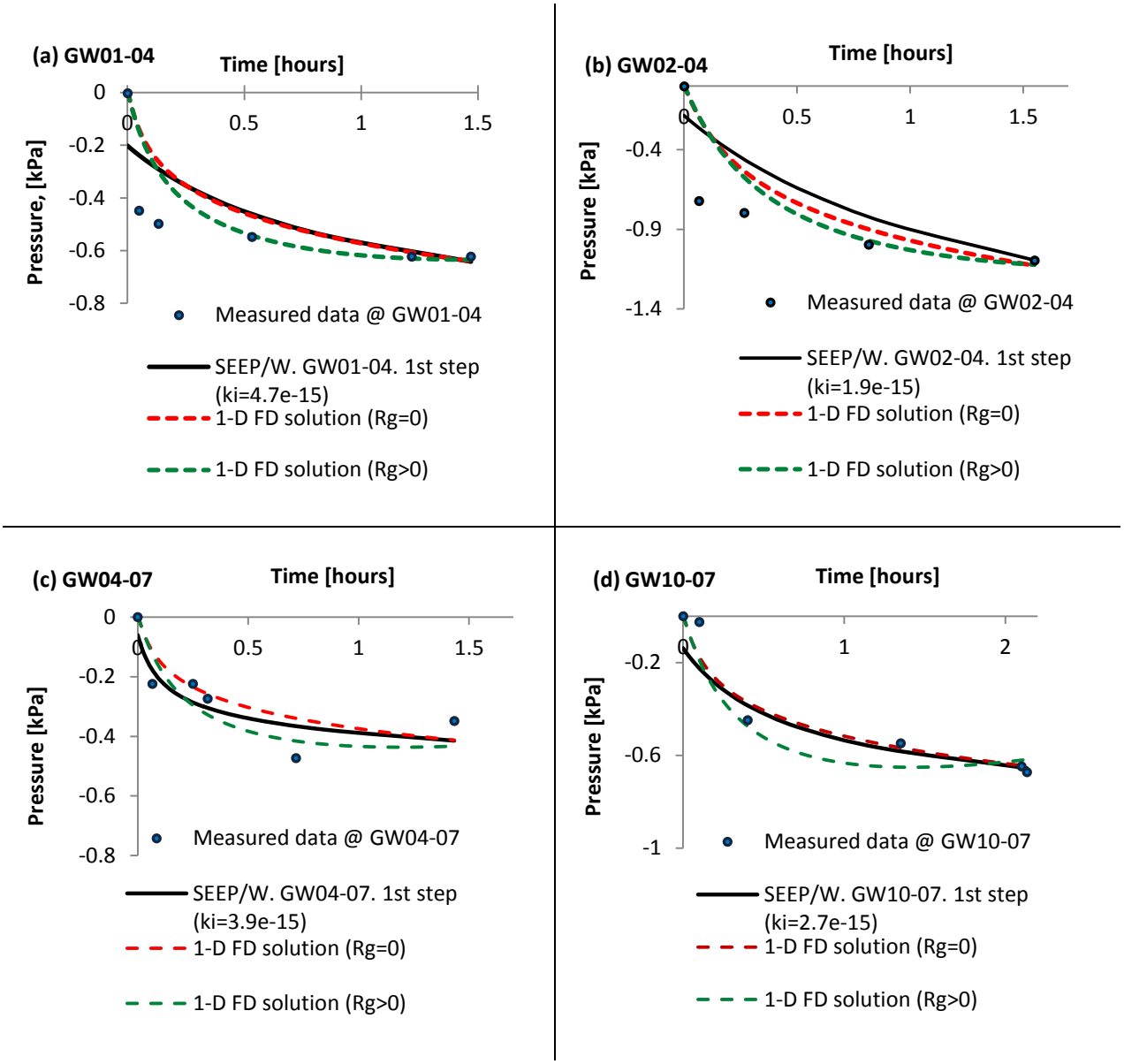

Fig. D. 2. Measured gas pressure during the short-term field test at all four test wells and SEEP/W and 1-D FD solution outputs based on the same best-fit values of air permeability respectively.

Table D.1 below shows the geometric mean of the obtained intrinsic permeability results within the parametric study of 1-D FD solution. The 1-D FD results of the calculated intrinsic permeability as the geometric mean, shown in Table D.1, demonstrate how the gas generation affected the defined intrinsic permeability values within the parametric studies for four test-wells.

Table D. 1. The geometric mean of air and intrinsic permeability results with its gas generation rate obtained using the 1-D FD analysis.

Test-well	Rg[m3/m3/ year]	k_{ir}, [m^2] Geom. MEAN	Rg[m3/m3/ year]	k_{ir}, [m^2] Geom. MEAN	Rg[m3/m3/ year]	k_{ir}, [m^2] Geom. MEAN	Rg[m3/m3/ year]	k_{ir}, [m^2] Geom. MEAN	Rg[m3/m3/ year]	k_{ir}, [m^2] Geom. MEAN	Rg[m3/m3/ year]	k_{ir}, [m^2] Geom. MEAN
GW-01-04	0	3.90E-14	1.2	1.63E-14	3.7	7.48E-15	4.9	5.83E-15	6.1	4.60E-15	12.3	2.19E-15
GW-02-04	0	2.21E-14	1.2	1.23E-14	3.7	6.60E-15	4.9	5.37E-15	6.1	4.38E-15	12.3	2.50E-15
GW-04-07	0	1.03E-14	1.3	7.80E-15	3.8	5.54E-15	5	4.70E-15	6.3	4.16E-15	12.5	2.54E-15
GW-10-07	0	2.67E-14	1.2	1.69E-14	3.7	8.03E-15	4.9	6.33E-15	6.1	5.36E-15	12.3	2.57E-15
kra=0.15		k_i, [m^2]		k_i, [m^2]		k_i, [m^2]		k_i, [m^2]		k_i, [m^2]		k_i, [m^2]
GW-01-04	0	2.60E-13	1.2	1.09E-13	3.7	4.99E-14	4.9	3.89E-14	6.1	3.07E-14	12.3	1.46E-14
GW-02-04	0	1.47E-13	1.2	8.20E-14	3.7	4.40E-14	4.9	3.58E-14	6.1	2.92E-14	12.3	1.67E-14
GW-04-07	0	6.87E-14	1.3	5.20E-14	3.8	3.69E-14	5	3.13E-14	6.3	2.77E-14	12.5	1.69E-14
GW-10-07	0	1.78E-13	1.2	1.13E-13	3.7	5.35E-14	4.9	4.22E-14	6.1	3.57E-14	12.3	1.71E-14

It might be found for someone easier to follow when the gas flow pumping rate is expressed in the unit of standard cubic feet per minute of "scfm" that is commonly used in the landfill engineering to measure the flow rate in a landfill. For this reason, the gas flow rate expressed in [scfm] as well as [m^3/s] in Table D.2. Table D.2 represents the 1-D FD solution results obtained through the parametric study for the following test-wells: GW01-04, GW02-04, GW04-07, and GW10-07.

Table D. 2. The 1-D FD solution results within the parametric studies and the AIR/W input intrinsic permeability values.

			1-D FD solution results				AIR/W	
GW01-04	R_{CH4} [m^3/Mg/year]	R_g [m^3/m^3/year]	Q_g [scfm]	12.33	19.8	0	k_i Geom. MEAN	k_i [m^2] L_S/D_{T2} & k_x/k_y=1
			Q_g [m^3/s]	0.0058	0.0093	0		
	R_{CH4}=0	0		3.13E-14	1.08E-13	5.20E-12	2.60E-13	2.55E-13
	R_{CH4}=1	1.2		2.62E-14	8.20E-14	6.00E-13	1.09E-13	k(AIR/W)&k(1D FD) differ by
	R_{CH4}=3	3.7	k_i [m^2]	2.17E-14	5.73E-14	1.00E-13	4.99E-14	-2%
	R_{CH4}=4	4.9		1.97E-14	4.97E-14	6.00E-14	3.89E-14	
	R_{CH4}=5	6.1		1.81E-14	4.33E-14	3.67E-14	3.07E-14	
	R_{CH4}=10	12.3		1.20E-14	2.67E-14	9.67E-15	1.46E-14	
			V_{waste} [m^3]	35931	51742	51742		
			ROI [m]	25	30	30		
GW02-04	R_{CH4} [m^3/Mg/year]	R_g [m^3/m^3/year]	Q_g [scfm]	11.4	20.75	0	k_i Geom. MEAN	k_i [m^2] L_S/D_{T2} & k_x/k_y=1
			Q_g [m^3/s]	0.0054	0.0098	0		
	R_{CH4}=0	0		1.27E-14	4.20E-14	6.00E-12	1.47E-13	1.50E-13
	R_{CH4}=1	1.2		1.13E-14	3.67E-14	1.33E-12	8.20E-14	k(AIR/W)&k(1D FD) differ by
	R_{CH4}=3	3.7	k_r [m^2]	9.33E-15	3.00E-14	3.00E-13	4.40E-14	2%
	R_{CH4}=4	4.9		9.33E-15	2.73E-14	1.80E-13	3.58E-14	
	R_{CH4}=5	6.1		8.67E-15	2.53E-14	1.13E-13	2.92E-14	
	R_{CH4}=10	12.3		6.67E-15	1.73E-14	4.00E-14	1.67E-14	
			V_{waste} [m^3]	32937	47430	47430		
			ROI [m]	25	30	30		
GW04-07	R_{CH4} [m^3/Mg/year]	R_g [m^3/m^3/year]	Q_g [scfm]	11.75	19.4	29.83	k_i Geom. MEAN	
			Q_g [m^3/s]	0.0056	0.0092	0.0141		
	R_{CH4}=0	0		2.59E-14	8.00E-14	1.57E-13	6.87E-14	N/A
	R_{CH4}=1	1.3		2.00E-14	5.87E-14	1.20E-13	5.20E-14	
	R_{CH4}=3	3.8	k_i [m^2]	1.60E-14	4.00E-14	7.87E-14	3.69E-14	
	R_{CH4}=4	5		1.33E-14	3.47E-14	6.67E-14	3.13E-14	
	R_{CH4}=5	6.3		1.20E-14	3.07E-14	5.87E-14	2.77E-14	
	R_{CH4}=10	12.5		7.67E-15	1.83E-14	3.47E-14	1.69E-14	
			V_{waste} [m^3]	9124	12573	17661		
			ROI [m]	23	27	32		
GW10-07	R_{CH4} [m^3/Mg/year]	R_g [m^3/m^3/year]	Q_g [scfm]	9.5	14.67	30	k_i Geom. MEAN	k_i [m^2] L_S/D_{T2} & k_x/k_y=1
			Q_g [m^3/s]	0.0045	0.0069	0.0142		
	R_{CH4}=0	0		1.80E-14	5.80E-14	1.20E-13	1.78E-13	1.87E-13
	R_{CH4}=1	1.2		1.47E-14	4.40E-14	9.00E-14	1.13E-13	k(AIR/W)&k(1D FD) differ by
	R_{CH4}=3	3.7	k_i [m^2]	1.11E-14	3.13E-14	5.93E-14	5.35E-14	5%
	R_{CH4}=4	4.9		1.00E-14	2.67E-14	5.10E-14	4.22E-14	
	R_{CH4}=5	6.1		9.00E-15	2.33E-14	4.47E-14	3.57E-14	
	R_{CH4}=10	12.3		5.33E-15	1.47E-14	2.73E-14	1.71E-14	
			V_{waste} [m^3]	22628	35357	48124		
			ROI [m]	24	30	35		

Fig. D.3 shows the logarithmic function of the intrinsic permeability correction factor due to gas generation and the gas ratio based on the data sets from the following test-wells: GW-01-04, GW-02-04; GW-04-07; GW-10-07.

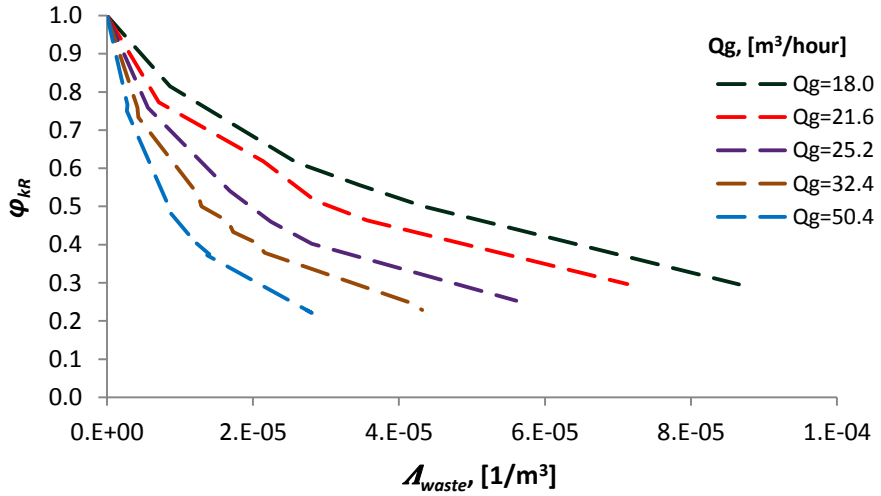

Fig. D. 3. The relationship between the intrinsic permeability correction factor due to gas generation and the gas ratio based on the data from the following test-wells: GW-01-04, GW-02-04; GW-04-07; GW-10-07.

Both Fig. D.3 and Table D.3 show the logarithmic functions that describe the relationship between the intrinsic permeability correction factor due to gas generation and the gas ratio for the correspondent gas pumping flow rate.

Table D. 3. The relationship between the intrinsic permeability correction factor due to gas generation and the gas ratio.

Q_g [m^3/hour]	$\varphi_{kR}=a\cdot ln(\Lambda_{waste})+b$	r_P	R^2
18.0	φ_{kR}= -0.2207*ln(Λ_{waste})-1.7337	0.9897	0.9796
21.6	φ_{kR}= -0.2078*ln(Λ_{waste})-1.6636	0.9858	0.9718
25.2	φ_{kR}= -0.2212*ln(Λ_{waste})-1.9090	0.9984	0.9969
32.4	φ_{kR}= -0.2216*ln(Λ_{waste})-1.9905	0.9982	0.9965
50.4	φ_{kR}= -0.2331*ln(Λ_{waste})-2.2279	0.9990	0.9980

The results of statistical analysis that evaluated the accuracy of fitting the 1-D FD solution results to their logarithmic functions provided there as well. Where the Pearson's correlation coefficient varies as r_P=98.6% to 99.9% and the coefficient of determination R^2=97.2% to 99.8% (Table D.3).

APPENDIX E. STATISTICAL ANALYSIS OF BEST-FIT

Statistical analysis is a necessity for any engineering research intended to compare simulated values with measured values on a basis of best-fit. In this particular research, in Chapter 3, Chapter 4, and the Appendices, the statistical analysis of fit between the measured field data and the model outputs (for all approaches) were made with the following statistics: the Pearson's correlation coefficient (r_p) and the coefficient of determination (R^2) (Taylor 2005).

Pearson's correlation coefficient measures the strength of the relationship between two variables: "*x*" and "*y*". Its ranges from plus one to minus one, and the closed-interval values of Pearson's correlation coefficient indicates a stronger relationship between the data-sets.

Pearson's correlation coefficient, r_p, can be expressed in the following form:

$$r_P = \frac{S_{xy}}{\sqrt{S_{xx}}.\sqrt{S_{yy}}} \quad \text{[E. 1]}$$

where S_{xx} and S_{yy} are the statistics: that used to measure variability in variable "x" and "y" correspondently, and S_{xy} is the statistic that used to measure correlation.

The statistic that used to measure variability in variable "*x*", S_{xx}, can be expressed is the following form:

$$S_{xx} = \sum_{i=1}^{n}(x_i - \bar{x})^2 \quad \text{[E. 2]}$$

where x_i is the value of *x* for case *i*, $\bar{x}$ is the arithmetic mean for *x*-variables, *i* is the case number, and *n* is the total number of cases.

The statistic that used to measure variability in variable "*y*", S_{yy}, can be expressed is the following form:

$$S_{yy} = \sum_{i=1}^{n}(y_i - \bar{y})^2 \quad \text{[E. 3]}$$

where y_i is the value of *y* for case *i*, and $\bar{y}$ is the arithmetic mean for *y*-variables.

The statistic that is used to measure correlation, S_{xy}, can be expressed is the following form:

$$S_{xy} = \sum_{i=1}^{n} (x_i - \bar{x}) \cdot (y_i - \bar{y}) \quad \text{[E. 4]}$$

The coefficient of determination, R^2, shows goodness of fitting, and it is the proportion of variability in "*y*" explained by "*x*":

$$R^2 = \frac{\sum_{i=1}^{n}(\hat{y}_i - \bar{y})^2}{\sum_{i=1}^{n}(y_i - \bar{y})^2} \quad \text{[E. 5]}$$

where $\hat{y}_i$ is the predicted value of *y* for case *i*.

Accordingly, in all figures in which estimated values of material properties are made on the basis of best-fit of predicted to measured data-sets, the calculated values of r_p and R^2 are reported for each measured/predicted data-sets.